Graphene-based functional materials

Zhang, Xiaoyan

Graphene-Based Functional Materials

Xiaoyan Zhang

university of groningen / zernike institute for advanced materials

The work described in this thesis was performed at the Stratingh Institute for Chemistry and the Zernike Institute for Advanced Materials, University of Groningen, the Netherlands.

This work is financially supported by 'Top Research School' program of the Zernike Institute for Advanced Materials under the Bonus Incentive Scheme (BIS) of the Netherlands' Ministry of Education, Science and Culture, and received additional support from the 'Stichting voor Fundamenteel Onderzoek de Materie (FOM)', which is financially supported by the 'Nederlandse Organisatie voor Wetenschappelijk Onderzoek (NWO)'.

Cover images: Porphyrins on graphene and self-assembly of *bis*-urea-terthiophene on graphene.

Printed by: Ipskamp Drukkers B.V., Enschede, The Netherlands.

RIJKSUNIVERSITEIT GRONINGEN

Graphene-based Functional Materials

Proefschrift

ter verkrijging van het doctoraat in de
Wiskunde en Natuurwetenschappen
aan de Rijksuniversiteit Groningen
op gezag van de
Rector Magnificus, dr. E. Sterken,
in het openbaar te verdedigen op
dinsdag 10 december 2013
om 09:00 uur

door
Xiaoyan Zhang
geboren op 20 februari 1982
te Henan, China

Promotores	: Prof. dr. B.L. Feringa Prof. dr. B.J. van Wees Prof. dr. W.R. Browne
Beoordelingscommissie	: Prof. dr. J.N. Coleman Prof. dr. M. Mayor Prof. dr. T. Banerjee

ISBN: 978-90-367-6616-6 (print)
978-90-367-6615-9 (electronic)

Dedicated to my family

Everyone has a dream, no matter that others care or not.

Anonymous

Contents

Chapter 1 Introduction 1

1.1 Graphene……2

1.2 Preparation of graphene…….....2

1.3 Functionalization of graphene…….……..3

1.4 Graphene field-effect transistors……...4

1.5 Outline and goal of the thesis…….……...6

1.6 Notes and references.……8

Chapter 2 Preparation of graphene by solvent dispersion methods and its functionalization through noncovalent and covalent approaches 11

2.1 Introduction……...……..12

2.2 Characterization techniques of graphene flakes……..…12

2.3 Preparation of graphene using solvent dispersion……...14

2.3.1 Exfoliation of graphene in solvents……...14

2.3.2 Exfoliation graphene in water/surfactant……...17

2.3.3 Solvent exchange method…….....19

2.4 Functionalization of graphene…….22

2.4.1 Functionalization of graphene using noncovalent methods…….....22

2.4.1.1 Noncovalent functionalization of graphene in aqueous media……22

2.4.1.2 Noncovalent functionalization of graphene in organic media.....27

2.4.2 Functionalization of graphene using covalent methods…….30

2.4.2.1 1,3-Dipolar cycloaddition……30

2.4.2.2 Zwitterion cycloaddition…….....32

2.4.2.3 Nitrene addition……...33

2.4.2.4 Nucleophilic addition……...34

2.4.2.5 Bingel reaction……35

2.4.2.6 Radical addition……...36

2.4.2.7 Click chemistry……....38

2.4.2.8 Hydrogenation……39

2.5 Conclusions and future aspects……41

2.6 Notes and references……...42

Chapter 3 Dispersion of graphene in ethanol using a simple solvent exchange method 51

3.1 Introduction……..52

3.2 Results……..53

3.3 Discussions……60

3.4 Conclusions……..61

3.5 Perspective……...62

3.6 Experimental……62

3.7 Notes and references……63

Chapter 4 Preparation of dispersible graphene through organic functionalization of graphene using a zwitterion intermediate cycloaddition approach 67

4.1 Introduction……..68

4.2 Results……..69

4.3 Conclusions……..79

4.4 Acknowledgement……...80

4.5 Experimental……80

4.6 Notes and references ……...84

Chapter 5 One-pot functionalization of graphene with porphyrin through cycloaddition reactions 89

5.1 Introduction……..90

5.2 Results……..91

5.3 Conclusions……105

5.4 Perspective……..106

5.5 Acknowledgement……..106

5.6 Experimental……..106

5.7 Notes and references ……..109

Chapter 6 Supramolecular chemistry on large area graphene field-effect transistors 117

6.1 Introduction……118

6.2 Results……119

6.3 Conclusions……131

6.4 Methods……132

6.5 Acknowledgement……..133

6.6 Notes and references ……..133

Chapter 7 Self-assembly of alkyl-porphyrins on large area chemical vapor deposition (CVD) graphene on nickel and SiO_2 substrates and the interaction between graphene and alkyl-porphyrins 137

7.1 Introduction……138

7.2 Results……139

7.3 Conclusions……147

7.4 Methods……148

7.5 Notes and references ……..150

Summary and outlook……155

总结与展望……159

Samenvatting en vooruitzichten……163

Acknowledgements……167

Abstract

Graphene-based functional materials are attracting increasing attention in recent years due to their potential applications in several fields, as diverse as electronic devices, composites and sensors. In this chapter, a brief introduction to graphene and its preparation, functionalization and application in field-effect transistors is provided, followed by an outline of the thesis and the aim of the research.

1.1 Graphene

Graphene, a monolayer of carbon atoms arranged in a hexagonal lattice, has attracted unprecedented interest due to its extraordinary properties, such as a room temperature quantum Hall effect, high charge carrier mobility, high transparency and good thermal conductivity.[1,2] Graphene is a semimetal, and its valence band and conduction band touch at the Dirac points (Figure 1).[3]

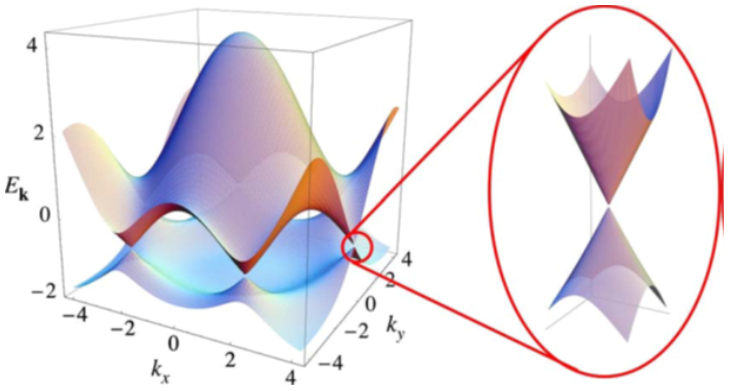

Figure 1. Band structure of graphene. Reproduced with permission from ref. 3. Copyright 2009 American Physical Society.

Graphene has already realised potential in several fields, such as transparent electrodes, sensors and composites.[4] In 2010, Andre Geim and Konstantin Novoselov were awarded the Nobel Prize in Physics 'for groundbreaking experiments regarding the two-dimensional material graphene'.[5] Over the past decade, graphene has been one of the hottest topics among materials scientists, physicists and chemists.

1.2 Preparation of graphene

There are primarily three approaches to prepare graphene, including mechanical, epitaxial and chemical routes (Chart 1).

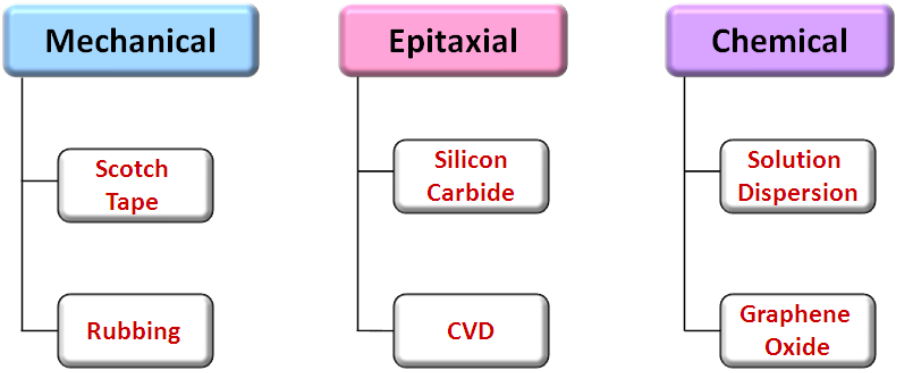

Chart 1. Methods to obtain graphene.

The mechanical method includes the famous scotch tape exfoliation method[1] and rubbing graphite against substrates.[6] Annealing silicon carbide at high temperatue[7] and chemical vapor deposition (CVD) on metal substrates are used to grow graphene epitaxially.[8,9] The chemical method involves either solution dispersion of graphite[10] or reduction of graphene oxide.[11] In this thesis, CVD grown graphene and solution dispersed graphene were used to prepare graphene-based functional materials.

1.3 Functionalization of graphene

In many applications, graphene needs to be combined with other materials, which requires functionalization of graphene. There are two approaches commonly taken to the functionalization of graphene: covalent and noncovalent.[12] Covalent functionalization involves covalently attachment of molecules onto graphene using organic reactions. Noncovalent functionalization involves binding molecules to graphene through π-π, hydrophobic and hydrogen bonding interactions. Examples of chemical functionalization of graphene are discussed in Chapter 2.

1.4 Graphene field-effect transistors

Graphene-based electronic devices have developed rapidly over the past years. In particular, graphene-based field-effect transistors are considered to be highly promising for high-frequency applications due to its two-dimensional structure and unique carrier transport properties.[13]

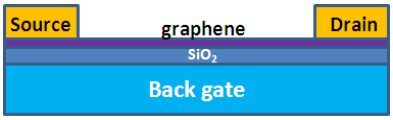

Scheme 1. Typical structure of a graphene field-effect transistor.

The first multilayer graphene field-effect transistors demonstrated by the Manchester team showed mobilities up to 1.5 × 10^4 cm^2 V^{-1} s^{-1} at 300 K and 6 × 10^4 cm^2 V^{-1} s^{-1} at 4 K, and on-off resistance ratios less than 30 at 300 K.[1] A typical structure of a graphene field-effect transistor is shown in Scheme 1 (source, drain, dielectric layer, graphene and back gate).

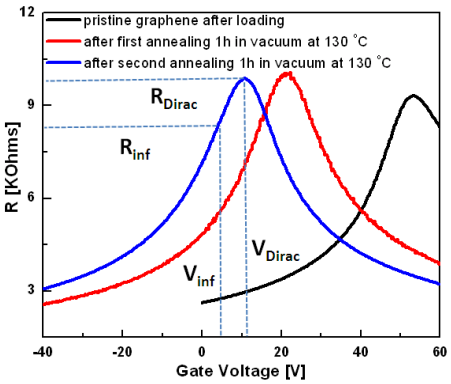

Figure 2. Gate spectroscopy of a large area graphene field-effect transistor before (black curve) and after thermal annealing in vacuum at 130 °C after first (red curve) and second (blue curve) annealing treatment. The resistance and gate voltage of the inflection point and Dirac point are labeled in the blue curve (data from Chapter 6).

The Dirac point described by gate spectroscopy in graphene field-effect transistors is defined as the gate voltage where the resistance is maximum. Ideally, the Dirac point of undoped graphene is at the zero gate voltage. However, graphene is typically contaminated by unwanted dopants from the environment and the processes used to fabricate transistors (Figure 2, black curve). Recovery of the intrinsic graphene can be achieved by annealing graphene to remove absorbates (Figure 2, red and blue curves, after first and second annealing, respectively).

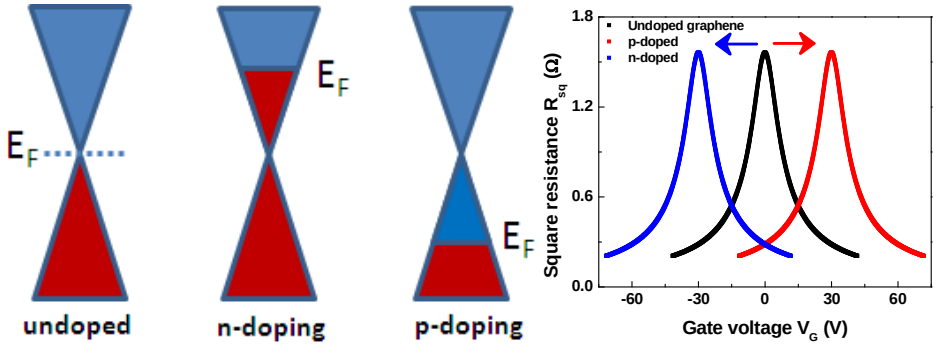

Figure 3. Shifts of the Fermi energy level (E_F) of graphene and Dirac point of gate spectroscopy due to doping (black: undoped; red: p-doped; blue: n-doped).

The effect of absorption of molecules onto graphene field-effect transistors could have two effects: shift of the Dirac point and change of the mobility. Molecules can dope graphene either in n- or p-type, which shifts the Fermi energy level (E_F) of graphene and also the Dirac point observed in gate spectroscopy (Figure 3).[14] Changes in the mobility can be induced when molecules act as (charged) impurity scatterers (decrease), on the other hand they may screen the electric field of coulomb scatterers present on the underlying substrate (increase).[15,16]

The mobility μ of graphene transistors can be calculated using the following formula.

$$\mu = \frac{1}{ne\rho} \qquad n = (V_{Dirac} - V) \cdot \alpha$$

$$\alpha = \frac{C}{e} \qquad \rho = \frac{RW}{L}$$

Here, n is the charge carrier density, ρ is the resistivity, e is the elementary charge, V_{Dirac} is the gate voltage at the Dirac point, V is the gate voltage, α is the effective capacitance in the units of $cm^{-2}\,V^{-1}$, C is the capacitance per unit area, R is the resistance, W is the width of the graphene channel and L is the length of the graphene channel. Usually, the mobility is calculated at the inflection points, where the derivative dρ/dn has an extreme (Figure 2).

In 2007, the first top gated graphene transistor was reported.[17] Subsequently, graphene transistors with a 240-nm gate showed a cutoff frequency of 100 GHz.[18] More recently, graphene transistors capable of detecting THz and IR waves over a wide band of frequencies (0.76–33 THz) were also reported.[19]

Although there has been considerable progress in the technology of graphene-based transistors, challenges remain.[13] For example, creating a well defined bandgap in graphene to allow logic graphene transistors to be switched off still needs to be explored.[20,21] Also, fabricating large area graphene transistors in a controllable and reproducible manner is highly desirable.[22]

1.5 Outline and goal of the thesis

The overall goal of the thesis work was to prepare graphene-based functional materials, including preparation of graphene, and its functionalization using covalent and noncovalent approaches.

In Chapter 2, an overview on the preparation of graphene by solvent dispersion methods and its functionalization through noncovalent and covalent approaches is discussed.

In Chapter 3, a simple solvent exchange method to disperse graphene in ethanol is described for the first time. The graphene dispersions were studied by several spectroscopic and microscopic techniques, and the film formed showed good conductivity. Considering the low boiling point of ethanol, this method will be useful in the preparation of composites, surface deposition and fabrication of graphene based materials, and will help to find other low boiling point solvents to disperse graphene.

In Chapter 4, highly functionalized graphene was obtained through a zwitterion intermediate cycloaddition onto exfoliated graphene flakes under new reaction conditions. The functionalized graphene formed stable dispersions in common solvents (most remarkably in water) and was characterized by several spectroscopic and microscopic techniques. Its dispersion in water is especially useful in a wide range of areas, such as composites, devices and biological applications.

In Chapter 5, two types of graphene-porphyrin hybrid materials were prepared using one pot cycloaddition reactions. The graphene-porphyrin hybrid materials were characterized using a number of spectroscopies and microscopy techniques. The relatively low degree of functionalization of these two hybrid materials may allow for retention of graphene's intrinsic properties, especially in comparison with materials prepared via graphene oxides for example. Considering the remarkable properties of both graphene and porphyrin, these two hybrid materials may have potential applications in a number of areas, such as solar cells, sensors and catalysis.

In Chapter 6, commercially available chemical vapor deposition (CVD) graphene was used as a template to study the self-assembly of *bis*-urea-terthiophene (**T_3**) molecular wires. The interaction between graphene and **T_3** molecular wires was studied by gate spectroscopy. It is shown that commercially available CVD graphene can be used as a substrate for the self-assembly of **T_3** molecular wires even when the graphene is highly undulating. Changes in doping levels and charge carrier mobility are observed in graphene transistors after **T_3** modification. We attribute these changes mostly to solvent induced cleaning of initially p-doped graphene. Nevertheless, occasionally clean transistors reveal that the doping induced by the molecular wires and the graphene is at least an order of magnitude less than the doping induced by unwanted adsorbates.

In Chapter 7, the self-assembly of two alkyl-Ni (II)-porphyrins on large area CVD graphene was studied using scanning tunneling microscopy (STM). The interaction between graphene and porphyrins was studied by Raman and UV spectroscopy. The data indicate that graphene and porphyrins can affect each other electronically.

1.6 Notes and references

1. K. S. Novoselov, A. K. Geim, S. V. Morozov, D. Jiang, Y. Zhang, S. V. Dubonos, I. V. Grigorieva and A. A. Firsov, Electric field effect in atomically thin carbon films, *Science*, 2004, **306**, 666.

2. A. K. Geim and K. S. Novoselov, The rise of graphene, *Nat. Mater.*, 2007, **6**, 183.

3. A. H. Castro Neto, F. Guinea, N. M. R. Peres, K. S. Novoselov and A. K. Geim, The electronic properties of graphene, *Rev. Mod. Phys.*, 2009, **81**, 109.

4. K. S. Novoselov, Graphene: materials in the flatland (Nobel lecture), *Angew. Chem. Int. Ed.*, 2011, **50**, 6986.

5. http://www.nobelprize.org/nobel_prizes/physics/laureates/2010/, accessed on 31/10/2013.

6. K. S. Novoselov, D. Jiang, F. Schedin, T. J. Booth, V. V. Khotkevich, S. V. Morozov and A. K. Geim, Two-dimensional atomic crystals, *Proc. Natl. Acad. Sci. U.S.A.*, 2005, **102**, 10451.

7. K. V. Emtsev, A. Bostwick, K. Horn, J. Jobst, G. L. Kellogg, L. Ley, J. L. McChesney, T. Ohta, S. A. Reshanov, J. Rohrl, E. Rotenberg, A. K. Schmid, D. Waldmann, H. B. Weber and T. Seyller, Towards wafer-size graphene layers by atmospheric pressure graphitization of silicon carbide, *Nat. Mater.*, 2009, **8**, 203.

8. X. Li, W. Cai, J. An, S. Kim, J. Nah, D. Yang, R. Piner, A. Velamakanni, I. Jung, E. Tutuc, S. K. Banerjee, L. Colombo and R. S. Ruoff, Large-area synthesis of high-quality and uniform graphene films on copper foils, *Science*, 2009, **324**, 1312.

9. K. S. Kim, Y. Zhao, H. Jang, S. Y. Lee, J. M. Kim, K. S. Kim, J.-H. Ahn, P. Kim, J.-Y. Choi and B. H. Hong, Large-scale pattern growth of graphene films for stretchable transparent electrodes, *Nature*, 2009, **457**, 706.

10. Y. Hernandez, V. Nicolosi, M. Lotya, F. M. Blighe, Z. Y. Sun, S. De, I. T. McGovern, B. Holland, M. Byrne, Y. K. Gun'ko, J. J. Boland, P. Niraj, G. Duesberg, S. Krishnamurthy, R. Goodhue, J. Hutchison, V. Scardaci, A. C. Ferrari and J. N. Coleman, High-yield production of graphene by liquid-phase exfoliation of graphite, *Nat. Nanotechnol.*, 2008, **3**, 563.

11. S. Stankovich, D. A. Dikin, R. D. Piner, K. A. Kohlhaas, A. Kleinhammes, Y. Jia, Y. Wu, S. T. Nguyen and R. S. Ruoff, Synthesis of graphene-based nanosheets via chemical reduction of exfoliated graphite oxide, *Carbon*, 2007, **45**, 1558.

12. V. Georgakilas, M. Otyepka, A. B. Bourlinos, V. Chandra, N. Kim, K. C. Kemp, P. Hobza, R. Zboril and K. S. Kim, Functionalization of graphene: covalent and non-covalent approaches, derivatives and applications, *Chem. Rev.*, 2012, **112**, 6156.

13. F. Schwierz, Graphene transistors, *Nat. Nanotechnol.*, 2010, **5**, 487.

14. H. T. Liu, Y. Q. Liu and D. B. Zhu, Chemical doping of graphene, *J. Mater. Chem.*, 2011, **21**, 3335.

15. J. H. Chen, C. Jang, S. Adam, M. S. Fuhrer, E. D. Williams and M. Ishigami, Charged-impurity scattering in graphene, *Nat. Phys.*, 2008, **4**, 377.

16. T. Ando, Screening effect and impurity scattering in monolayer graphene, *J. Phys. Soc. Jpn.*, 2006, **75**, 074716.

17. M. C. Lemme, T. J. Echtermeyer, M. Baus and H. Kurz, A graphene field-effect device, *IEEE Electron Dev. Lett.*, 2007, **28**, 282.

18. Y.-M. Lin, C. Dimitrakopoulos, K. A. Jenkins, D. B. Farmer, H.-Y. Chiu and A. Grill, 100-GHz transistors from wafer-scale epitaxial graphene, *Science*, 2010, **327**, 662.

19. Y. Kawano, Wide-band frequency-tunable terahertz and infrared detection with graphene, *Nanotechnology*, 2013, **24**, 214004.

20. M. Y. Han, B. Ozyilmaz, Y. B. Zhang and P. Kim, Energy band-gap engineering of graphene nanoribbons, *Phys. Rev. Lett.*, 2007, **98**, 206805.

21. H. Zhang, E. Bekyarova, J.-W. Huang, Z. Zhao, W. Bao, F. Wang, R. C. Haddon and C. N. Lau, Aryl functionalization as a route to band gap engineering in single layer graphene devices, *Nano Lett.*, 2011, **11**, 4047.

22. J. Chan, A. Venugopal, A. Pirkle, S. McDonnell, D. Hinojos, C. W. Magnuson, R. S. Ruoff, L. Colombo, R. M. Wallace and E. M. Vogel, Reducing extrinsic performance-limiting factors in graphene grown by chemical vapor deposition, *ACS Nano*, 2012, **6**, 3224.

Chapter 2

Preparation of graphene by solvent dispersion methods and its functionalization through noncovalent and covalent approaches

Abstract

In this chapter, a review of recent developments in the preparation of graphene using the solvent dispersion method will be discussed followed by a survey of the non-covalent approaches taken to disperse graphene. Finally, chemical reactions performed on solvent dispersed graphene, including 1,3-dipolar cycloaddition, zwitterion cycloaddition, nitrene addition, nucleophilic addition, the Bingel reaction, radical addition and click chemistry, will be discussed.

This chapter has been published:

Xiaoyan Zhang, Wesley R. Browne, Bart J. van Wees and Ben L. Feringa, ***Handbook of Graphene Science (CRC press)***, *in press.*

2.1. Introduction

The unique properties of graphene, a one atom thick layer of connected carbon atoms with a two-dimensional honeycomb lattice, has attracted increasing attention over the last decade due to its promising materials properties for a wide range of applications varying from electronic devices, to composites and biological applications.[1-3] However, a prerequisite to its application is the availability of methods to obtain high quality graphene on a large scale. Several approaches have been developed, including mechanical cleavage,[4] epitaxial growth,[5-7] reduction of graphene oxide,[8] and solvent dispersion of graphite.[9] Among these methods, solvent dispersion of graphite seems to be the simplest approach to prepare dispersible and near defect-free graphene sheets. However, graphene sheets tend to precipitate due to aggregation as a result of strong π-π interactions even in aromatic solvents. Chemical functionalization of graphene through noncovalent or covalent approaches holds potential in improving the stability and processing of dispersed graphene, and may also introduce new properties as well as allowing tuning of the properties of graphene. In this chapter, a review of recent developments in the preparation of graphene using the solvent dispersion method will be discussed followed by a survey of the non-covalent approaches taken to disperse graphene. Finally, chemical reactions performed on solvent dispersed graphene, including 1,3-dipolar cycloaddition, zwitterion cycloaddition, nitrene addition, nucleophilic addition, the Bingel reaction, radical addition and click chemistry, will be discussed.

2.2 Characterization techniques of graphene flakes

The quality of exfoliated graphene dispersions is usually determined using a number of spectroscopic and microscopic techniques.

Transmission electron microscopy (TEM) is a convenient technique to assess the exfoliation of graphene flakes. The number of layers can be determined by

examining the edges of graphene flakes. Furthermore, electron diffraction can also be performed to confirm the presence of single-layer graphene flakes.[10] If the innermost spots are more intense stronger than the outer spots, it indicates a single-layer graphene flake. Otherwise, it is a multi-layer graphene flake.[10]

Atomic force microscopy (AFM) allows for measurement of the height of the graphene flakes, from which the presence of single-layer graphene can be confirmed.[4,10] However, the measured thickness of graphene depends on the substrates used, and also the presence of water increases the apparent height. A problem often encountered is the aggregation of the graphene flakes when deposited onto substrates,[9,10] which can make it difficult to perform analysis of the graphene dispersions.

Raman spectroscopy is an invaluable technique in the study of the quality of graphene.[11] The characteristic Raman bands for graphitic materials are: a disorder-induced D band at ~1350 cm^{-1}, a doubly degenerate zone centre E_{2g} mode at about 1580 cm^{-1} (G band, indicative to sp^2 carbon bonds), and a two phonon double resonance Raman band at ~ 2700 cm^{-1} (2D band). The number of layers of graphene flakes can be determined from the shape and full-width at half-maximum (FWHM) of the 2D band. The ratio of intensity between the D band and G band (I_D/I_G) is often used to quantify the defect level in graphene materials, and can therefore give direct evidence for covalent functionalization of graphene.[12]

Techniques such as Fourier transform infrared spectroscopy (FTIR) and X-ray photoelectron spectroscopy (XPS) can also be used to study the quality of graphene, with XPS providing the composition of graphene samples. Thermal gravimetric analysis (TGA) is typically used to determine the content of defects or amount of functional groups of the graphene samples.

2.3 Preparation of graphene using solvent dispersion

2.3.1 Exfoliation of graphene in solvents

The method of solvent exfoliation of graphite to yield graphene with the aid of sonication was first described by Coleman and co-workers.[10] Graphite flakes were sonicated gently in *N*-methyl-2-pyrrolidone (NMP) for half an hour, the mixture was centrifuged and the supernatant was collected. The concentration of the dispersions was ca. 0.01 mg ml^{-1}. The presence of single-layer graphene

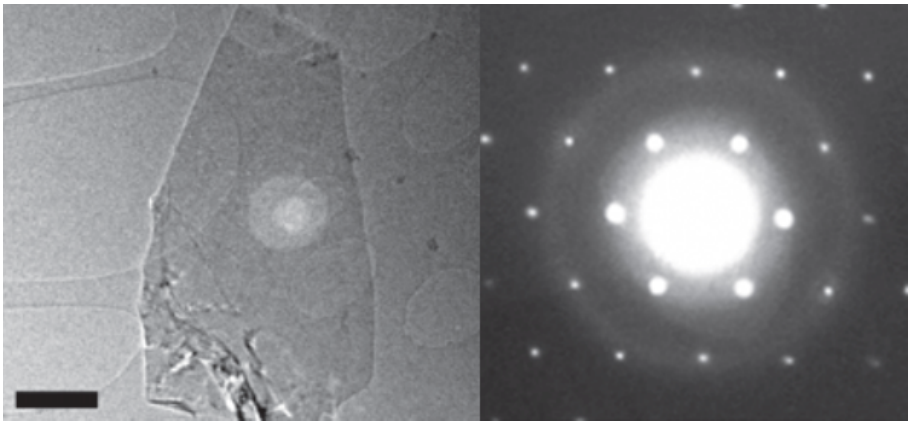

Figure 1. TEM image of single-layer graphene flake from NMP dispersion (left) and the corresponding electron diffraction pattern (right). Reproduced with permission from ref. 10. Copyright 2008 Nature Publishing Group.

flakes was confirmed by transmission electron microscopy (TEM, by checking the number of layers at the edges, Figure 1), electron diffraction (the intensity of the innermost spots is stronger than that of the outer spots) and Raman spectroscopy (from the shape of the 2D band). The quality of the graphene flakes was analyzed by X-ray photoelectron, infrared and Raman spectroscopy, which indicated a low content of defects. Graphene thin films were fabricated using a vacuum filtration method, which, after thermal annealing of the graphene films showed conductivity comparable to that of reduced graphene

oxide. Polymer/graphene nanocomposites were also tested and showed enhanced electrical conductivity. The authors also pointed out that the optimal solvents for the exfoliation of graphite are those whose surface tension best matched with the surface energy of graphene.

After the first report, other solvents such as dimethylformamide (DMF),[13] *o*-dichlorobenzene (ODCB),[14] perfluorinated aromatic solvents[15] and ionic liquids[16] (Figure 2) were also used to exfoliate graphite into graphene. The obtained graphene dispersions consisted mainly of single- and few-layer graphene flakes as confirmed by TEM, AFM and Raman spectroscopy. Coleman and co-workers further tested the dispersibility of graphene in 40 solvents and concluded that good solvents for graphene dispersion are those for which the Hildebrand solubility parameter is near to $\delta_T \sim 23$ MPa$^{1/2}$ and the Hansen solubility parameters are near $\delta_D \sim 18$ MPa$^{1/2}$, $\delta_P \sim 9.3$ MPa$^{1/2}$ and $\delta_H \sim 7.7$ MPa$^{1/2}$.[17]

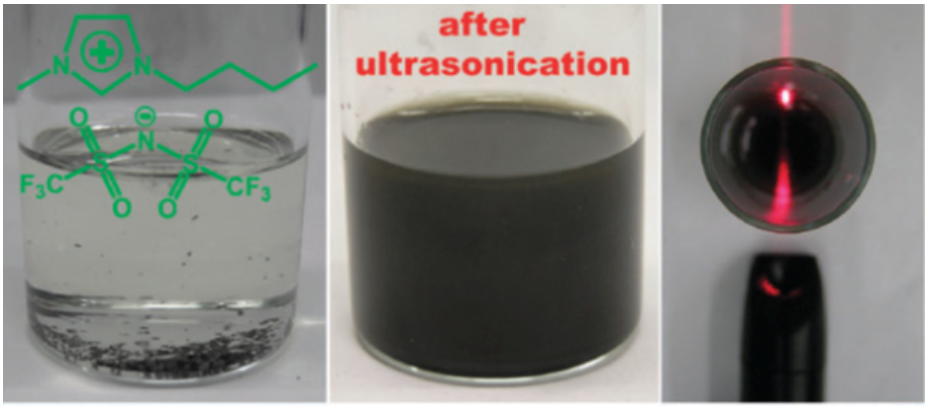

Figure 2. Graphite in ionic liquids before (left) and after (middle) sonication. The Tyndall effect of graphene dispersions (right). Reproduced with permission from ref. 16. Copyright 2010 Royal Society of Chemistry.

Mild sonication for short period only yields low concentrations of graphene dispersions in the above mentioned solvents. With prolonged sonication, high

concentrations of graphene in NMP could be obtained (up to 1.2 mg ml^{-1}).[18] TEM images showed that the size of the graphene flakes reduced as a function of time. Raman spectroscopic analysis indicated that the D band intensity increased with time as $t^{1/2}$, which means new edges were created during sonication and the defects were mainly distributed on the edge of the graphene flakes. Extended sonication of graphite in ionic liquids yields high concentrations of graphene dispersions of up to 5.33 mg ml^{-1}.[19] High concentrations of graphene dispersions can also be obtained by the addition of NaOH to the solvents (NMP, *N,N*-dimethylacetamide and cyclohexanone).[20] NaOH is proposed to intercalate graphite, thereby improving the exfoliation efficiency. Organic salts such as sodium citrate can also dramatically enhance the exfoliation efficiency up to 123 times.[21]

Besides using various solvents, several graphite sources can be used also. For example, worm-like exfoliated graphite was used to prepare graphene flakes in NMP with the aid of sonication and centrifugation.[22] Expandable graphite was first heated and then quenched in cooled hydrazine hydrate (20%) or concentrated ammonia (28%) to generate single- and few-layer graphene flakes.[23]

Other methods to disperse graphene in organic solvents have been reported.[24-27] Ball milling is an optional method to exfoliate graphite into graphene.[24] Single- and few-layer graphene flakes with thicknesses of around 0.8-1.8 nm were prepared by ball milling of thin graphite in DMF. The graphene dispersions were characterized by TEM, electron diffraction, AFM and Raman spectroscopy. The electrical conductivity of the graphene film was ca. 1.2×10^3 S m^{-1} at room temperature. Supercritical fluid exfoliation of graphite into graphene in NMP, DMF and ethanol was also developed.[25] AFM and Raman analysis indicated that about 90-95% of the graphene sheets were <8 layers, with approximately 6-10% monolayers. Vortex fluidic devices, which produce

shear forces, can be used as a 'soft energy' source to exfoliate graphite in NMP.[26] Ionic liquid assisted grinding of graphite into graphene was reported by Shang and co-workers.[27] The graphene sheets obtained were only two to five layers thick. These recent methods significantly broaden the range of preparation of graphene dispersions.

2.3.2 Exfoliation graphene in water/surfactant

Dispersion of graphene in aqueous solution is appealing for biological applications. However, water has a surface tension of 72.8 mJ m^{-2}, which is unsuitable for the direct exfoliation of graphite. Coleman and co-workers demonstrated that graphite could be exfoliated into single- and few-layer graphene with the aid of sodium dodecylbenzene sulfonate (SDBS, Figure 3).[28] An absorption coefficient of $\alpha = 1390$ mL mg^{-1} m^{-1} at 660 nm was determined by fitting the absorption data at different graphite concentration. The dispersions are stabilized by Coulombic repulsion of the surfactant. X-ray photoelectron, infrared and Raman spectroscopies indicate that the graphene flakes contain few defects. The graphene films showed a conductivity of 1.5×10^3 S m^{-1} after annealing. Other surfactants such as sodium cholate can also be used to exfoliate graphite in aqueous solution.[29] The annealed graphene films show a conductivity of 1.5×10^4 S m^{-1}.

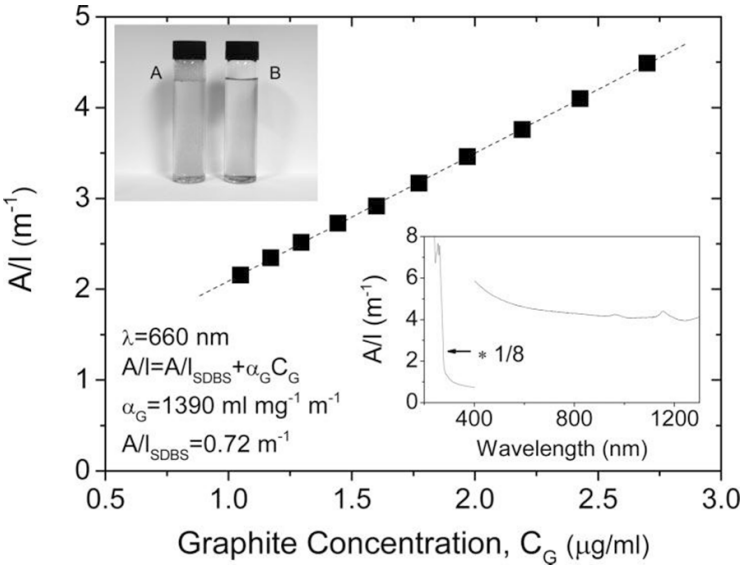

Figure 3. Absorbance per unit length (λ = 660 nm) as a function of graphite concentration at a SDBS concentration of 0.5 mg ml^{-1}. Reproduced with permission from ref. 28. Copyright 2009 American Chemical Society.

The concentrations of the graphene/surfactant dispersions can be further improved by sonication for longer periods (up to 0.3 mg ml^{-1} after 400 h sonication).[30] The size of the graphene flakes does not decrease with the increase in sonication time, and the yield of single-layer graphene can be up to 10%. High concentrations of graphene dispersions (~ 15 mg ml^{-1}) can be prepared by continuous addition of the surfactant during the exfoliation process, which is believed to lower the surface tension during sonication.[31] Gum Arabic assisted exfoliation of graphite in water by sonication was reported by Yu et al.[32] The surfactant residues could be removed completely by acid hydrolysis to produce pure graphene. The fabricated graphene films showed 20 times higher electrical conductivity than reduced graphene oxide.

The properties of graphene depend on thickness, lateral area and shape.[33] Therefore, preparation of monodispersed graphene dispersions is useful for

device applications. Graphene flakes with controlled thickness could be obtained by density gradient ultracentrifugation of graphene/sodium cholate dispersions.[34] The sorted graphene flakes were characterized by AFM and Raman spectroscopy. Graphene films prepared using this method showed enhanced performance in transparent conducting films compared with previous sedimentation-based centrifugation approach.

2.3.3 Solvent exchange method

Solvents such as NMP, DMF and ODCB, whose surface tensions are close to 40 mJ m^{-2}, are suitable for the direct exfoliation of graphite to yield graphene. However, their high boiling points limit their use in composites and surface deposition. In these cases, solvents with low boiling point are preferred. However, most low boiling point solvents (for example, water and ethanol) are unsuitable for the direct exfoliation of graphite because their surface tensions do not match the surface energy of graphene.

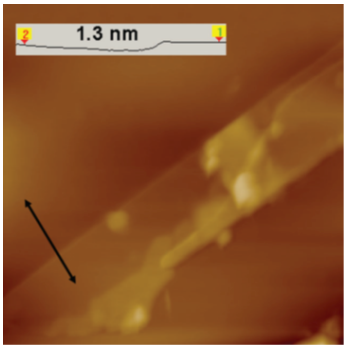

Figure 4. An AFM image of graphene from a dispersion of ethanol using the solvent exchange method (size: 2.0 × 2.0 μm, ref. 35).

Recently, our group reported the preparation of graphene dispersion in ethanol using a solvent exchange method.[35] Graphene was first exfoliated in NMP, and the graphene flakes were collected on a membrane by filtration. The filter cake was redispersed in ethanol several times to remove residual NMP (<0.3 vol%,

as determined by FTIR spectroscopy). After the solvent exchange, the concentration of graphene in ethanol can reach 0.04 mg ml^{-1}. The graphene dispersion in ethanol showed at most 20% sedimentation over one week, which is comparable to a graphene dispersion in NMP diluted with water (NMP: water = 1:99).[18] The presence of single-and few-layer graphene flakes in ethanol was confirmed by TEM, AFM (Figure 4) and Raman spectroscopy. The graphene films showed electrical conductivity of ca. 1130 S m^{-1}. The solvent exchange method indicates that the solvent properties that are optimum for initial exfoliation are not necessarily the same as those required to maintain the dispersion.

Different approaches to preparation of graphene dispersions in various solvents are summarized below (Table 1).

Table 1. Comparision of available approaches to disperse graphene in solvents

Ref.	Starting materials	Solvents	Method	Concentra-tions/mg ml^{-1}	Size	Thickness /nm	Conducti-vity/S m^{-1}
10	Graphite powders	NMP	Sonication/0.5 h	0.01	A few µm	Single- and few-layer	6500
13	Natural graphite crystal	DMF	Sonication/3 h	—	Sub-µm	Single- and few-layer	5 kΩ
14	Microcrystalline synthetic graphite/ expanded graphite/HOPG	ODCB	High-shear mix 1 h plus sonication 0.5 h	0.03/<0.02	100–500 nm	Single- and few-layer	1500
15	Graphite powders	Perfluorinat-ed aromatic solvents	Sonication/1 h	0.05–0.1	Sub-µm to µm	Single- and few-layer	—

16	Natural graphite flakes	Ionic liquids	Sonication/1 h	0.95	μm	<5 layers	—
18	Natural graphite powders	NMP	Sonication 0.5–462 h	0.06–1.2	Several μm	Single- and few-layer	$1.8\pm0.1\times10^4$
19	Graphite flakes	Ionic liquids	Grinding and sonication 24h	5.33	3–4 μm	average ~ 2 nm	—
22	Worm-like graphite	NMP	Sonication/0.5 h	—	Several μm	Single- and few-layer	—
24	Graphite nanosheets	DMF	Ball milling 30 h	—	—	≤ 3 layers (0.8–1.8 nm)	1200
26	Pristine graphite	NMP	Vortex fluidic exfoliation/0.5 h	—	≤ 1 μm	Single- and few-layer	—
28	Graphite power	SDBS/H_2O	Sonication	0.002–0.05	Several μm	Single- and few-layer	1500
29	Natural flake graphite	Sodium cholate/H_2O	Sonication	0.05–0.3	Several hundred nm to 1 μm	Single- and few-layer	17500
32	Natural graphite powder	Gum Arabic/H_2O	Sonication	—	Several hundred nm to 2 μm	Single- and few-layer	10000
35	Graphite flakes	Ethanol	Sonication and solvent exchange	0.04	Several hundred nm to several μm	Single- and few-layer	1130

— data not available

Sonication is still the most commonly used method to prepare graphene dispersions in various solvents. Mild sonication with low power input is normally needed to prepare graphene flakes with a low defect content. For other methods such as high-power ball milling or grinding, care should be taken to prevent the introduction of defects on the basal plane of graphene. Vortex fluidic, as a relatively soft energy tool, can also be used for the exfoliation of graphene, but this method is mainly limited by the availability of Vortex fluidic instrument.

2.4. Functionalization of graphene

Although graphene can be dispersed in various solvents using the methods above, graphene flakes still tend to precipitate in these solvents due to the strong π-π interactions between the individual flakes. In order to solve this issue and further improve their dispersibility, stability and processability, a range of methods to functionalize graphene non-covalently and covalently have been developed.[36-84]

2.4.1 Functionalization of graphene using noncovalent methods

Graphene has a large π system, which facilitates π-π interactions with other conjugated molecules. The advantage of the noncovalent methods to modify graphene is that they do not destroy the sp^2 structure of graphene, and have the potential to tune the properties of graphene due to the electronic interactions with the molecules.

2.4.1.1 Noncovalent functionalization of graphene in aqueous media

Aqueous dispersed graphene could be obtained via first grinding expanded graphite with 7,7,8,8-tetracyanoquinodimethane (TCNQ) using a mortar and pestle, then dimethyl sulfoxide was added to faciliate the diffusion of TCNQ into the interlayer of expanded graphite, and finally the mixture was sonicated

in aqueous KOH solution (Figure 5).[36] The TCNQ anion stabilized graphene could also be dispersed in DMF and DMSO. The hybrid materials were characterized by TEM, AFM, FTIR and Raman spectroscopy.

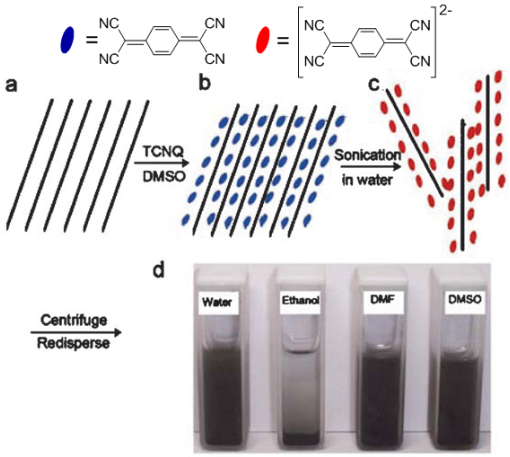

Figure 5. Preparation of aqueous graphene dispersions stabilized with the TCNQ anion and the redispersion in water, ethanol, DMF and dimethyl sulfoxide. Reproduced with permission from ref. 36. Copyright 2008 Royal Society of Chemistry.

Graphite was exfoliated in an aqueous solution of a perylene-based bolaamphiphile detergent, which yielded single-layer and few-layer graphene flakes in water by taking advantage of π-π and hydrophobic interactions between the detergent and graphene.[37] The dispersions formed were spin-coated onto silicon wafers, which were characterized by optical and Raman microscopy. AFM showed that the height of the graphene flakes have a distribution ranging from 0.5 to 2 nm. A perylene dye covalently linked to hydrophilic poly(vinyl alcohol) (PVA) chains was employed to prepare stable aqueous graphene dispersions, as demonstrated by UV/Vis absorption and Raman spectroscopy.[38] The obtained graphene dispersions were used to

fabricate transparent and flexible films. The presence of graphene dramatically increased the glass transition temperature of PVA.

Other stable aqueous graphene dispersions were prepared by sonicating graphite in the presence of 1-pyrenecarboxylic acid (PCA).[39] PCA acted as both a molecular wedge to cleave graphite layers, and also as a stabilizer to disperse graphene due to π-π interactions between the pyrene unit and graphene. Furthermore, the hydrophilic carboxylic acid groups in PCA facilitated graphene to form stable dispersion in water. The PCA functionalized graphene was used as a sensor to detect ethanol vapor, and the resistance of the functionalized graphene changed rapidly > 10000 %. This can be potentially used for breathalyzers and industrial alcohol leakage sensing. Ultracapacitors with very high specific capacitance (~ 120 F/g), power density (~ 105 kW/Kg), and energy density (~ 9.2 Wh/Kg) were also fabricated using this functionalized graphene.[39] The PCA functionalized graphene were also laminated onto flexible and transparent polydimethylsiloxane (PDMS) membranes.[40] The hybrid structure can block 70-95% of ultraviolet (UV) light, while allowing ≥ 65% transmittance in the visible region. The PCA-graphene-PDMS hybrids could potentially be used in flexible UV absorbing/filtering applications. Furthermore, the electrical resistance of these structures showed high sensitivity to visible light, pressure change and the presence of molecular analytes.

An amphiphilic pyrene was employed to exfoliate graphite into single- and bi-layer graphene flakes in aqueous solution (Figure 6).[41] The π-π interactions between the pyrene units and graphene were confirmed by UV/Vis absorption and fluorescence spectroscopy. AFM measurements indicated that the graphene flakes were composed of single-layer sheets with a thickness of ca. 2 nm. TEM and SEM images showed that the sizes of the graphene flakes are 2–4 μm in diameter. Raman spectra demonstrated that the graphene dispersions

predominantly consisted of single- and bi-layer graphene flakes. The prepared graphene films showed high transparency and conductivity. Pyrene-conjugated hyaluronan could also be used to exfoliate graphite in water with the assistance of sonication, and the hybrid material could have potential biomedical applications.[42]

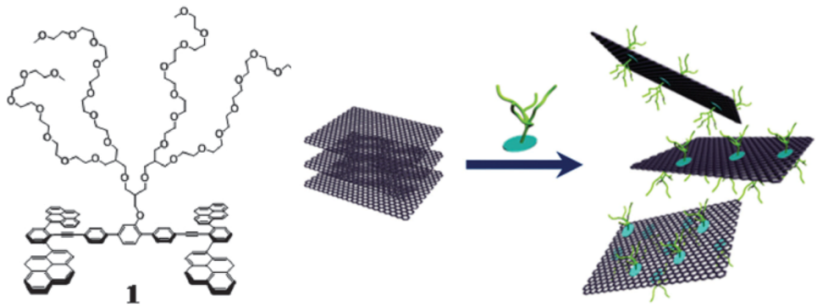

Figure 6. Exfoliation of graphite using an amphiphilic pyrene **1**. Reproduced with permission from ref. 41. Copyright 2011 Royal Society of Chemistry.

p-Phosphonic acid calix[8]arene assisted exfoliation and stabilization of graphene dispersions in water was reported by Raston and co-workers.[43] The as prepared graphene was characterized by XPS, TEM, AFM, SEM and Raman spectroscopy. Non-covalent functionalization of graphene in water using triphenylene derivatives was demonstrated by Green *et al.*[44] The obtained graphene dispersions were mixed with poly (vinyl alcohol) using a simple solution casting process. The composites showed enhanced mechanical and electrical properties at low filler fraction.

Water dispersible graphene/porphyrin hybrids were obtained by combining a positively charged pyrene derivative and negatively charged porphyrins.[45] The hybrid materials were characterized by UV and fluorescence titration experiments. Photoelectrodes were fabricated using the hybrid materials through layer by layer deposition, and a photocurrent response of up to 360 nA was achieved. CdTe quantum dots were also immobilized onto graphene to

form stable aqueous dispersions.[46] Two strategies were used to incorporate CdTe quantum dots onto graphene (Figure 7). In the first appoach, CdTe quantum dots were covalently modified with pyrene, which provided for π-π interactions with exfoliated graphite. In the second method, positively charged pyrene was used to exfoliate graphite into water, and subsequently negatively charged CdTe quantum dots were immobilized via electrostatic interactions. From spectroscopic measurements, it is evident that the degree of graphene exfoliation affected very much the electronic communication between graphene and the CdTe quantum dots. A clear transient bleach in the near-infrared region was observed in the hybrid materials.

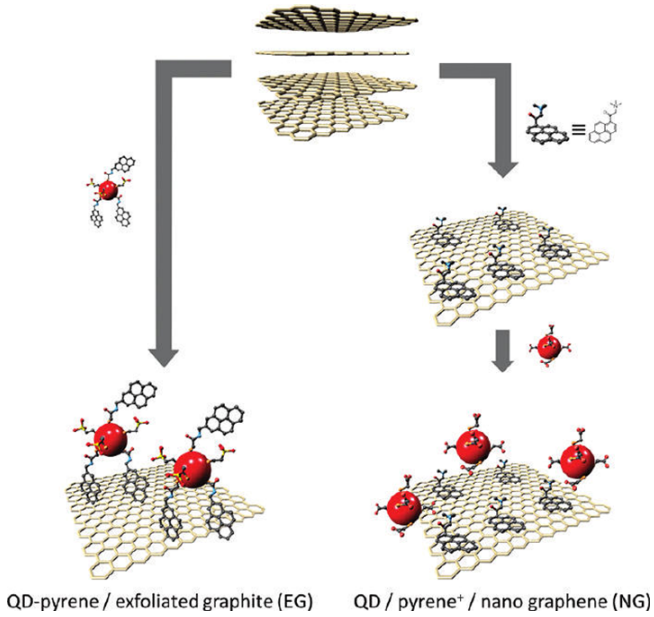

Figure 7. The two approaches to prepare graphene/CdTe quantum dots hybrid materials. Reproduced with permission from ref. 46. Copyright 2012 American Chemical Society.

In a more recent report, diazaperopyrenium dications were used to assist the direct exfoliation of graphite into graphene in aquous media.[47] The graphene

dispersions were stable for more than three weeks without precipitation. Several microscopic and spectroscopic measurements were performed to confirm the exfoliation behavior of graphene in water. Fluorescence quenching of the hybrid material indicated interactions between graphene and the diazaperopyrenium dications in the excited state.

2.4.1.2 Noncovalent functionalization of graphene in organic media

Graphite can be exfoliated in NMP using both porphyrins and ammonium ions.[48] The proposed mechanism is that first a ammonium ion intercalates the interlayer of graphite followed by porphyrin induced exfoliation. The graphene/porphyrin hybrid materials were characterized by TEM, AFM, FTIR, UV/Vis absorption and Raman spectroscopy. A zinc phthalocyanine-poly(*p*-phenylene vinylene) oligomer was used to exfoliate graphite forming stable graphene dispersions in THF.[49] The functionalized graphene was characterized by TEM, UV/Vis absorption and Raman spectroscopy. Transient absorption measurements indicated electron transfer from zinc phthalocyanine to graphene took place upon excitation. Using a similar method, the same group also prepared porphycenes/graphene hybrids, which were studied by TEM, UV/Vis absorption, FL and Raman spectroscopy.[50] Time-resolved photophysical measurements confirmed electron transferred from graphene to porphycenes, which is the first report on the electron donating features of graphene in solution. Dye-sensitized solar cells (DSSCs) was also tested using the porphycenes/graphene hybrids, which led to an improved device performance due to the efficient electron transfer process from graphene to porphycene and finally to the ZnO photoanode.

Phthalocyanines and porphyrins bearing four pyrene units were used to form donor-acceptor hybrids with graphene through π-π interactions (Figure 8).[51] Femtosecond transient absorption spectroscopy indicated that ultrafast charge separation and relatively slow charge recombination processes occurred.

Noncovalent functionalization of graphene in NMP using dendronized perylene bisimides was reported by Hirsch and co-workers.[52] The electronic interactions between graphene and dendronized perylene bisimides were confirmed by fluorescence quenching.

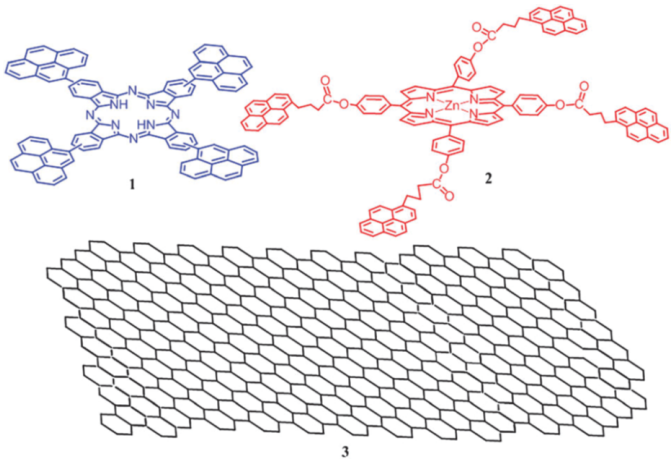

Figure 8. Chemical structures of phthalocyanine and porphyrin bearing four pyrene units. Reproduced with permission from ref. 51. Copyright 2012 Royal Society of Chemistry.

Benzylamine-assisted noncovalent exfoliation of graphite in isopropyl/water mixture was reported by Kuo et al.[53] The exfoliated graphene, with a low defect content, was characterized by TEM and Raman spectroscopy. Platinum nanoparticles were anchored to the graphene with benzylamine as a stabilizer. The graphene/platinum hybrids were used as electrode material, which showed increase catalytic activity toward methanol oxidation compared with commercial electrodes. A similar system composed of graphene/1-pyrenamine/platinum was developed.[54,55] The hybrid materials exhibited higher electrocatalytic activity (1.4 times) and stability (3.5 times) toward methanol oxidation than commercial Pt/Vulcan XC-72R catalysts. Melamine was also used to exfoliate graphite using a ball-milling method.[56] The graphene flakes

were characterized by XPS, TEM, UV/Vis absorption and Raman spectroscopy, indicating that few-layer graphene flakes with low defects were prepared. The dispersions were stable in water and DMF for weeks.

1-Cyanoethyl-2-ethyl-4-methylimidazole was employed as a stabilizer for graphene dispersions in acetonitrile and also acted as a reducing agent for silver to enable silver nanoparticles to deposit on graphene flakes.[57] Highly conductive epoxy-based composites were prepared by using the graphene/silver nanoparticles obtained as a nanoscale filler. Non-covalent functionalized graphene using 1-pyrenebutyric acid was incorporated into the epoxy matrix, and the nanocomposites showed enhanced mechanical properties and thermal conductivity due to the homogeneous dispersibility and compatibility of graphene with the polymer matrix.[58]

Poly(fluorene-*alt*-phenylene) appended with redox-active anthraquinone moieties and graphene hybrid materials, obtained with the help of mild sonication in NMP, were reported by Segura and co-workers.[59] The presence of the conjugated polymer was confirmed by UV/Vis absorption spectroscopy. The interactions between the polymer and graphene were characterized by fluorescence quenching and the anodic shift of the reduction potential of anthraquinone as described by cyclic voltammetry (0.81 V). Oligothiophene-terminated poly(ethylene glycol) was used to exfoliate graphite to yield graphene in ethanol.[60] Graphene films were fabricated from the exfoliated graphene dispersions by vacuum filtration. The film shows high performance with a sheet resistance of 0.3 $k\Omega\ sq^{-1}$ and a transparency of 74% at 550 nm after being treated with nitric acid and thionyl chloride. Nitric acid and thionyl chloride were used to remove the surfactant residues, and also increase the transmittance and conductivity of the graphene films. Water-soluble polymer functionalized graphene dispersions in dimethyl sulfoxide were prepared by Wang and co-workers.[61] The polyvinyl pyrrolidone (PVP)/graphene based

catalyst showed better methanol oxidation performance than the prepared PVP/reduced graphene oxide catalyst. Poly(4-vinylpyridine)/graphene hybrids were also prepared and showed a stable and reversible response to pH change, which could potentially be used in sensors. Pyrene-based amphiphilic block copolymer exfoliated graphene in aqueous and organic media was also reported.[62] The as prepared graphene/polymer composites showed enhanced tensile strength compared with pristine graphene.

2.4.2 Functionalization of graphene using covalent methods

Covalent functionalization of graphene has recently seen increased attention, as it potentially provides more stable and robust hybrid materials compared with noncovalent functionalized graphene. Covalently functionalized graphene can also be used for subsequent chemical processes, which are incompatible with noncovalently functionalized graphene. Although the chemical reactivity of graphene is less than that of fullerenes and carbon nanotubes, the wrinkled and folded structure and defects present in graphene can increase its reactivity towards organic reagents.[63,64]

2.4.2.1 1,3-Dipolar cycloaddition

The 1,3-dipolar cycloaddition reaction was performed previously on fullerenes and carbon nanotubes.[65] Recently, it was also successfully applied to graphene.[66-68] Georgakilas and co-workers prepared hydroxyl functionalized graphene by reacting graphene with *N*-methyl-glycine and 3,4-dihydroxybenzaldehyde in a mixture of pyridine/DMF.[66] The increased D to G band ratio in the Raman spectra indicate the successful functionalization of graphene. The functionalization degree was estimated to be one functional group per 40 carbon atoms. The hydroxyl functionalized graphene showed good dispersibility in ethanol and DMF. Using gold nanorods as an indicator,

Prato and co-workers demonstrated that the 1,3-dipolar cycloaddition reaction can occur both on the edges and basal plane of graphene (Figure 9).[67]

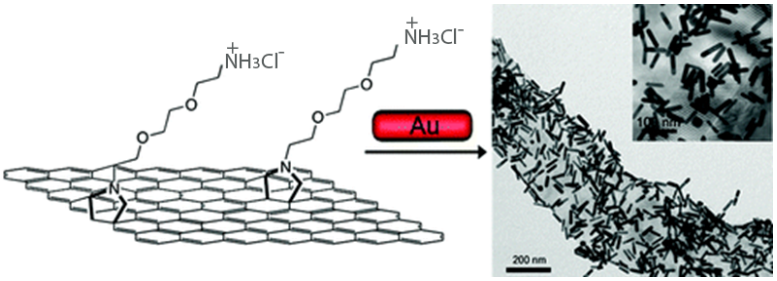

Figure 9. 1,3-Dipolar cycloaddition functionalized graphene derivatives with amino groups can selectively bind to gold nanorods. Reproduced with permission from ref. 67. Copyright 2010 American Chemical Society.

Photoactive materials such as porphyrins and Pd (II)-porphyrin were chemically attached onto graphene by Feringa et al (Figure 10).[68] The presence of porphyrin was confirmed by UV/Vis spectroscopy and XPS. Fluorescence and phosphorescence quenching together with decreased excited state lifetimes indicate that energy- and/or electron-transfer quenching between graphene and the covalently bound porphyrins occurs. The relatively low content of prophyrin in the hydrids is benefical to retain the inherent properties of graphene. The hybrid materials could be potentially used in electrochemical cells and catalysis.[69]

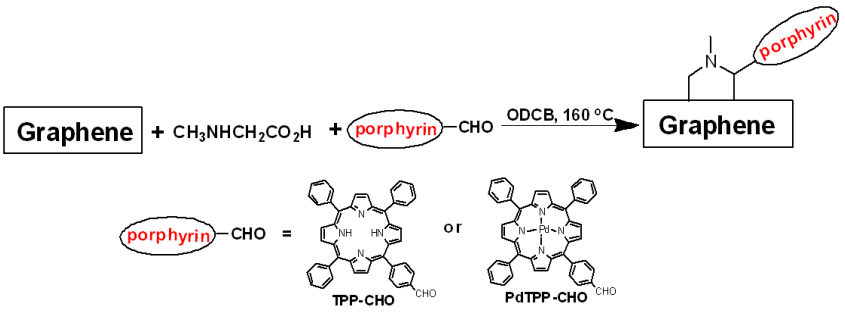

Figure 10. Synthesis of graphene-porphyrin hybrids (ref. 68).

Later on, Guldi *et al.* reported that phthalocyanines were chemically linked to graphene using a similar method.[70] Physicochemical measurements revealed an ultrafast charge separation from the phthalocyanines to graphene followed by a slower charge recombination. Triphenylamine functionalized graphene was also prepared and modified with platinum nanoparticles.[71] The hybrid materials was used as a photocatalyst for H_2 evolution.

2.4.2.2 Zwitterion cycloaddtion

Functionalized graphene can also be obtained through a zwitterion intermediate cycloaddition approach on solvent dispersed graphene flakes as shown by Feringa and co-workers.[72] 4-Dimethylaminopyridine (DMAP) adds to the triple bond of acetylene dicarboxylates to form a zwitterionic intermediate, which then reacts with a double bond of graphene followed by reaction with the carbonyl group. Finally, the positively charged DMAP moiety is substituted by an alkoxy group, yielding the functionalized graphene product (Figure 11). The functionalized graphene obtained formed stable dispersions in common solvents, including DMF, $CHCl_3$ and water. Its dispersion in water is especially useful in a wide range of areas, such as composites, devices and biological applications.

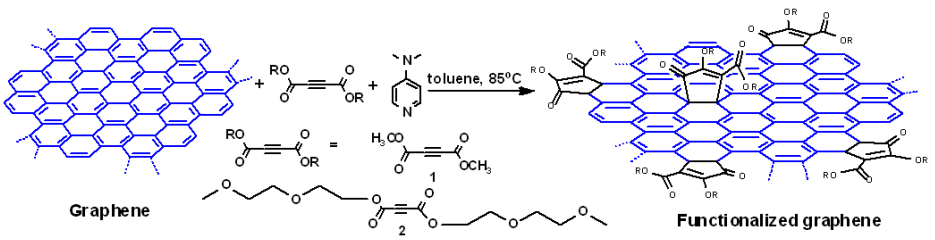

Figure 11. Preparation of functionalized graphene using a zwitterion cycloaddition approach (ref. 72).

2.4.2.3 Nitrene addition

Barron and co-workers reported the functionalization of exfoliated graphene using azido-phenylalanine by doing a nitrene addition.[73] The degree of functionalization of the covalently modified graphene flakes is 1 phenylalanine substituent per 13 carbons as determined by X-ray photoelectron spectroscopy (XPS). The functionalization took place on the edges and basal plane of graphene. Valiyaveettil et al. demonstrated functionalization of surfactant/graphene flakes using alkyl azides.[74] The alkyl functionalized graphene showed enhanced dispersibility in acetone and toluene. The free carboxylic acid groups at the end of alkyl chains can be used to bind gold nanoparticles, which acted as markers for the reactive sites on graphene.

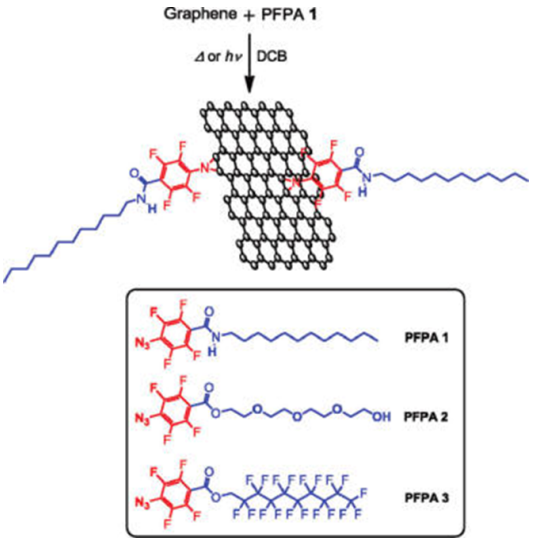

Figure 12. Fuctionalization of graphene with perfluorophenylazides using nitrene addition. Reproduced with permission from ref. 75. Copyright 2010 American Chemical Society.

Perfluorophenylazides were reacted with graphene by photochemical or thermal activation (Figure 12).[75] Alkyl, ethylene oxide or perfluoroalkyl groups

were attached to graphene, which provided either organic or water dispersible graphene. In a recent report by Li and co-workers,[76] graphene was functionalized with tetraphenylethylene by nitrene addition and the obtained functionalized graphene showed good dispersion stability in both polar and apolar solvents.

2.4.2.4 Nucleophilic addition

A zinc phthalocyanine−graphene hybrid material was prepared by Tagmatarchis and co-workers using nucleophilic addition of primary amines to exfoliated graphene (Figure 13), which was obtained by sonication in ODCB.[77]

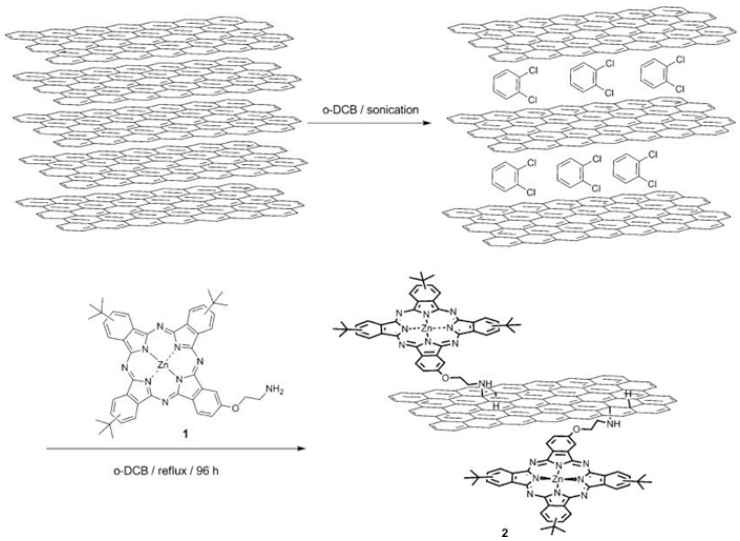

Figure 13. Covalent functionalization of graphene with zinc phthalocyanine using nucleophilic addition. Reproduced with permission from ref. 77. Copyright 2012 American Chemical Society.

The hybrid material was stable in common organic solvents without precipitation for several weeks. The degree of functionalization of the hybrid was 1 zinc phthalocyanine per 518 carbon atoms determined by TGA. Spectroscopic studies indicate that electronic interaction occurs between

graphene and phthalocyanine both in the ground and excited state. The zinc phthalocyanine-graphene hybrid was used as a photoanode in a photoelectrochemical cell, which showed a prompt, stable, and reproducible photocurrent.

2.4.2.5 Bingel reaction

Highly functionalized graphene can also be obtained using the Bingel reaction, in which cyclopropanated malonates covalently attach to the double bond of the graphene lattice.[78] In this case, graphene flakes were prepared by sonication of graphite in benzylamine. Then the exfoliated graphene flakes were reacted with bromo-malonates in the presence of 1,8-diazabicycloundec-7-ene (DBU) under microwave irradiation conditions (Figure 14). The functionalized graphene materials form stable dispersions in common organic solvents and were characterized by several spectroscopic and microscopy techniques. The authors also pointed out that the choice of solvent for the reaction is crucial for the production of functionalized graphene. This method was used to link redox-active tetrathiafulvalene (TTF) units covalently to graphene. Electrochemical measurements indicated the formation of a radical ion pair between graphene and TTF.

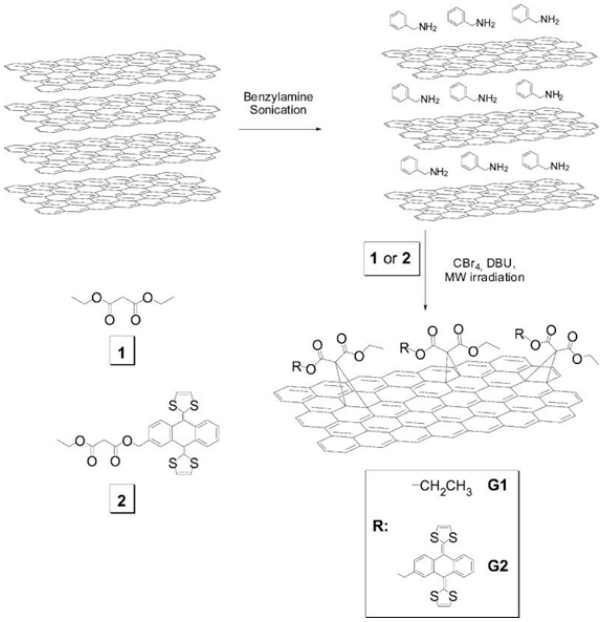

Figure 14. Preparation of functionalized graphene using Bingel reaction. Reproduced with permission from ref. 78. Copyright 2010 American Chemical Society.

In a recent report, TEMPO radicals were covalently attached on graphene using the Bingel reaction.[79] The TEMPO radical modified graphene was characterized by TGA, Raman, XPS and also electron paramagnetic resonance (EPR) measurements. Transport measurements indicate that the properties of graphene were affected by the density of radicals attached. A low field magnetoresistance (LFMR) effect was also observed at low temperatures for the hybrid material.

2.4.2.6 Radical addition

Radical addition of perfluorinated alkyl iodides to graphene was performed under thermal or UV photolysis conditions.[80] Graphene flakes was prepared by sonication graphite in ODCB. The perfluorinated functionalized graphene was characterized by XPS, Raman and AFM measurements, and also showed

enhanced dispersibility in $CHCl_3$. Polystyrene functionalized graphene can be obtained by sonication of graphite in styrene via a one step sonochemically initiated radical polymerization.[81] The successful functionalization of graphene with polystyrene was confirmed by XPS, FTIR and Raman spectroscopy. The morphology of both graphene and functionalized graphene was characterized by AFM, TEM and SEM. The content of polystyrene in the functionalized graphene is about 18%, as determined by TGA. The graphene-polystyrene hybrid material forms stable dispersions for several months in common organic solvents, such as DMF, THF, toluene, and chloroform, which provides potential for their use in graphene-based composites materials.

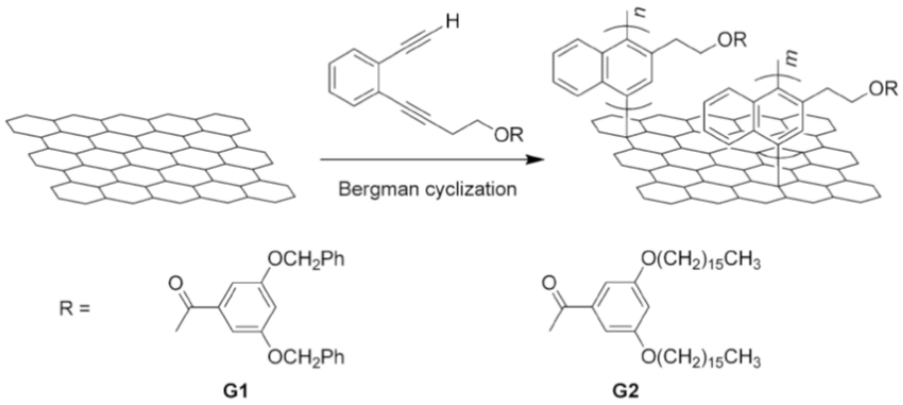

Figure 15. Functionalization of exfoliated graphene using Bergman cyclization. Reproduced with permission from ref. 82. Copyright 2012 Wiley.

Another example of graphene-polymer hybrid was prepared using Bergman cyclization.[82] Enediyne-containing dendrimers were reacted with graphene in NMP through addition and propagation of diradicals, which formed conjugated polymers on graphene (Figure 15). The functionalized graphene was characterized with AFM, FTIR and Raman spectroscopy. The degree of functionalization was 1 functional group per ~ 960 carbon atoms according to TGA. The low degree of functionalization of graphene allows the sp^2 structure

of graphene to be preserved, which results in good electrical conductivity of the functionalized graphene. The graphene-polymer products form stable dispersions in NMP, DMF, ODCB, THF, chloroform, toluene and ethyl acetate.

2.4.2.7 Click chemistry

The click reaction on graphene was reported by Strano and co-workers.[83] Graphene flakes were prepared by sonication of graphite in sodium cholate solution. Alkyne terminated groups were then introduced onto graphene via a diazonium reaction (Figure 16). Subsequently, polyethylene glycol chains were attached onto graphene using the azide–alkyne cycloaddition reaction. The functionalized graphene was characterized by FTIR and Raman spectroscopy. It forms stable dispersions in water after dialysis to remove the surfactant. The functionalized graphene dispersions also show increased zeta-potential and surface tension compared to pristine graphene dispersions. Raman mapping suggested that edges and defects are the preferred reactive sites.

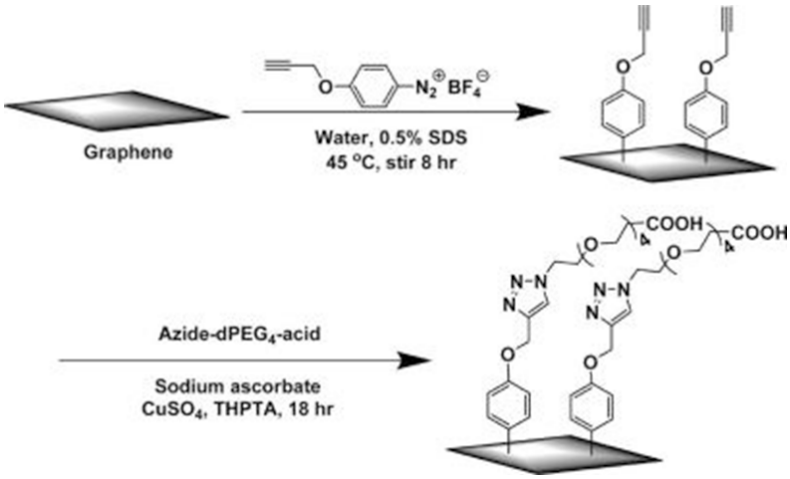

Figure 16. Functionalization of graphene using the diazonium reaction and subsequent click reaction. Reproduced with permission from ref. 83. Copyright 2011 American Chemical Society.

2.4.2.8 Hydrogenation

Graphite powder was hydrogenated using lithium in liquid ammonia with *tert*-butyl alcohol as the source of protons (Figure 17).[84] The hydrogenated graphene was highly exfoliated, which was characterized by XRD, AFM and electron microscopy. The chemical composition of the hydrogenated graphene was expressed as $(C_{1.3}H)_n$ determined by elemental analysis. Electron energy loss spectroscopy mapping studies showed that both the basal plane and edges of graphene were covered by hydrogen. UV/Vis absorption spectroscopy of the hydrogenated graphene indicated a large band gap of ~4 eV. Using a similar method, Hirsch and co-workers reported the preparation of polyhydrogenated graphene by reacting graphite in NH_3/ND_3 with Li, using H_2O/D_2O as the quenching reagents.[85] The polyhydrogenated graphene was characterized by TGA, ^{13}C NMR, XPS, FTIR and Raman spectroscopy. The exfoliation of the functionalized graphene was confirmed by AFM. The polyhydrogenated graphene showed strong fluorescence, indicating that isolated and electronically decoupled domains of π-conjugated regions are formed.

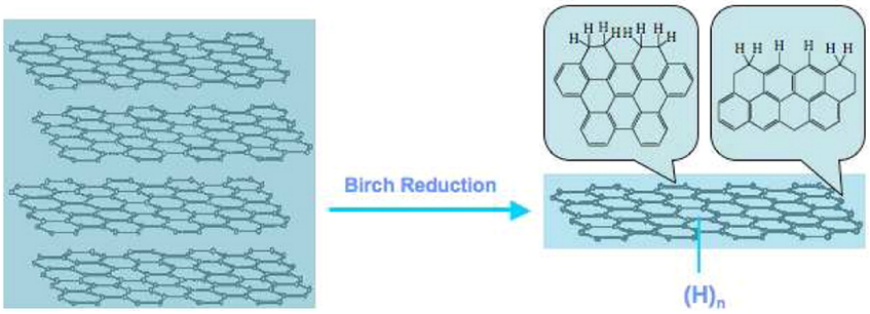

Figure 17. Chemical hydrogenation of graphene. Reproduced with permission from ref. 84. Copyright 2012 American Chemical Society.

Table 2 summarizes the various methods and conditions used for the covalent functionalization of graphene.

Table 2. Comparison of approaches to covalent functionalization of graphene

Ref.	Graphene materials	Reagents	Methods	Temperature /Time	Characterization techniques	Functionali-zation degree
66	Graphene in pyridine/DMF	*N*-methyl-glycine and 3,4-dihydroxybenzaldehyde	1,3-Dipolar cycloaddition	145–150 °C 96 h	TEM, AFM, Raman, TGA, FTIR and UV	Every 40 carbon atoms
67	Graphene in NMP	Paraformaldehyde and modified α-amino acid	1,3-Dipolar cycloaddition	125 °C/5 d	TEM, Raman, XPS, TGA and UV	Every 128 carbon atoms
68	Graphene in ODCB	Sarcosine and aldehyde porphyrins	1,3-Dipolar cycloaddition	160 °C/7 d	UV, TGA, XPS, FTIR, Raman, TEM, emission and lifetime measurements	Every ~ 240 carbon atoms
72	Graphene in toluene	DMAP and acetylene dicarboxylates	Zwitterion cycloaddition	85 °C/3 d	FTIR, TGA, TEM, Raman and control	Every ~ 10 or ~ 50 carbon atoms
73	Graphene in ODCB	Azido-phenylalanine	Nitrene addition	165 °C/4 d	TEM, AFM, Raman, STEM, TGA, IR and XPS	Every 13 carbon atoms
77	Graphene in ODCB	(2-aminoethoxy)(tri-*tert*-butyl) zinc phthalocyanine	Nucleophilic addition	120 °C/96 h	TEM, AFM, DLS, Raman, TGA, UV, emission, time-resolved transient absorption, EPR and photoelectrochemical measurements	Every 518 carbon atoms
78	Graphene in benzylamine	Bromo-malonates and DBU	Bingel reaction	130 °C/180 s	Raman, TGA, TEM, UV, IR and cyclic voltammetry	Every ~ 44 or ~ 198 carbon atoms
82	Graphene in NMP	Enediyne-containing dendrimers	Bergman cyclization	Reflux/16 h	TGA, FTIR, Raman, AFM and DSC	Every ~ 940 or ~ 980 carbon atoms

83	Graphene in water/SDS	4-propargyloxybenzene-diazonium tetrafluoroborate and azido-PEG-COOH	Diazonium reaction and click chemistry	45 °C/8 h, RT/18 h	FTIR, UV, zeta-potential and Raman	—
84	Graphite/ lithium in liquid ammonia	*tert*-Butyl alcohol	Birch reduction	-78 °C/1 h, -33 °C /4 h	Raman, FTIR, TGA, NMR, UV, XPS, elemental analysis, XRD, AFM, SEM and TEM	$(C_{1.3}H)_n$

— data not available

2.5. Conclusions and future aspects

The preparation of graphene using the solvent dispersion method has already seen impressive progress during the last five years. Single- and few-layer graphene flakes with relatively small size can be prepared in various solvents. Toward future improvements of the solvent dispersion method of graphene, the preparation of graphene with large size and low content of defects is highly desirable. Also, developing new mild and effective method to exfoliate graphite to graphene is appealing. Controlling the nature of the graphene flakes and selecting graphene flakes with uniform thickness and size, and avoiding of contamination are important aspects for device applications.

The functionalization of graphene using noncovalent and covalent approaches has seen major developments over the past decade, especially combining graphene with functional molecules bearing photoactive or redox active units. However, functionalization of graphene is still immature. For the noncovalent functionalization of graphene, methodology for understanding the charge transfer process and the spatial distribution of charge carriers will be fundamentally important to further design novel graphene-based hybrid materials.

Covalent functionalization on graphene may affect the electronic properties of graphene. Therefore, controlling the degree of functionalization of graphene is

important for graphene-based device applications. Site selective functionalized graphene, for example, edge selective functionalized graphene, is expected to preserve the intrinsic properties of graphene and at the same time may introduce novel properties to these hybrid materials. On the other hand, incorporating covalently functionalized graphene into polymers or other matrices is expected to allow nanocomposites with enhanced mechanical, electrical and thermal properties to be fabricated. In particular, milder approaches to covalent functionalization of graphene still need to be developed to broaden the chemistry of graphene and their applications.

2.6. Notes and references

1. A. K. Geim and K. S. Novoselov, The rise of graphene, *Nat. Mater.,* 2007, **6**, 183.

2. A. K. Geim, Graphene: status and prospects. *Science*, 2009, **324**, 1530.

3. K. S. Novoselov, V. I. Falko, L. Colombo, P. R. Gellert, M. G. Schwab and K. Kim, A roadmap for graphene, *Nature*, 2012, **490**, 192.

4. K. S. Novoselov, A. K. Geim, S. V. Morozov, D. Jiang, Y. Zhang, S. V. Dubonos, I. V. Grigorieva and A. A. Firsov, Electric field effect in atomically thin carbon films, *Science*, 2004, **306**, 666.

5. C. Berger, Z. M. Song, T. B. Li, X. B. Li, A. Y. Ogbazghi, R. Feng, Z. T. Dai, A. N. Marchenkov, E. H. Conrad, P. N. First and W. A. de Heer, Ultrathin epitaxial graphite: 2D electron gas properties and a route toward graphene-based nanoelectronics, *J. Phys. Chem. B*, 2004, **108**, 19912.

6. K. S. Kim, Y. Zhao, H. Jang, S. Y. Lee, J. M. Kim, K. S. Kim, J.-H. Ahn, P. Kim, J.-Y. Choi and B. H. Hong, Large-scale pattern growth of graphene films for stretchable transparent electrodes, *Nature*, 2009, **457**, 706.

7. X. Li, W. Cai, J. An, S. Kim, J. Nah, D. Yang, R. Piner, A. Velamakanni, I. Jung, E. Tutuc, S. K. Banerjee, L. Colombo and R. S. Ruoff, Large-area synthesis of high-quality and uniform graphene films on copper foils, *Science*, 2009, **324**, 1312.

8. S. Pei and H.-M. Cheng, The reduction of graphene oxide, *Carbon*, 2012, **50**, 3210.

9. J. N. Coleman, Liquid exfoliation of defect-free graphene, *Acc. Chem. Res.*, 2013, **46**, 14.

10. Y. Hernandez, V. Nicolosi, M. Lotya, F. M. Blighe, Z. Y. Sun, S. De, I. T. McGovern, B. Holland, M. Byrne, Y. K. Gun'ko, J. J. Boland, P. Niraj, G. Duesberg, S. Krishnamurthy, R. Goodhue, J. Hutchison, V. Scardaci, A. C. Ferrari and J. N. Coleman, High-yield production of graphene by liquid-phase exfoliation of graphite, *Nat. Nanotechnol.*, 2008, **3**, 563.

11. A. C. Ferrari, J. C. Meyer, V. Scardaci, C. Casiraghi, M. Lazzeri, F. Mauri, S. Piscanec, D. Jiang, K. S. Novoselov, S. Roth and A. K. Geim, Raman spectrum of graphene and graphene layers, *Phys. Rev. Lett*., 2006, **97**, 187401.

12. M. A. Pimenta, G. Dresselhaus, M. S. Dresselhaus, L. G. Cancado, A. Jorio and R. Saito, Studying disorder in graphite-based systems by Raman spectroscopy, *Phys. Chem. Chem. Phys.*, 2007, **9**, 1276.

13. P. Blake, P. D. Brimicombe, R. R. Nair, T. J. Booth, D. Jiang, F. Schedin, L. A. Ponomarenko, S. V. Morozov, H. F. Gleeson, E. W. Hill, A. K. Geim and K. S. Novoselov, Graphene-based liquid crystal device, *Nano Lett*., 2008, **8**, 1704.

14. C. E. Hamilton, J. R. Lomeda, Z. Z. Sun, J. M. Tour and A. R. Barron, High-yield organic sispersions of unfunctionalized graphene, *Nano Lett*., 2009, **9**, 3460.

15. A. B. Bourlinos, V. Georgakilas, R. Zboril, T. A. Steriotis and A. K. Stubos, Liquid-phase exfoliation of graphite towards solubilized graphenes, *Small*, 2009, **5**, 1841.

16. X. Q. Wang, P. F. Fulvio, G. A. Baker, G. M. Veith, R. R. Unocic, S. M. Mahurin, M. F. Chi and S. Dai, Direct exfoliation of natural graphite into micrometre size few layers graphene sheets using ionic liquids, *Chem. Commun*., 2010, **46**, 4487.

17. Y. Hernandez, M. Lotya, D. Rickard, S. D. Bergin and J. N. Coleman, Measurement of multicomponent solubility parameters for graphene facilitates solvent discovery, *Langmuir*, 2010, **26**, 3208.

18. U. Khan, A. O'Neill, M. Lotya, S. De and J. N. Coleman, High-concentration solvent exfoliation of graphene, *Small*, 2010, **6**, 864.

19. D. Nuvoli, L. Valentini, V. Alzari, S. Scognamillo, S. B. Bon, M. Piccinini, J. Illescas and A. Mariani, High concentration few-layer graphene sheets obtained by liquid phase exfoliation of graphite in ionic liquid, *J. Mater. Chem.*, 2011, **21**, 3428.

20. W. W. Liu and J. N. Wang, Direct exfoliation of graphene in organic solvents with addition of NaOH, *Chem. Commun.*, 2011, **47**, 6888.

21. W. C. Du, J. Lu, P. P. Sun, Y. Y. Zhu and X. Q. Jiang, Organic salt-assisted liquid-phase exfoliation of graphite to produce high-quality graphene, *Chem. Phys. Lett.*, 2013, **568–569**, 198–201.

22. W. T. Gu, W. Zhang, X. M. Li, H. W. Zhu, J. Q. Wei, Z. Li, Q. Shu, C. Wang, K. Wang, W. Shen, F. Kang and D. Wu, Graphene sheets from worm-like exfoliated graphite, *J. Mater. Chem.*, 2009, **19**, 3367.

23. B. Jiang, C. Tian, L. Wang, Y. Xu, R. Wang, Y. Qiao, Y. Ma and H. Fu, Facile fabrication of high quality graphene from expandable graphite: simultaneous exfoliation and reduction, *Chem. Commun.*, 2010, **46**, 4920.

24. W. F. Zhao, M. Fang, F. R. Wu, H. Wu, L. W. Wang, and G. H. Chen, Preparation of graphene by exfoliation of graphite using wet ball milling, *J. Mater. Chem.*, 2010, **28**, 5817.

25. D. Rangappa, K. Sone, M. Wang, U. K. Gautam, D. Golberg, H. Itoh, M. Ichihara and I. Honma, Rapid and direct conversion of graphite crystals into high-yielding, good-quality graphene by supercritical fluid exfoliation, *Chem. Eur. J.*, 2010, **16**, 6488.

26. X. Chen, J. F. Dobson and C. L. Raston, Vortex fluidic exfoliation of graphite and boron nitride, *Chem. Commun.*, 2012, **48**, 3703.

27. N. G. Shang, P. Papakonstantinou, S. Sharma, G. Lubarsky, M. Li, D. W. McNeill, A. J. Quinn, W. Zhou and R. Blackley, Controllable selective exfoliation of high-quality graphene nanosheets and nanodots by ionic liquid assisted grinding, *Chem. Commun.*, 2012, **48**, 1877.

28. M. Lotya, Y. Hernandez, P. J. King, R. J. Smith, V. Nicolosi, L. S. Karlsson, F. M. Blighe, S. De, Z. M. Wang, I. T. McGovern, G. S. Duesberg and J. N. Coleman, Liquid phase production of graphene by exfoliation of graphite in surfactant/water solutions, *J. Am. Chem. Soc.*, 2009, **131**, 3611.

29. S. De, P. J. King, M. Lotya, A. O'Neill, E. M. Doherty, Y. Hernandez, G. S. Duesberg and J. N. Coleman, Flexible, transparent, conducting films of randomly stacked graphene from surfactant-stabilized, oxide-free graphene dispersions, *Small*, 2010, **6**, 458.

30. M. Lotya, P. J. King, U. Khan, S. De and J. N. Coleman, High-concentration, surfactant-stabilized graphene dispersions, *ACS Nano*, 2010, **4**, 3155.

31. S. M. Notley, Highly concentrated aqueous suspensions of graphene through ultrasonic exfoliation with continuous surfactant addition, *Langmuir*, 2012, **28**, 14110.

32. V. Chabot, B. Kim, B. Sloper, C. Tzoganakis and A. P. Yu, High yield production and purification of few layer graphene by Gum Arabic assisted physical sonication, *Sci. Rep.*, 2013, **3**, 1378.

33. A. A. Green and M. C. Hersam, Emerging methods for producing monodisperse graphene dispersions. *J. Phys. Chem. Lett.*, 2010, **1**, 544.

34. A. A. Green and M. C. Hersam, Solution phase production of graphene with controlled thickness via density differentiation, *Nano Lett.*, 2009, **9**, 4031.

35. X. Y. Zhang, A. C. Coleman, N. Katsonis, W. R. Browne, B. J. van Wees and B. L. Feringa, Dispersion of graphene in ethanol using a simple solvent exchange method, *Chem. Commun.*, 2010, **46**, 7539.

36. R. Hao, W. Qian, L. Zhang and Y. Hou, Aqueous dispersions of TCNQ-anion-stabilized graphene sheets, *Chem. Commun.*, 2008, 6576.

37. J. M. Englert, J. Röhrl, C. D. Schmidt, R. Graupner, M. Hundhausen, F. Hauke and A. Hirsch, Soluble graphene: generation of aqueous graphene solutions aided by a perylenebisimide-based bolaamphiphile. *Adv. Mater.*, 2009, **21**, 4265.

38. H. J. Salavagione, G. Ellis, J. L. Segura, R. Gomez, G. M. Morales and G. Martinez, Flexible film materials from conjugated dye-modified polymer surfactant-induced aqueous graphene dispersions, *J. Mater. Chem.*, 2011, **21**, 16129.

39. X. An, T. Simmons, R. Shah, C. Wolfe, K. M. Lewis, M. Washington, S. K. Nayak, S. Talapatra and S. Kar, Stable aqueous dispersions of noncovalently functionalized graphene from graphite and their multifunctional high-performance applications, *Nano Lett.*, 2010, **10**, 4295.

40. X. An, T. W. Butler, M. Washington, S. K. Nayak and S. Kar, Optical and sensing properties of 1-pyrenecarboxylic acid-functionalized graphene films laminated on polydimethylsiloxane membranes, *ACS Nano*, 2011, **5**, 1003.

41. D.-W. Lee, T. Kim and M. Lee, An amphiphilic pyrene sheet for selective functionalization of graphene, *Chem. Commun.*, 2011, **47**, 8259.

42. F. Zhang, X. J. Chen, R. A. Boulos, F. M. Yasin, H. B. Lu, C. Raston, and H. B. Zhang, Pyrene-conjugated hyaluronan facilitated exfoliation and

stabilisation of low dimensional nanomaterials in water, *Chem. Commun.* 2013, **49**, 4845.

43. X. J. Chen, R. A. Boulos, P. K. Eggers and C. L. Raston, *p*-Phosphonic acid calix[8]arene assisted exfoliation and stabilization of 2D materials in water, *Chem. Commun.*, 2012, **48**, 11407.

44. S. Das, F. Irin, H. S. Tanvir Ahmed, A. B. Cortinas, A. S. Wajid, D. Parviz, A. F. Jankowski, M. Kato and M. J. Green, Non-covalent functionalization of pristine few-layer graphene using triphenylene derivatives for conductive poly (vinyl alcohol) composites, *Polymer*, 2012, **53**, 2485.

45. J. Malig, C. Romero-Nieto, N. Jux and D. M. Guldi, Integrating water–soluble graphene into porphyrin nanohybrids, *Adv. Mater.*, 2012, **24**, 800.

46. G. Katsukis, J. Malig, C. Schulz-Drost, S. Leubner, N. Jux and D. M. Guldi, Toward combining graphene and QDs: assembling CdTe QDs to exfoliated graphite and nanographene in water, *ACS Nano*, 2012, **6**, 1915.

47. S. Sampath, A. N. Basuray, K. J. Hartlieb, T. Aytun, S. I. Stupp and J. F. Stoddart, Direct exfoliation of graphite to graphene in aqueous media with diazaperopyrenium dications, *Adv. Mater.*, 2013, **25**, 2740.

48. J. Geng, B. S. Kong, S. B. Yang and H. T. Jung, Preparation of graphene relying on porphyrin exfoliation of graphite, *Chem. Commun.*, 2010, **46**, 5091.

49. J. Malig, N. Jux, D. Kiessling, J.-J. Cid, P. Vázquez, T. Torres and D. M. Guldi, Towards tunable graphene/phthalocyanine–PPV hybrid systems, *Angew. Chem., Int. Ed.*, 2011, **50**, 3561.

50. R. D. Costa, J. Malig, W. Brenner, G. Katsukis, N. Jux and D. M. Guldi, Electron accepting porphycenes on graphene, *Adv. Mater.*, 2013, **25**, 2600.

51. C. B. K. C., S. K. Das, K. Ohkubo, S. Fukuzumi and F. D'Souza, Ultrafast charge separation in supramolecular tetrapyrrole–graphene hybrids, *Chem. Commun.*, 2012, **48**, 11859.

52. N. V. Kozhemyakina, J. M. Englert, G. Yang, E. Spiecker, C. D. Schmidt, F. Hauke and A. Hirsch, Non-covalent chemistry of graphene: electronic communication with dendronized perylene bisimides, *Adv. Mater.*, 2010, **22**, 5483.

53. C.-H. Hsu, H.-Y. Liao, Y.-F. Wu, and P.-L. Kuo, Benzylamine-assisted noncovalent exfoliation of graphite-protecting Pt nanoparticles applied as catalyst for methanol oxidation, *ACS Appl. Mater. Interfaces*, 2011, **3**, 2169.

54. X. Zheng, Q. Xu, J. Li, L. Li and J. Wei, High-throughput, direct exfoliation of graphite to graphene via a cooperation of supercritical CO_2 and pyrene-polymers, *RSC Adv.*, 2012, **2**, 10632.

55. L. H. Li, J. N. Zhang, Y. Q. Liu, W. M. Zhang, H. X. Yang, J. Chen and Q. Xu, Facile fabrication of Pt nanoparticles on 1-pyrenamine functionalized graphene nanosheets for methanol electrooxidation, *ACS Sustainable Chem. Eng.*, 2013, **1**, 527.

56. V. León, M. Quintana, M. A. Herrero, J. L. G. Fierro, A. d. l. Hoz, M. Prato and E. Vazquez, Few-layer graphenes from ball-milling of graphite with melamine, *Chem. Commun.*, 2011, **47**, 10936.

57. K. Liu, L. Liu, Y. Luo and D. Jia, One-step synthesis of metal nanoparticle decorated graphene by liquid phase exfoliation, *J. Mater. Chem.*, 2012, **22**, 20342.

58. S. H. Song, K. H. Park, B. H. Kim, Y. W. Choi, G. H. Jun, D. J. Lee, B.-S. Kong, K.-W. Paik and S. Jeon, Enhanced thermal conductivity of epoxy-graphene composites by using non-oxidized graphene flakes with non-covalent functionalization. *Adv. Mater.*, 2013, **25**, 732.

59. M. Castelaín, H. J. Salavagione, R. Gómez and J. L. Segura, Supramolecular assembly of graphene with functionalized poly(fluorene-*alt*-phenylene): the role of the anthraquinone pendant groups. *Chem. Commun.*, 2011, **47**, 7677.

60. M. S. Kang, K. T. Kim, J. U. Lee and W. H. Jo, Direct exfoliation of graphite using a non-ionic polymer surfactant for fabrication of transparent and conductive graphene films, *J. Mater. Chem. C*, 2013, **1**, 1870.

61. H. B. Wang, B. Y. Xia, Y. Yan, N. Li, J.-Y. Wang and X. Wang, Water-soluble polymer exfoliated graphene: as catalyst support and sensor. *J. Phys. Chem. B*, 2013, **117**, 5606.

62. Z. Liu, J. Q. Liu, L. Cui, R. Wang, X. Luo, C. J. Barrow and W. R. Yang, Preparation of graphene/polymer composites by direct exfoliation of graphite in functionalised block copolymer matrix. *Carbon*, 2013, **51**, 148.

63. K. P. Loh, Q. L. Bao, P. K. Ang and J. X. Yang, The chemistry of graphene, *J. Mater. Chem.*, 2010, **20**, 2277.

64. L. Yan, Y. B. Zheng, F. Zhao, S. Li, X. Gao, B. Xu, P. S. Weiss and Y. Zhao, Chemistry and physics of a single atomic layer: strategies and challenges for functionalization of graphene and graphene-based materials, *Chem. Soc. Rev.*, 2012, **41**, 97.

65. N. Tagmatarchis and M. Prato, Carbon-based materials: from fullerene nanostructures to functionalized carbon nanotubes, *Pure Appl. Chem.*, 2005, **77**, 1675.

66. V. Georgakilas, A. B. Bourlinos, R. Zboril, T. A. Steriotis, P. Dallas, A. K. Stubos and C. Trapalis, Organic functionalisation of graphenes, *Chem. Commun.*, 2010, **46**, 1766.

67. M. Quintana, K. Spyrou, M. Grzelczak, W. R. Browne, P. Rudolf and M. Prato, Functionalization of graphene via 1,3-dipolar cycloaddition, *ACS Nano*, 2010, **4**, 3527.

68. X. Y. Zhang, L. L. Hou, A. Cnossen, A. C. Coleman, O. Ivashenko, P. Rudolf, B. J. van Wees, W. R. Browne and B. L. Feringa, One-pot functionalization of graphene with porphyrin through cycloaddition reactions, *Chem. Eur. J.*, 2011, **17**, 8957.

69. D. M. Guldi, G. M. A. Rahman, V. Sgobba and C. Ehli, Multifunctional molecular carbon materials–from fullerenes to carbon nanotubes, *Chem. Soc. Rev.*, 2006, **35**, 471.

70. M.-E. Ragoussi, J. Malig, G. Katsukis, B. Butz, E. Spiecker, G. de la Torre, T. Torres and D. M. Guldi, Linking photo- and redoxactive phthalocyanines covalently to graphene, *Angew. Chem., Int. Ed.*, 2012, **51**, 6421.

71. Z. Li, Y. Chen, Y. Du, X. Wang, P. Yang and J. Zheng, Triphenylamine-functionalized graphene decorated with Pt nanoparticles and its application in photocatalytic hydrogen production, *Int. J. Hydrogen Energy*, 2012, **37**, 4880.

72. X. Y. Zhang, W. R. Browne and B. L. Feringa, Preparation of dispersible graphene through organic functionalization of graphene using a zwitterion intermediate cycloaddition approach, *RSC Adv.*, 2012, **2**, 12713.

73. T. A. Strom, E. P. Dillon, C. E. Hamilton and A. R. Barron, Nitrene addition to exfoliated graphene: a one-step route to highly functionalized graphene, *Chem. Commun.*, 2010, **46**, 4097.

74. S. Vadukumpully, J. Gupta, Y. Zhang, G. Xu and S. Valiyaveettil, Functionalization of surfactant wrapped graphene nanosheets with alkylazides for enhanced dispersibility, *Nanoscale*, 2011, **3**, 303.

75. L.-H. Liu, M. M. Lerner and M. Yan, Derivitization of pristine graphene with well-defined chemical functionalities, *Nano Lett.*, 2010, **10**, 3754.

76. X. Xu, W. Lv, J. Huang, J. Li, R. Tang, J. Yan, Q. Yang, J. Qin and Z. Li, Functionalization of graphene by tetraphenylethylene using nitrene chemistry, *RSC Adv.*, 2012, **2**, 7042.

77. N. Karousis, J. Ortiz, K. Ohkubo, T. Hasobe, S. Fukuzumi, A. Sastre-Santos and N. Tagmatarchis, Zinc phthalocyanine–graphene hybrid material for energy conversion: synthesis, characterization, photophysics, and photoelectrochemical cell preparation, *J. Phys. Chem. C*, 2012, **116**, 20564.

78. S. P. Economopoulos, G. Rotas, Y. Miyata, H. Shinohara and N. Tagmatarchis, Exfoliation and chemical modification using microwave irradiation affording highly functionalized graphene, *ACS Nano*, 2010, **4**, 7499.

79. C. Bosch-Navarro, F. Busolo, E. Coronado, Y. Duan, C. Martí-Gastaldo and H. Prima-Garcia, Influence of the covalent grafting of organic radicals to graphene on its magnetoresistance. *J. Mater. Chem. C*, 2013, **1**, 4590.

80. C. E. Hamilton, J. R. Lomeda, Z. Z. Sun, J. M. Tour and A. R. Barron, Radical addition of perfluorinated alkyl iodides to multi-layered graphene and single-walled carbon nanotubes, *Nano Res.*, 2010, **3**, 138.

81. H. X. Xu and K. S. Suslick, Sonochemical preparation of functionalized graphenes, *J. Am. Chem. Soc.*, 2011, **133**, 9148.

82. X. W. Ma, F. Li, Y. F. Wang and A. G. Hu, Functionalization of pristine graphene with conjugated polymers through diradical addition and propagation. *Chem. Asian. J.*, 2012, **7**, 2547.

83. Z. Jin, T. P. McNicholas, C. Shih, Q. Wang, G. L. C. Paulus and M. S. Strano, Click chemistry on solution-dispersed graphene and monolayer CVD graphene, *Chem. Mater.*, 2011, **23**, 3362.

84. Z. Yang, Y. Sun, L. B. Alemany, T. N. Narayanan and W. E. Billups, Birch reduction of graphite. edge and interior functionalization by hydrogen, *J. Am. Chem. Soc.*, 2012, **134**, 18689.

85. R. A. Schäfer, J. M. Englert, P. Wehrfritz, W. Bauer, F. Hauke, T. Seyller and A. Hirsch, On the way to graphane–pronounced fluorescence of polyhydrogenated graphene, *Angew. Chem., Int. Ed.*, 2013, **52**, 754.

Chapter 3

Dispersion of graphene in ethanol using a simple solvent exchange method

Abstract

The preparation of a dispersion of graphene in ethanol was achieved using solvent exchange from *N*-methyl-2-pyrrolidone (NMP). The dispersion is relatively stable and the small amount of sedimentation can be redispersed by mild sonication. The graphene sheets contain few defects and the conductivity of the film is 1130 S m^{-1} after drying under vacuum at room temperature for 24 h. Considering the low boiling point of ethanol, this method will be useful in the preparation of composites, surface deposition and fabrication of graphene based materials, and will help to find other low boiling point solvents to disperse graphene.

This chapter has been published:

Xiaoyan Zhang, Anthony C. Coleman, Nathalie Katsonis, Wesley R. Browne, Bart J. van Wees and Ben L. Feringa, ***Chem. Commun.***, 2010, 46, 7539-7541.

3.1 Introduction

Since its isolation by Geim and coworkers in 2004,[1] graphene has attracted widespread attention due to its unique properties, such as room temperature quantum effects, ambipolar electric field effects, and high carrier mobility.[2] Graphene of less than 10 layers shows properties distinct from those of bulk graphite[3] and hence single- and few-layer graphenes are highly attractive materials for electronics, composites and devices. As with carbon nanotubes, a major problem encountered is the preparation of graphene on a large scale. To date, several methods have been reported, including mechanical,[1] epitaxial,[4,5] reduction of graphene oxide,[6-10] and solvent dispersion of graphite.[11-14] Though the mechanical method can yield high quality single-layer graphene sheets, it is time consuming and features low throughput, which makes it unsuitable for large scale production. There are also reports on epitaxial growth of graphene on metal substrates,[4,5] but this process requires high temperatures and subsequent transfer of the sample to other substrates. Compared with these methods, the reduction of graphene oxide and solvent dispersion of graphite have obvious advantages, such as scalable production and ease of solution processing. For example, chemical or thermal treatment of graphene oxide provides a material that is conductive and can be used in device applications.[9,10] However, the reduced graphene oxide still contains defects and the original properties of graphene are not recovered.[15] Recently, several groups have shown that graphene can be prepared by exfoliation of graphite in certain solvents, such as *N*-methyl-2-pyrrolidone (NMP),[11] dimethylformamide (DMF),[12] and *o*-dichlorobenzene (ODCB)[13] to produce single and few-layer graphene sheets. These solvents have surface tensions close to 40 mJ m^{-2}, and are suitable for direct exfoliation of graphite.[11] However, these solvents hold their own disadvantages. Their high boiling points limit their viability for real manipulation. Thus, dispersion of graphene in low boiling solvents without surfactants or other stabilizers is useful in many applications. For example, in

composites and surface deposition, low boiling point solvents are preferred. However, most low boiling solvents, for example, water and ethanol, have surface tension (72.8 mJ m^{-2} and 22.1 mJ m^{-2}, respectively) that are unsuitable for the direct exfoliation of graphite. Therefore, a more suitable method is required.

Coleman and coworkers recently reported that graphene could be prepared by exfoliation of graphite in a surfactant/water solution, to yield large amounts of few-layer graphene sheets and small quantities of single-layer graphene sheet with the aid of the surfactant.[16]

In this chapter, we report the discovery that graphene can form a relatively stable high concentration dispersion in ethanol using a solvent exchange process from NMP. The preparation of the graphene dispersion in ethanol is confirmed by spectroscopic and microscopic methods, and the generated film shows good conductivity.

3.2 Results

The preparation of the graphene dispersion in ethanol is shown in Scheme 1. Approximately, 200 mg of graphite in 200 ml NMP was sonicated for 2 h, and centrifuged at 4000 rpm for 30 min to remove large and thick particles. The supernatant of graphene in NMP was decanted, and 150 ml of the above supernatant was filtered through a 0.45 μm nylon membrane. The obtained filter cake was dispersed in 50 ml ethanol with mild sonication and filtered again. This process was repeated five times (each time with 50 ml ethanol and ca. 10 min of sonication) and finally the filter cake was redispersed in 30 ml ethanol. This suspension was centrifuged at 1000 rpm for 30 min, the supernatant was decanted and further sonicated for several minutes to give the required homogeneous graphene dispersion in ethanol (the sample vial was sealed to prevent evaporation of ethanol).

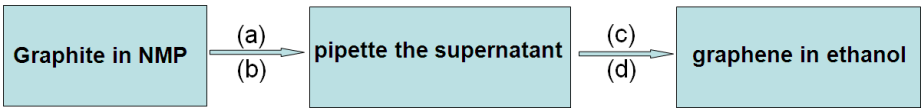

Scheme 1. Procedure for the preparation of graphene in ethanol: (a) sonicate for 2 h, (b) centrifuge at 4000 rpm/30 min, (c) filter, redisperse the filter cake in ethanol, and repeat this process 5 times, (d) redisperse the filter cake in ethanol, centrifuge at 1000 rpm/30 min, then pipette the supernatant and sonicate for several minutes.

Using the solvent exchange process, graphene can form a relatively stable dispersion in ethanol, at a concentration of up to 0.04 mg ml^{-1} (Fig. 1a, right). Fig. 1b shows the absorption spectrum of graphene in ethanol after dilution with ethanol, which is flat and featureless. Over one week, the sample shows at most 20% sedimentation (as determined by UV/Vis absorption spectroscopy). A graphene dispersion in NMP diluted with water (NMP : water = 1 : 99) shows 25% sedimentation over 160 h,[17] which is slightly higher than graphene in ethanol. In addition, the sedimentation in ethanol can be redispersed by mild sonication. By contrast, as a control, graphite which was directly sonicated in ethanol for several hours, showed complete precipitation on standing for 4 h (Fig. 1a, left). The repeated washing steps using the solvent exchange method yield a stable dispersion of graphene in ethanol containing < 0.3 vol% NMP (Fig. 1c).

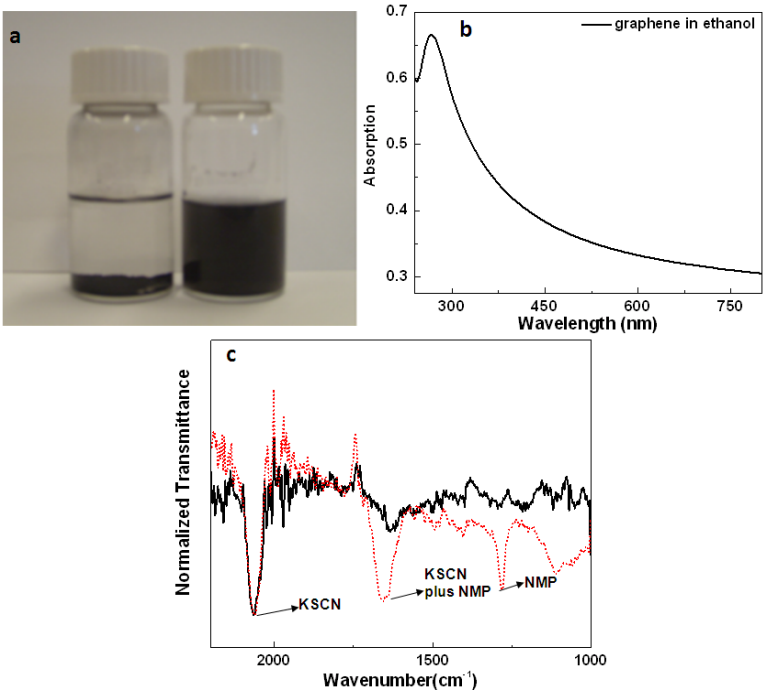

Figure 1. (a) Direct sonication of graphite in ethanol results in complete precipitation after 4 h (left) while a relatively stable graphene dispersion in ethanol is obtained using the solvent exchange process (right). (b) UV/Vis absorption spectrum of graphene in ethanol after dilution with ethanol. (c) FTIR spectrum of graphene in ethanol with 0.5% KSCN (solid line), and ethanol with 0.5% KSCN plus 0.3% NMP (dotted line). The contents of KSCN and NMP are expressed in vol%. KSCN was used as a reference, and the volume content of KSCN in the two samples are identical. The spectra were obtained by dropping a certain volume (5 µl) of the two samples on the FTIR crystal plate, followed by 128 scans after the evaporation of ethanol. The spectrum of ethanol with 0.5% KSCN plus 0.3% NMP shows a stronger NMP signal than graphene in ethanol containing 0.5% KSCN alone, which indicates that the content of NMP should be below 0.3% volume for the sample of graphene in ethanol.

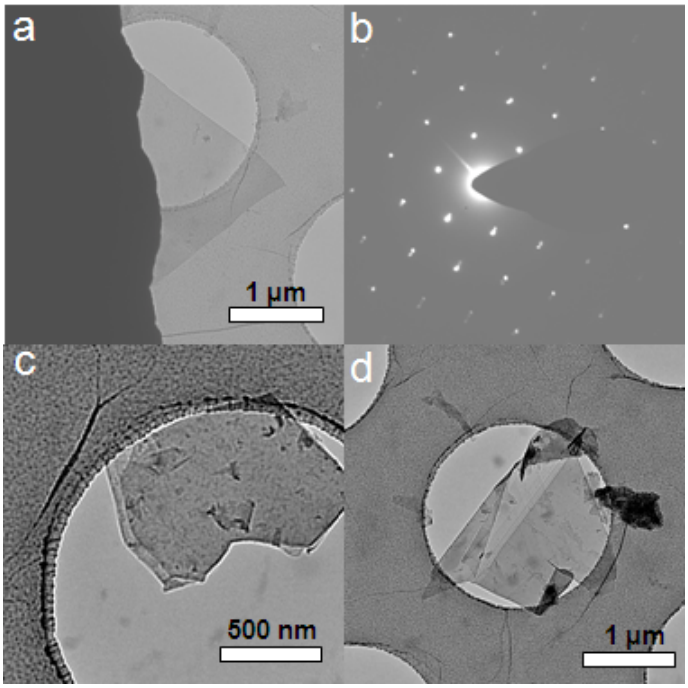

Figure 2. TEM images of a single-layer graphene sheet (a), the corresponding electron diffraction pattern of the sheet (b), a bi-layer graphene sheet (c), and few-layer graphene sheets (d).

Transmission electron microscopy (TEM) was performed to investigate the quality and exfoliation behaviour of the graphene sheets obtained in ethanol. Fig. 2a shows a single-layer graphene sheet, which is confirmed by the corresponding electron diffraction pattern (Fig. 2b). The intensity of the innermost spots is stronger than the outer spots, indicating it is a single-layer graphene sheet.[11] Checking the edge of the sheets showed that some bi-layer graphene sheets were also present (Fig. 2c). In addition, a large number of few-layer graphene sheets were observed, as shown in Fig. 2d. There are also some graphene nanoribbons in the graphene dispersion of ethanol (Fig. 3). This indicates that graphene in ethanol predominantly consists of single- and few-layer graphene sheets.

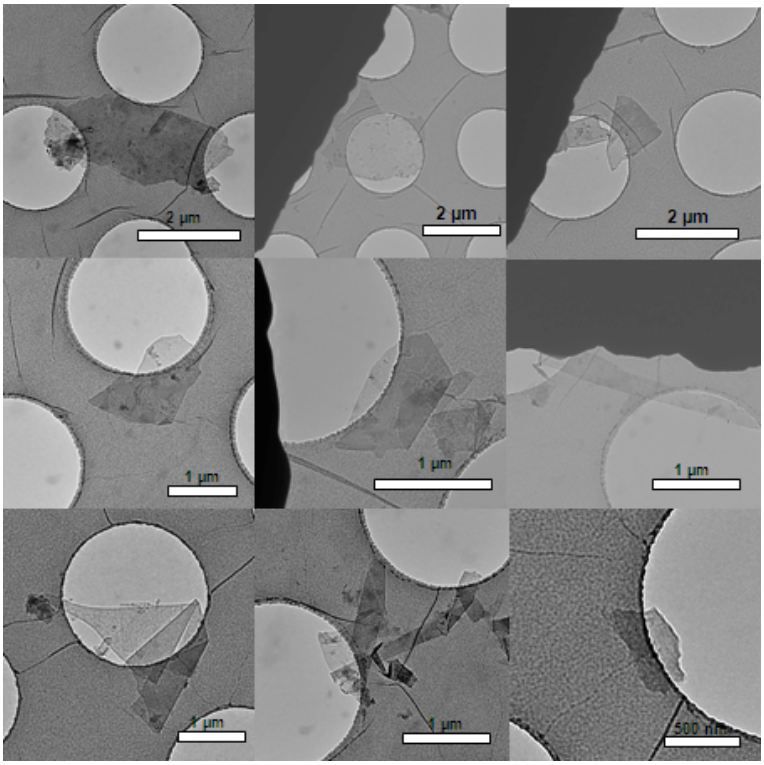

Figure 3. Additional TEM images of graphene in ethanol.

The exfoliation of graphene in ethanol is confirmed by tapping mode atomic force microscopy (AFM). The sample was prepared by drop casting the graphene dispersion in ethanol onto a hot mica surface to enable rapid evaporation of ethanol. Fig. 4 shows a large graphene flake composed of a single- or bi-layer graphene sheet. This assignment is based on the sheet height of ca. 1.3 nm, which is in agreement with the height of 1-2 nm observed elsewhere for single- or bi-layer graphene sheets.[11,16] Analysis of the height of the flakes indicates that most of the graphene sheets are below 10 nm.

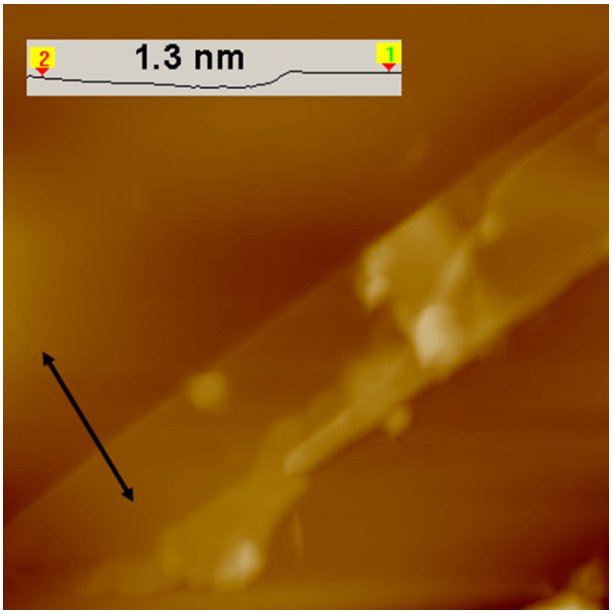

Figure 4. An AFM image of graphene from ethanol by drop-casting onto freshly cleaved mica. The scan area is 2.0 × 2.0 μm.

Raman spectroscopy was employed to analyze the quality of the graphene sheets obtained using this solvent exchange method. The most prominent Raman features for graphitic materials are: a defect-induced D band at 1350 cm^{-1}, an in-plane vibration of sp^2 carbon at 1580 cm^{-1} (G band), and a two phonon double resonance process at about 2700 cm^{-1} (2D band).[18,19] As shown in Fig. 5a, the D band of graphite is weak, while graphene shows a small D band. The relatively low intensity of the D band indicates that the graphene flakes contain few defects. According to Coleman and coworkers,[16] these defects are predominantly located at the edges of the graphene flakes, and the basal plane of the flakes are relatively defect free. In the present case, the small size of the flakes precludes spatial mapping of the defects and hence identification of their location on the edge or in the basal plane. However, the positions and shapes of the spectra (2D band) of graphene indicates that the graphene flakes are a mixture of single- and few-layer graphene.[11,18] Additional

evidence of the low defect content is also provided by FTIR spectroscopy (Fig. 5b). The spectrum of graphene flakes from ethanol is almost featureless, confirming the low content of defects in the graphene sample.

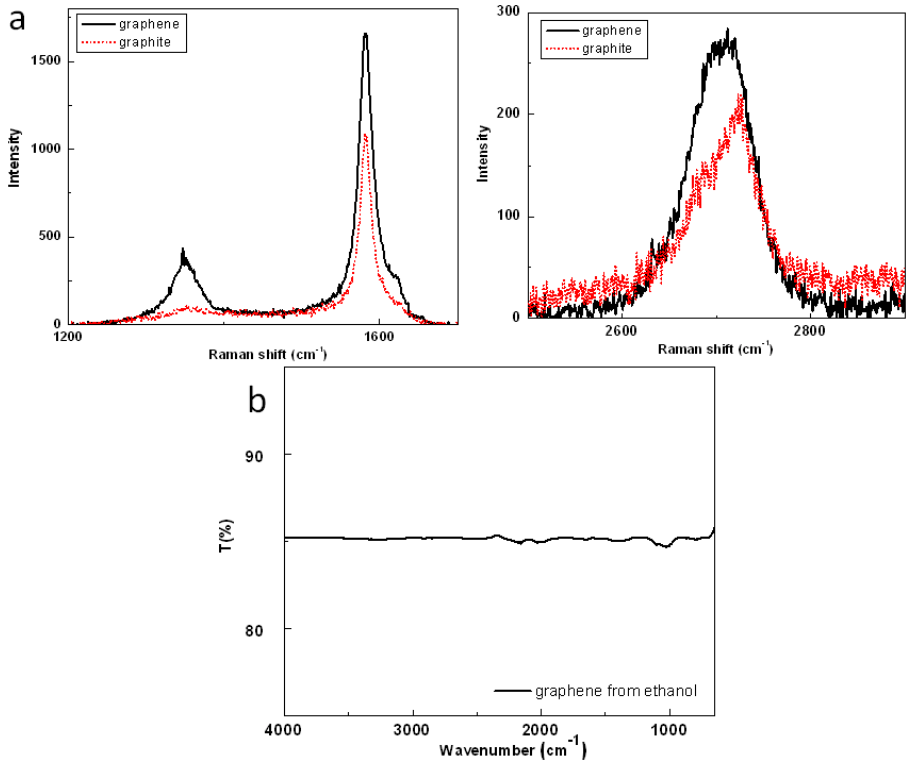

Figure 5. (a) Raman spectra of graphene from an ethanol dispersion (solid line) and graphite (dotted line). (b) FTIR spectrum of graphene from ethanol. The spectrum is almost featureless, confirming the low content of defects in the graphene sample.

The conductivity of the film from graphene in ethanol was also determined using the standard four-point probe method. The film was made by vacuum filtration of graphene dispersions in ethanol. The film shows a conductivity of 1130 S m^{-1} after drying under vacuum at room temperature for 24 h (without annealing). This value is comparable with the reported conductivity value

(1500 S m^{-1}) of an annealed graphene film (250 ^{o}C in Ar/N_2) from a surfactant/water system,[16] and also the conductivity (1200 S m^{-1}) of graphene powder using the wet ball milling exfoliation method.[20]

The same solvent exchange process was also applied using other solvents, such as methanol, dichloromethane (DCM) and toluene. However, graphene was found to completely precipitate after the final centrifugation process (1000 rpm/30 min) in these three solvents.

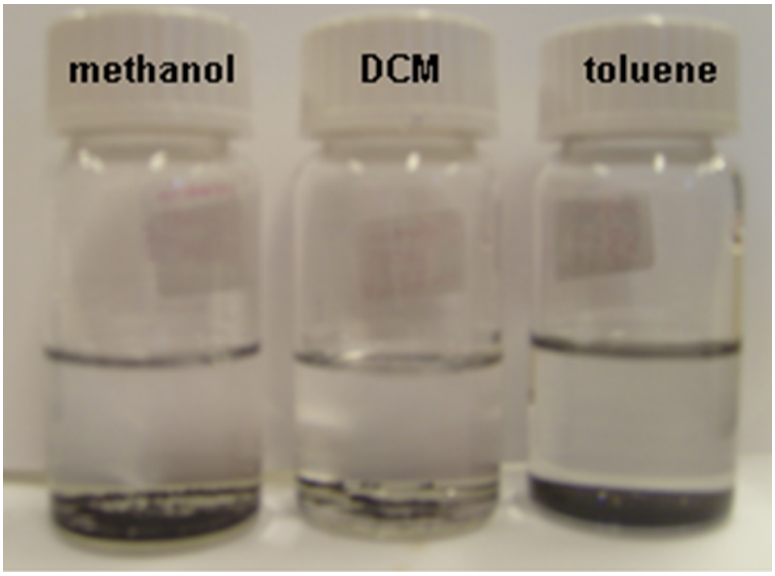

Figure 6. Precipitates obtained from the solvent exchange process, as described for ethanol, applied using methanol, dichloromethane and toluene.

3.3 Discussions

The reason for the difference between ethanol and other solvents is rationalized as follows. NMP is a good solvent for the exfoliation of graphite, which produces single- and few-layer graphene sheets.[11,17] After the filtration process, the filter cake still contains single- and few-layer graphene flakes. During the solvent exchange process, the above materials were redispersed into the

corresponding solvents. However, the interactions of graphene with different solvents are not the same, so the dispersion behaviours in these solvents are different. Ethanol shows better dispersibility and stability than the other three solvents. However, the exact mechanism of stabilization in ethanol is still not clear, and needs further study. Importantly it should be noted that direct exfoliation in ethanol leads to much reduced stability compared with initial exfoliation in NMP followed by solvent exchange with ethanol. This indicates that the solvent properties that are optimum for initial exfoliation are not necessarily the same as that required to maintain the dispersion.

These data are consistent with the molecular dynamics simulations by Shih et al.[21] When the solvent-graphene interaction is not strong enough to overcome the π-π interactions between the graphene sheets, the solvent itself cannot directly exfoliate graphite. However, once the graphene sheets are dispersed in the solvent, the solvent molecules confined between the graphene sheets generate a high energy barrier which repels the sheets by steric repulsions between the solvent molecules and the graphene sheets.

3.4 Conclusions

In summary, we present a simple solvent exchange method to prepare graphene in ethanol, which consists of single- and few-layer graphene sheets. The dispersion is relatively stable and the small amount of sedimentation can be redispersed by mild sonication. The graphene sheets contain few defects and the conductivity of the film is 1130 S m^{-1} after drying under vacuum at room temperature for 24 h. Considering the low boiling point of ethanol, this method will be very useful in the preparation of composites, surface deposition and fabrication of graphene based materials, and will help to find other low boiling point solvents to disperse graphene.

3.5 Perspective

The solvent dispersion method developed by our group has already been used by others.[22-27] For example, Hempel et al. used the same appoach to transfer graphene from NMP to ethanol, which is better suited for spray coating onto polyethylene terephthalate (PET) substrates.[22] This method can also be applied to graphene oxide dispersions. Tang and co-workers showed that graphene oxide can form stable dispersion in DMF by solvent exchange from water, while directly sonicated graphene oxide in DMF cannot form stable dispersions.[24] The authors concluded that graphene oxide cannot be directly exfoliated in DMF due to the strong hydrogen bonding between the graphene oxide layers.

Therefore, it is reasonable to expect that the solvent exchange method may offer the opportunity of achieve stable graphene dispersion in a wide range of solvents, which could later be used in graphene-based functional materials through a solution process. This method could also potentially be used in other two-dimensional systems.[28]

3.6 Experimental

Chemicals. Graphite flakes (Sigma-Aldrich), N-methyl-2-pyrrolidone (NMP, Acros Organics, 99%, extra pure), ethanol (absolute, AR, Merck), methanol (99.8%, AR, Lab-Scan), dichloromethane (99.8%, AR, Lab-Scan) and toluene (99.5%, AR, Lab-Scan) were used as received without further purification.

Instruments. Sonication was conducted using a low power sonication bath (Bransonic, PC 620). Centrifugation was performed on a Hermle Z323K Centrifuge. Filtration was carried out using a Sintered Micro Filter holder through a 0.45 μm nylon membrane. UV/Vis spectra were obtained on a JASCO V-630 UV/Vis spectrometer. Transmission electron microscopy (TEM) characterization was undertaken on a PHILIPS CM10 operating at 100 KV. A

drop of graphene in ethanol was deposited on a holey carbon grid. Atomic force microscopy (AFM) was obtained with a PicoScan LE (Molecular Imaging) in tapping mode. The sample was prepared by drop casting a few drops of the graphene dispersion in ethanol onto a hot freshly cleaved mica surface (The mica was contained in a glass petri dish, which was placed in a hot oven at 90 ^{o}C). Raman spectra were measured on a JOBIN-YVON model T 64000 triple grating spectrometer (excitation at 532 nm). Fourier Transform Infrared Spectroscopy (FTIR) were collected using a Perkin Elmer spectrophotometer equipped with a UATR attachment. Conductivity measurement was determined using the standard four-point probe method on a Keithley 2410 Source Meter.

3.7 Notes and references

1. K. S. Novoselov, A. K. Geim, S. V. Morozov, D. Jiang, Y. Zhang, S. V. Dubonos, I. V. Grigorieva and A. A. Firsov, Electric field effect in atomically thin carbon films, *Science*, 2004, **306**, 666.

2. A. K. Geim and K. S. Novoselov, The rise of graphene, *Nat. Mater.*, 2007, **6**, 183; N. Tombros, C. Jozsa, M. Popinciuc, H. T. Jonkman and B. J. van Wees, Electronic spin transport and spin precession in single graphene layers at room temperature, *Nature*, 2007, **448**, 571; C. Jozsa, M. Popinciuc, N. Tombros, H. T. Jonkman and B. J. van Wees, Electronic spin drift in graphene field-effect transistors, *Phys. Rev. Lett*., 2008, **100**, 236603.

3. B. Partoens and F. M. Peeters, From graphene to graphite: electronic structure around the K point, *Phys. Rev. B*, 2006, **74**, 075404.

4. P. W. Sutter, J. I. Flege and E. A. Sutter, Epitaxial graphene on ruthenium, *Nat. Mater*., 2008, **7**, 406.

5. J. Coraux, A. T. N'Diaye, C. Busse and T. Michely, Structural coherency of graphene on Ir(111), *Nano Lett*., 2008, **8**, 565.

6. S. Stankovich, D. A. Dikin, R. D. Piner, K. A. Kohlhaas, A. Kleinhammes, Y. Jia, Y. Wu, S. T. Nguyen and R. S. Ruoff, Synthesis of graphene-based

nanosheets via chemical reduction of exfoliated graphite oxide, *Carbon*, 2007, **45**, 1558.

7. D. Li, M. B. Müller, S. Gilje, R. B. Kaner and G. G. Wallace, Processable aqueous dispersions of graphene nanosheets, *Nat. Nanotechnol*., 2008, **3**, 101.

8. H. L. Wang, J. T. Robinson, X. L. Li and H. J. Dai, Solvothermal reduction of chemically exfoliated graphene sheets, *J. Am. Chem. Soc.*, 2009, **131**, 9910.

9. X. Wang, L. J. Zhi and K. Müllen, Transparent, conductive graphene electrodes for dye-sensitized solar cells, *Nano Lett*., 2008, **8**, 323.

10. M. D. Stoller, S. Park, Y. W. Zhu, J. An and R. S. Ruoff, Graphene-based ultracapacitors, *Nano Lett.*, 2008, **8**, 3498.

11. Y. Hernandez, V. Nicolosi, M. Lotya, F. M. Blighe, Z. Y. Sun, S. De, I. T. McGovern, B. Holland, M. Byrne, Y. K. Gun'ko, J. J. Boland, P. Niraj, G. Duesberg, S. Krishnamurthy, R. Goodhue, J. Hutchison, V. Scardaci, A. C. Ferrari and J. N. Coleman, High-yield production of graphene by liquid-phase exfoliation of graphite, *Nat. Nanotechnol.*, 2008, **3**, 563.

12. P. Blake, P. D. Brimicombe, R. R. Nair, T. J. Booth, D. Jiang, F. Schedin, L. A. Ponomarenko, S. V. Morozov, H. F. Gleeson, E. W. Hill, A. K. Geim and K. S. Novoselov, Graphene-based liquid crystal device, *Nano Lett*., 2008, **8**, 1704.

13. C. E. Hamilton, J. R. Lomeda, Z. Z. Sun, J. M. Tour and A. R. Barron, High-yield organic sispersions of unfunctionalized graphene, *Nano Lett.*, 2009, **9**, 3460.

14. X. Q. Wang, P. F. Fulvio, G. A. Baker, G. M. Veith, R. R. Unocic, S. M. Mahurin, M. F. Chi and S. Dai, Direct exfoliation of natural graphite into micrometre size few layers graphene sheets using ionic liquids, *Chem. Commun*., 2010, **46**, 4487.

15. S. Park and R. S. Ruoff, Chemical methods for the production of graphenes, *Nat. Nanotechnol*., 2009, **4**, 217.

16. M. Lotya, Y. Hernandez, P. J. King, R. J. Smith, V. Nicolosi, L. S. Karlsson, F. M. Blighe, S. De, Z. M. Wang, I. T. McGovern, G. S. Duesberg and J. N. Coleman, Liquid phase production of graphene by exfoliation of graphite in surfactant/water solutions, *J. Am. Chem. Soc*., 2009, **131**, 3611.

17. U. Khan, A. O'Neill, M. Lotya, S. De and J. N. Coleman, High-concentration solvent exfoliation of graphene, *Small*, 2010, **6**, 864.

18. A. C. Ferrari, J. C. Meyer, V. Scardaci, C. Casiraghi, M. Lazzeri, F. Mauri, S. Piscanec, D. Jiang, K. S. Novoselov, S. Roth and A. K. Geim, Raman spectrum of graphene and graphene layers, *Phys. Rev. Lett*., 2006, **97**, 187401.

19. C. Casiraghi, A. Hartschuh, H. Qian, S. Piscanec, C. Georgi, A. Fasoli, K. S. Novoselov, D. M. Basko and A. C. Ferrari, Raman spectroscopy of graphene edges, *Nano Lett*., 2009, **9,** 1433.

20. W. F. Zhao, M. Fang, F. R. Wu, H. Wu, L. W. Wang, and G. H. Chen, Preparation of graphene by exfoliation of graphite using wet ball milling, *J. Mater. Chem*., 2010, **28**, 5817.

21. C.-J. Shih, S. C. Lin, M. S. Strano and D. Blankschtein, Understanding the stabilization of liquid-phase-exfoliated graphene in polar solvents: molecular dynamics simulations and kinetic theory of colloid aggregation, *J. Am. Chem. Soc.*, 2010, **132**, 14638.

22. M. Hempel, D. Nezich, J. Kong and M. Hofmann, A novel class of strain gauges based on layered percolative films of 2D materials, *Nano Lett*., 2012, **12**, 5714.

23. J. Li, F. Ye, S. Vaziri, M. Muhammed, M. C. Lemme and M. Östling, A simple route towards high-concentration surfactant-free graphene dispersions, *Carbon*, 2012, **50**, 3113.

24. Z. Tang, H. Kang, Z. Shen, Baochun Guo, L. Zhang and D. Jia, Grafting of polyester onto graphene for electrically and thermally conductive composites, *Macromolecules*, 2012, **45**, 3444.

25. J.-Y. Hong and J. Jang, Highly stable, concentrated dispersions of graphene oxide sheets and their electro-responsive characteristics, *Soft Matter*, 2012, **8**, 7348.

26. S. Lee, J.-Y. Hong and J. Jang, Multifunctional graphene sheets embedded in silicone encapsulant for superior performance of light-emitting diodes, *ACS Nano*, 2013, **7**, 5784.

27. D. P. Wong, H.-P. Tseng, Y.-T. Chen, B.-J. Hwang, L.-C. Chen and K.-H. Chen, A stable silicon/graphene composite using solvent exchange method as anode material for lithium ion batteries, *Carbon*, 2013, **63**, 397.

28. J. N. Coleman, M. Lotya, A. O'Neill, S. D. Bergin, P. J. King, U. Khan, K. Young, A. Gaucher, S. De, R. J. Smith, I. V. Shvets, S. K. Arora, G. Stanton, H. Y. Kim, K. Lee, G. T. Kim, G. S. Duesberg, T. Hallam, J. J. Boland, J. J. Wang, J. F. Donegan, J. C. Grunlan, G. Moriarty, A. Shmeliov, R. J. Nicholls, J. M. Perkins, E. M. Grieveson, K. Theuwissen, D. W. McComb, P. D. Nellist and V. Nicolosi, Two-dimensional nanosheets produced by liquid exfoliation of layered materials, *Science*, 2011, **331**, 568.

Chapter 4

Preparation of dispersible graphene through organic functionalization of graphene using a zwitterion intermediate cycloaddition approach

Abstract

Highly functionalized graphene was obtained through a zwitterion intermediate cycloaddition onto exfoliated graphene flakes under new reaction conditions. The functionalized graphene obtained formed stable dispersions in common solvents, including dimethylformamide (DMF), $CHCl_3$ and water. Its dispersion in water is especially useful in a wide range of areas, such as composites, devices and biological applications.

This chapter has been published:

Xiaoyan Zhang, Wesley R. Browne and Ben L. Feringa, ***RSC Adv.***, 2012, 2, 12173-12176.

4.1 Introduction

Over the last decade, graphene, a single-layer of graphite with a two-dimensional honeycomb lattice, has emerged as one of the most promising future materials due to its unique physical, mechanical and thermal properties.[1] Potential applications of graphene in Li-ion batteries, supercapacitors, transparent electrode, sensors and composites have already been demonstrated.[2] However, a key challenge in handling graphene based materials is in how to obtain a large amount of dispersible graphene flakes in either organic solvents or water for certain uses, such as in composites, devices and biological applications.[3] Several chemical methods have been developed, including reduction of graphene oxide,[4] bottom-up organic synthesis[5] and dispersion of graphite in certain solvents.[6-8] Methods employing the reduction of graphene oxide requires harsh oxidation conditions to prepare graphene oxide and a subsequent chemical and/or thermal reduction step. Graphene prepared by organic synthesis routes are impeded by limitations to size.[5] Of these approaches, direct sonication of graphite in solvents promises to be the simplest method to obtain dispersible and relatively defect-free graphene flakes. However, the graphene flakes suspended in solvents (such as in N-methyl pyrrolidone,[6] ortho-dichlorobenzene[7a] and ethanol[8a]) tend to aggregate due to the strong π–π interactions between the individual flakes, which seriously limits their application. In order to solve this problem and further improve their dispersibility, stability and processability, considerable efforts have been devoted to functionalize graphene flakes by noncovalent[9] or covalent methods.[10] In contrast to noncovalent methods, covalent methods can provide for more stable and robust materials. Covalently attached functional groups on graphene can improve the dispersibility of graphene, and also increase compatibility with various interfaces and matrices. Furthermore, covalently functionalized graphene can be applied in subsequent chemical processes that are usually unsuitable for non-covalent/physisorbed functionalized graphene.

More importantly, covalently functionalized graphene can yield graphene samples that show long-term stability when dispersed in solvents, which is necessary for application. However, covalent functionalization may affect the electronic properties of graphene. Thus, controlling the degree of functionalization of graphene is essential. Although the reactivity of graphene is less than those of fullerenes and carbon nanotubes, the wrinkled and folded structure and defects present in graphene can increase its reactivity towards organic reagents.[11] To date, a number of chemical reactions on graphene have been reported, including 1,3-dipolar cycloaddition,[10] diazonium chemistry,[12] nitrene addition,[13] radical addition[14] and click chemistry.[15] Through these reactions, a range of functional groups can be introduced and also the degree of functionalization of graphene can be tuned. However, chemical modification of graphene has yet to be fully studied and more facile and mild methods are highly desirable.

Here, we take a zwitterion intermediate cycloaddition functionalization approach, which was previously applied to fullerenes and carbon nanotubes,[16] to functionalize graphene obtained using the solvent dispersion and exchange method.[10a] The functionalized graphene formed stable dispersions in common solvents (most remarkably in water) and was characterized by several spectroscopic and microscopic methods.

4.2 Results

Functionalization of graphene through the zwitterion approach is shown in Scheme 1 (see Scheme 2 for the proposed mechanism).[16] 4-Dimethylaminopyridine (DMAP) reacts with the triple bond of acetylene dicarboxylates to form a zwitterionic intermediate, which then reacts with a double bond of graphene followed by reaction with the carbonyl group. Finally, the positively charged DMAP moiety is substituted by an alkoxy group, yielding the functionalized graphene product. Graphene in ODCB was prepared

by the solvent dispersion method,[10a] followed by a solvent exchange process developed by our group to transfer graphene into dry toluene (see experimental part).[8a] The graphene dispersed in dry toluene was reacted with DMAP, and acetylenedicarboxylates **1** or **2** at 85 ^{o}C under Ar atmosphere for 3 d. The functionalized graphene was purified by multiple filtration/redispersion cycles (see experimental part). Notably, the functionalized graphene is no longer dispersible in ODCB but **1** functionalized graphene shows good dispersion in both DMF (~ 0.28 mg mL^{-1}) and $CHCl_3$ (~ 0.19 mg mL^{-1}), while **2** functionalized graphene shows good dispersion in water (~ 0.06 mg mL^{-1}) (Fig. 1).[17] UV/Vis absorption spectrometry can be used to investigate the stability of graphene samples in the solvents by measuring the changes in apparent absorption (in actual fact the changes in scattering of light by the graphene) with time.[6,8a] In the present case, **1** functionalized graphene was stable in DMF and $CHCl_3$ for at least two months, while **2** functionalized graphene dispersed in water was stable for at least one month. The stability is comparable with the 1,3-dipolar cycloaddition functionalized graphene dispersed in ethanol (at least 30 days).[10c]

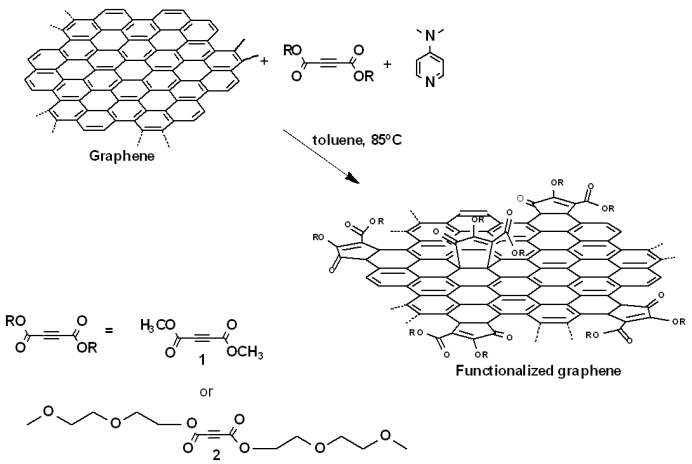

Scheme 1. Preparation of functionalized graphene through the zwitterion approach.

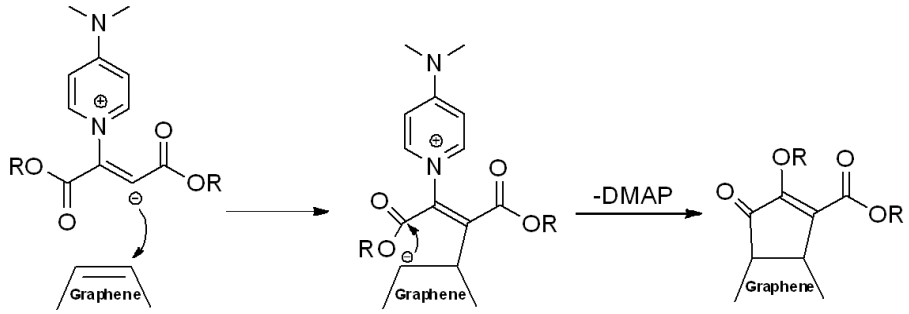

Scheme 2. Proposed mechanism for the zwitterion cycloaddition reaction.[16]

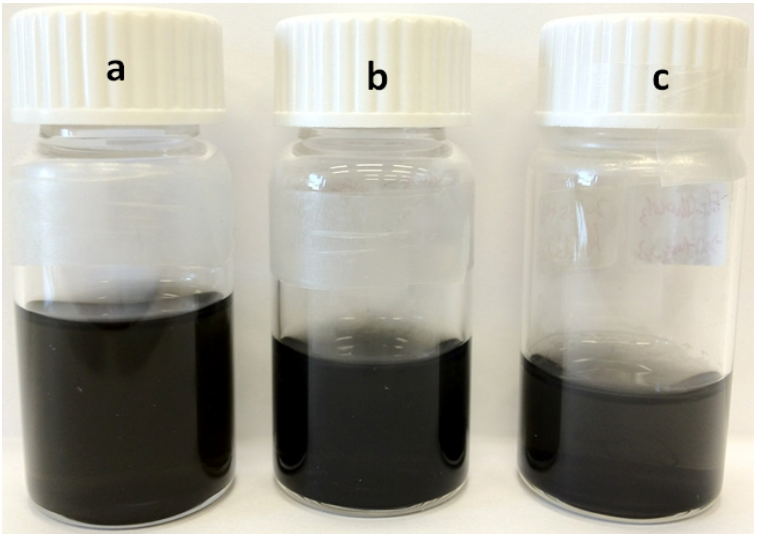

Figure 1. a, b: **1** functionalized graphene dispersion in DMF and $CHCl_3$; c: **2** functionalized graphene dispersion in water.

Fourier transform infrared (FTIR) spectra of graphene, **1** and **2** functionalized graphene, and the control samples are shown in Fig. 2. The FTIR spectrum of graphene itself is almost featureless, indicative of a low content of defects in the graphene. For both **1** and **2** functionalized graphene, the absorption bands at 1715 and 1240 cm^{-1} correspond to carbonyl and ether groups, respectively. The spectra of the control samples (Control 1: graphene reacted with **1** only;

Control 2 : graphene reacted with **2** only; Control 3: graphene reacted with DMAP only), did not show the above mentioned absorptions. This strongly supports that the modification is covalent in the two functionalized graphene samples and is not due to physisorption.

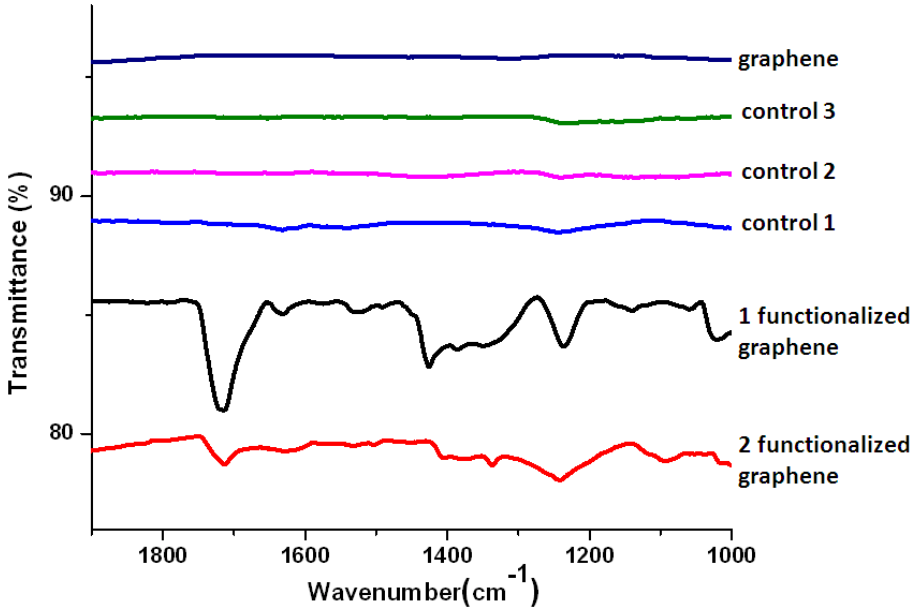

Figure 2. FTIR spectra of graphene, **1** and **2** functionalized graphene, and control samples.

The presence of organic functional groups in the functionalized graphene products is further confirmed by thermal gravimetric analysis (TGA). Fig. 3 shows the TGA curves of graphene, **1** and **2** functionalized graphene. The weight loss of graphene is about 5% between 200 ^{o}C and 450 ^{o}C, which is due to the defects caused by sonication, and also residual solvents. In the same temperature range, **1** and **2** functionalized graphene show about 54% and 36% weight loss, respectively. This weight loss is attributed to the decomposition of organic functional groups attached onto graphene. The degree of functionalization was estimated to be one functional group per 10 carbon atoms

for **1** functionalized graphene, and per 50 carbon atoms for **2** functionalized graphene.

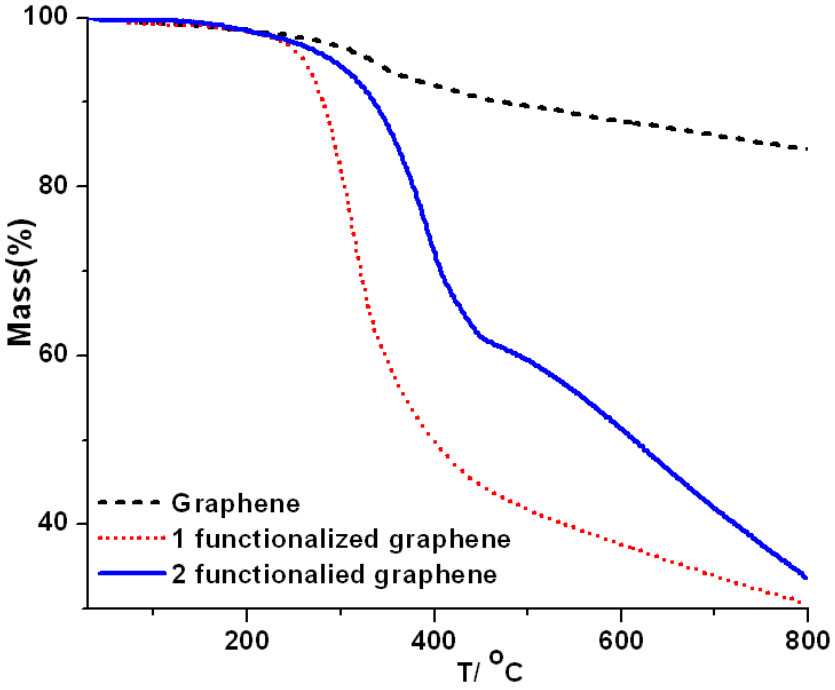

Figure 3. TGA curves of graphene, **1** and **2** functionalized graphene.

Raman spectroscopy is widely used to study the structural and electronic properties of graphitic materials.[18] The typical Raman bands for graphitic materials are: a disorder-induced D band at ~1350 cm^{-1}, a doubly degenerate zone centre E_{2g} mode at about 1580 cm^{-1} (G band, indicative to sp^2 carbon bonds), and a two phonon double resonance Raman process at ~ 2700 cm^{-1} (2D band).[18] The intensity ratio I_D/I_G between the D band and G band is often used to quantify the defects in graphitic materials. Graphene shows a small D band and a strong G band, with a I_D/I_G ratio of 0.3 (Fig. 4). For **1** and **2** functionalized graphene, an increased I_D/I_G ratio (0.54 and 0.4, respectively) is observed compared with graphene. Attachment of organic functional groups changes some carbon atoms from sp^2 to sp^3 and therefore results in an

increased I_D/I_G ratio, which indicates successful covalent functionalization.[10,19] Due to the relatively small size of the graphene flakes and aggregation when deposited onto the substrate, it is difficult to distinguish single-layer graphene by Raman spectroscopy in the present case. However, the positions and band shapes in the spectra of graphene and functionalized graphene indicate that the graphene flakes are a mixture of single- and few-layer graphene.[6,8a,10]

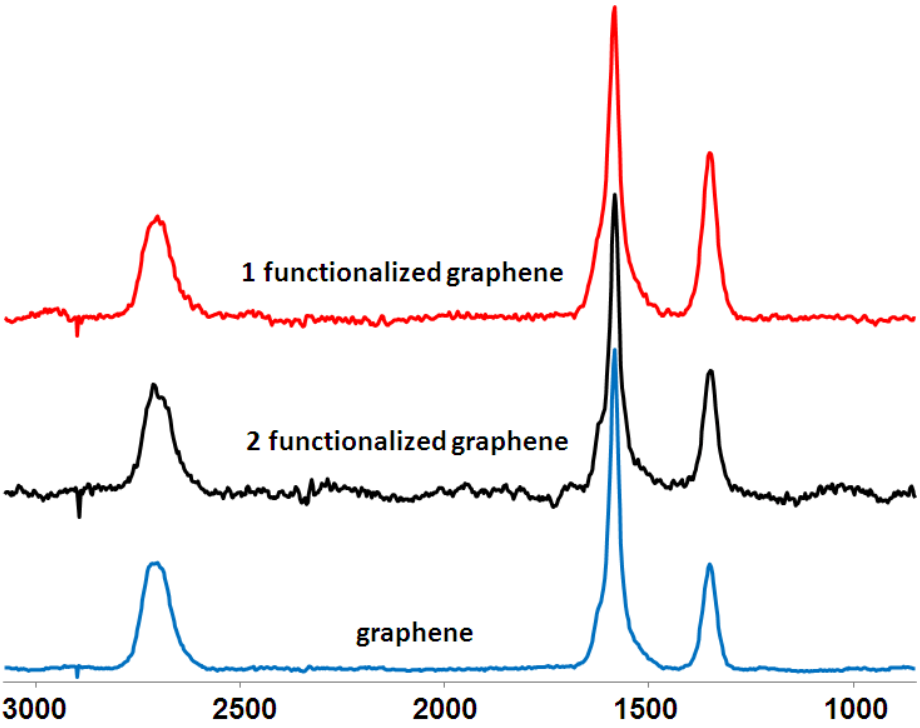

Figure 4. Raman spectra of graphene, **1** and **2** functionalized graphene (λ_{exc} = 532 nm).

The morphologies of graphene before and after functionalization were studied by transmission electron microscopy (TEM) analysis. The presence of single-layer graphene flakes is shown in Fig. 5a, which is confirmed by its electron diffraction pattern (Fig. 6, the intensity of innermost spots is stronger than the outer spots).[6,8a,10a] A large number of few-layer graphene flakes are also present

in the graphene samples used for functionalization (Fig. 5b). **1** functionalized graphene shows good dispersion behaviour both in DMF and $CHCl_3$ (Fig. 5c and Fig. 5d), while **2** functionalized graphene disperse well in water (Fig. 5e, Fig. 5f and Fig. 7). The HRTEM images of both graphene and functionalized graphene are shown in Fig. 8. After functionalization, little change in the morphology of graphene is observed, and importantly, the size of the graphene flakes is not decreased. This is an advantage compared with the harsh oxidation methods used to prepare graphene oxide, in which the flake size is normally significantly reduced.

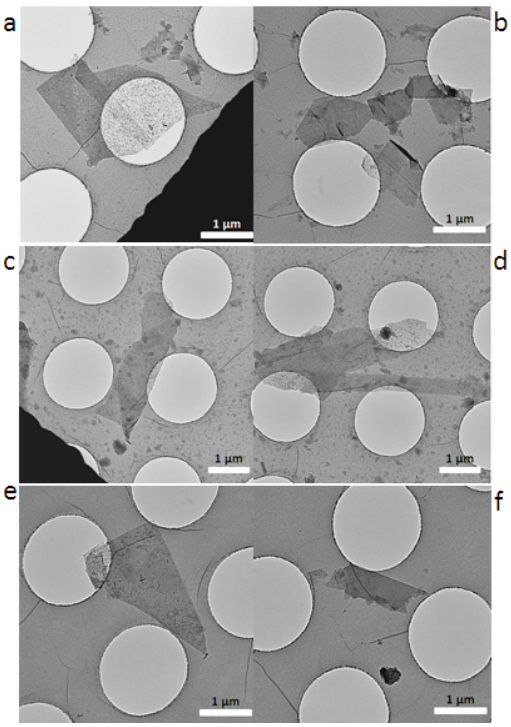

Figure 5. TEM images of graphene in ODCB (a, b), **1** functionalized graphene in DMF (c) and $CHCl_3$ (d) and **2** functionalized graphene in H_2O (e, f). The samples were prepared by drop-casting the dispersion onto a holey carbon grid.

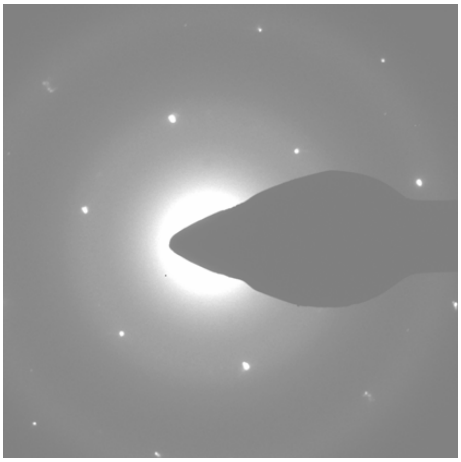

Figure 6. Electron diffraction (ED) pattern of the graphene flake shown in Figure 5a. The intensity of the innermost spots is more intense relative to the outer spots, indicating it is a single-layer graphene flake.[6,8a,10a]

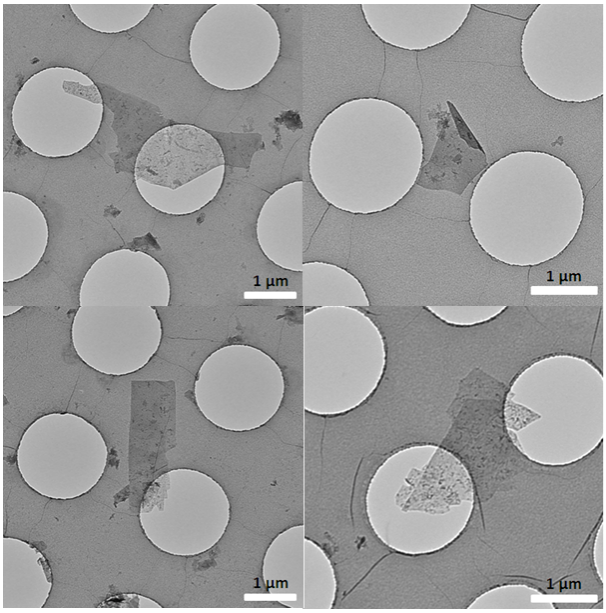

Figure 7. Additional TEM image of **2** functionalized graphene in H_2O.

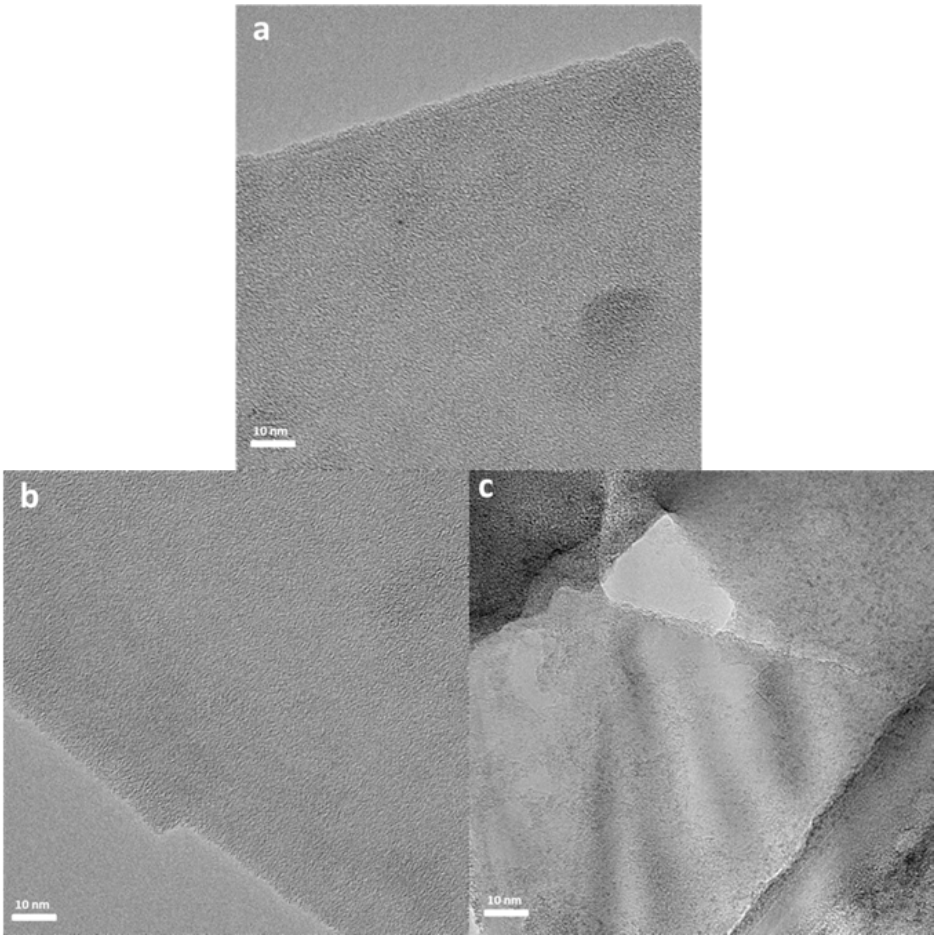

Figure 8. HRTEM images of graphene in ODCB (a), **1** functionalized graphene in DMF (b) and **2** functionalized graphene in H_2O (c). Scale bar: 10 nm.

The conductivity of films of graphene, **1** and **2** functionalized graphene was also determined using the standard four-point probe method. The films were prepared by vacuum filtration of the corresponding dispersions.

Table 1. Conductivity values of graphene, **1** and **2** functionalized graphene.

Name of the samples	$R_{\square}$ (Ω)	σ (S m^{-1})	Average σ (S m^{-1})	Standard deviation of σ (S m^{-1})
graphene	219 202 210	3136 3400 3271	3269	± 132
1 functionalized graphene	77000 85000 78000	7.136 6.464 7.044	6.88	± 0.36
2 functionalized graphene	1944 2065 1997	684 644 666	665	± 20

$$\sigma = \frac{1}{R_{\square} h} \qquad h = \frac{m}{\rho_G \pi r^2}$$

σ -conductivity of the films, $R_{\square}$-sheet resistance, h-thickness of the films, m-mass of the films (which was determined by measuring the mass difference of the films before and after filtration), ρ_G-density of graphene (which is 2000 Kg m^{-3} according to literature),[7c] r-radius of the films.

The graphene film shows a conductivity of 3269 ± 132 S m^{-1}, whereas for **1** and **2** functionalized graphene films a conductivity of 6.88 ± 0.36 and 665 ± 20 S m^{-1} was determined, respectively (see Table 1 for details). The difference between the conductivity of the two functionalized graphene films is due to the different degree of functionalization. The reduced conductivity of the two functionalized graphene films compared to graphene itself is due to covalent modification of the graphene. However, it should be noted that the two conductivity values are still much higher than that of graphene oxide (10^{-8}–10^{-5} S m^{-1}).[20]

4.3 Conclusions

In conclusion, functionalized graphene has been successfully prepared using a zwitterion intermediate cycloaddition approach under new reaction conditions, and was characterized by FTIR, Raman spectroscopy and by additional control experiments. The degree of functionalization on graphene was determined by TGA and more interestingly it was relevant to the starting acetylenedicarboxylates uses. TEM images show that the functionalized graphene has good dispersibility in common solvents, such as DMF, $CHCl_3$ and especially water. The functionalized graphene films show conductivity several orders of magnitude higher than graphene oxide. It is anticipated that this novel zwitterion functionalization method will broaden the chemistry of graphene substantially and that these functionalized graphene materials could be useful

in composites, devices and biological applications (sensing, drug loading and delivery).[3]

4.4 Acknowledgement

We thank María Jesús Ortiz Iniesta for assistance with TGA measurements and Dr Marc Stuart for assistance in obtaining high resolution TEM images.

4.5 Experimental

Chemicals. Graphite flakes (Sigma-Aldrich), *ortho*-dichlorobenzene (ODCB, 98%, AR, Merck), 4-dimethylaminopyridine (DMAP, ≥ 99%, Aldrich), dimethyl-acetylene-dicarboxylate (compound **1**, Sigma-Aldrich, 99%) were used as received without further purification. Dry toluene was used from a solvent purification system (MB SPS-800). Compound **2** was synthesized according to literature procedures.[21]

Instruments. Sonication was conducted with a low-power sonication bath (Bransonic, PC 620). Centrifugation was performed with a Hermle Z323K centrifuge. Filtration was carried out with a Sintered Micro Filter holder through a 0.45 μm nylon membrane. NMR spectra were recorded using a Varian VXR-400 spectrometer (400 MHz). Fourier transform infrared spectroscopy (FTIR) was performed with a Perkin-Elmer Spectrum 400 instrument and a UATR attachment. Raman spectra at 532 nm were obtained using a home built system comprising of a iDus-DU420A CCD detector coupled to a Shamrock163i spectrograph (Andor Technology) and a 25 mW 532 nm DPSS laser (Cobolt Lasers) fibre coupled to an Olympus BX51 microscope (equipped with laserline clean up and edge filters from Semrock) with long working distance objectives. Samples for Raman analysis were prepared by spin coating a few drops of the graphene and functionalized graphene on fresh gold substrates followed by drying under vacuum. Thermal gravimetric analysis (TGA) was carried out under N_2 with a Mettler Toledo

TGA/SDTA851e system. Transmission electron microscopy (TEM) images were acquired using a PHILIPS CM12 instrument operating at 120 KV. High resolution transmission electron microscopy (TEM) images were taken using a PHILIPS CM120 instrument operating at 120 KV. Conductivity was determined using the standard four-point probe method on a Keithley 2410 Source Meter. The films were prepared by vacuum filtration of the corresponding dispersions of graphene, **1** or **2** functionalized graphene followed by drying *in vacuo* at 60 ^{o}C for 48 h.

Preparation of graphene and functionalized graphene

Preparation of graphene in ODCB: Graphite (300 mg) was sonicated for 2 h in ODCB (300 mL), and the obtained suspension was centrifuged at 3000 rpm for 30 min to remove large and thick flakes. The supernatant was decanted to afford graphene in ODCB (the concentration of graphene in ODCB was about 0.01 mg mL^{-1}).[6,10a]

Transfer of graphene from ODCB to toluene: Dry toluene was chosen as the solvent for functionalization reactions. Therefore, a solvent exchange process was carried out to transfer graphene from ODCB to dry toluene.[8a] Graphene in ODCB (200 ml) was filtered through a 0.45 μm nylon membrane, then the filter cake was redispersed in toluene (50 ml) with sonication (5 min) and filtered again. This process was repeated twice and the filter cake was dispersed in 30 ml toluene and centrifuged at 4000 rpm for 10 min. The supernatant was decanted and 30 ml dry toluene was added (under Ar atmosphere), sonicated and centrifuged again (this process was repeated twice). Finally, 35 ml of dry toluene was added to the solid residue, and the suspension was transferred into a 100 ml three-neck round bottom flask and used for the functionalization reactions.

Functionalization of graphene: Compound **1** (177.6 mg in 5 ml dry toluene) or compound **2** (360 mg in 5 ml dry toluene) and DMAP (153 mg in 5 ml dry toluene) were added dropwise into the above graphene suspension in toluene, and the mixture was reacted at 85 ^{o}C under Ar atmosphere for 3 d. The reaction mixture was filtered through a 0.45 μm nylon membrane and washed subsequently with toluene (3 times, 30 ml each time), $CHCl_3$ (3 times, 30 ml each time), water (3 times, 30 ml each time) and acetone (3 times, 30 ml each time) using repeated redispersion, sonication, and filtration steps. The final suspension in acetone was centrifuged at 4000 rpm for 20 min and the solid residue was dried under vacuum to afford the desired functionalized graphene products.

Control samples: The covalent linkage between graphene and the organic functional groups was confirmed by control experiments to confirm that the improved dispersibility is not due to physisorption. Compound **1** (177.6 mg in 5 ml dry toluene) or compound **2** (360 mg in 5 ml dry toluene) or DMAP was added dropwise into the graphene suspension in toluene and the mixture was reacted at 85 ^{o}C under Ar atmosphere for 3 d. The handling procedures were as above for the functionalized graphene.

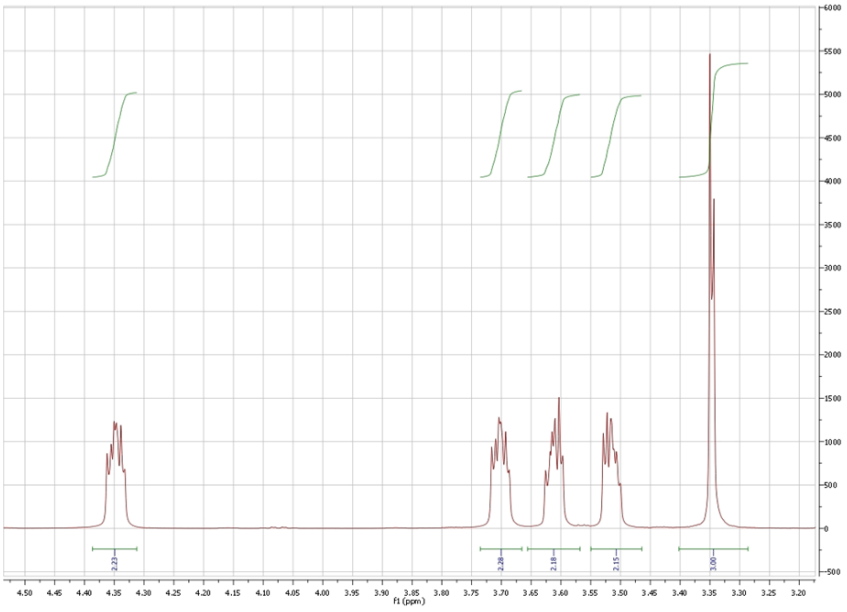

^{1}H NMR spectrum of compound **2** ($CDCl_3$, 400 MHz).

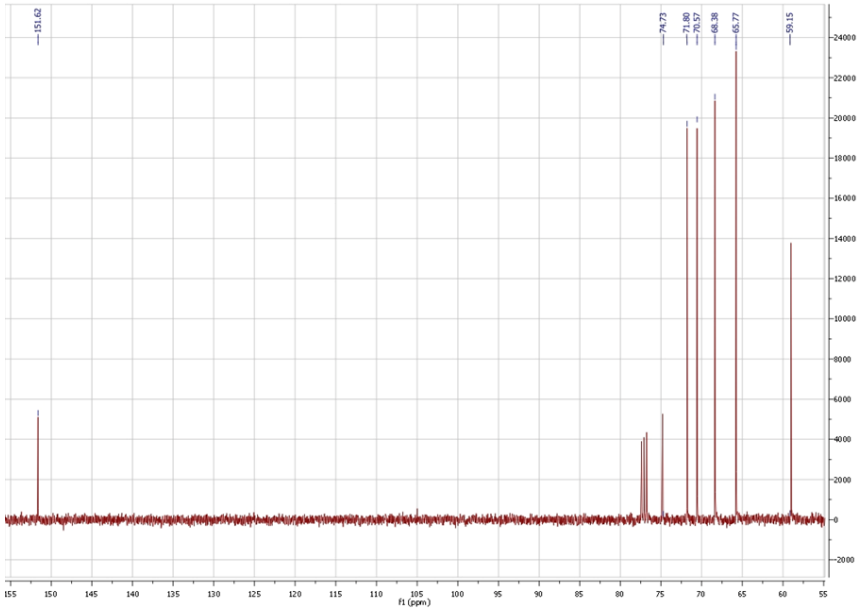

^{13}C NMR spectrum of compound **2** ($CDCl_3$, 100 MHz).

4.6 Notes and references

1. A. K. Geim and K. S. Novoselov, The rise of graphene, *Nat. Mater.*, 2007, **6**, 183.

2. (a) Y. Zhu, S. Murali, W. Cai, X. Li, J. Suk, J. Potts and R. Ruoff, Graphene and graphene oxide: synthesis, properties, and applications, *Adv. Mater.*, 2010, **22**, 3906; (b) S. J. Guo and S. J. Dong, Graphene nanosheet: synthesis, molecular engineering, thin film, hybrids, and energy and analytical applications, *Chem. Soc. Rev.*, 2011, **40**, 2644; (c) C. N. R. Rao, A. K. Sood, K. S. Subrahmanyam and A. Govindaraj, Graphene: the new two-dimensional nanomaterial, *Angew. Chem., Int. Ed.*, 2009, **48**, 7752; (d) M. Pumera, Graphene-based nanomaterials and their electrochemistry, *Chem. Soc. Rev.*, 2010, **39**, 4146.

3. X. Huang, Z. Y. Yin, S. X. Wu, X. Y. Qi, Q. Y. He, Q. C. Zhang, Q. Y. Yan, F. Boey and H. Zhang, Graphene-based materials: synthesis, characterization, properties, and applications, *Small*, 2011, **7**, 1876.

4. G. Eda, G. Fanchini and M. Chhowalla, Large-area ultrathin films of reduced graphene oxide as a transparent and flexible electronic material, *Nat. Nanotechnol.*, 2008, **3**, 270.

5. J. Wu, W. Pisula and K. Müllen, Graphenes as potential material for electronics, *Chem. Rev.*, 2007, **107**, 718.

6. Y. Hernandez, V. Nicolosi, M. Lotya, F. M. Blighe, Z. Sun, S. De, I. T. McGovern, B. Holland, M. Byrne, Y. K. Gun'ko, J. J. Boland, P. Niraj, G. Duesberg, S. Krishnamurthy, R. Goodhue, J. Hutchison, V. Scardaci, A. C. Ferrari and J. N. Coleman, High-yield production of graphene by liquid-phase exfoliation of graphite, *Nat. Nanotechnol.*, 2008, **3**, 563.

7. (a) C. E. Hamilton, J. R. Lomeda, Z. Z. Sun, J. M. Tour and A. R. Barron, High-yield organic sispersions of unfunctionalized graphene, *Nano Lett.*, 2009, **9**, 3460; (b) A. Catheline, C. Valles, C. Drummond, L. Ortolani, V. Morandi, M. Marcaccio, M. Iurlo, F. Paolucci and A. Pénicaud, Graphene solutions, *Chem. Commun.*, 2011, **47**, 5470; (c) M. Lotya, Y. Hernandez, P. J. King, R. J. Smith, V. Nicolosi, L. S. Karlsson, F. M. Blighe, S. De, Z. M. Wang, I. T. McGovern, G. S. Duesberg and J. N. Coleman, Liquid phase production of graphene by exfoliation of graphite in surfactant/water solutions, *J. Am. Chem. Soc.*, 2009, **131**, 3611.

8. (a) X. Y. Zhang, A. C. Coleman, N. Katsonis, W. R. Browne, B. J. van Wees and B. L. Feringa, Dispersion of graphene in ethanol using a simple solvent exchange method, *Chem. Commun.*, 2010, **46**, 7539; (b) W. F. van Dorp, X. Y. Zhang, B. L. Feringa, J. B. Wagner, T. W. Hansen and J. Th. M. De Hosson, Nanometer-scale lithography on microscopically clean graphene, *Nanotechnology*, 2011, **22**, 505303; (c) W. F. van Dorp, X. Y. Zhang, B. L. Feringa, T. W. Hansen, J. B. Wagner and J. Th. M. De Hosson, *ACS Nano*, 2012, **6**, 10076.

9. (a) Y. Xu, H. Bai, G. Lu, C. Li and G. Shi, Flexible graphene films via the filtration of water-soluble noncovalent functionalized graphene sheets, *J. Am. Chem. Soc.*, 2008, **130**, 5856; (b) D.-W. Lee, T. Kim and M. Lee, An amphiphilic pyrene sheet for selective functionalization of graphene, *Chem. Commun.*, 2011, **47**, 8259; (c) J. M. Englert, J. Röhrl, C. D. Schmidt, R. Graupner, M. Hundhausen, F. Hauke and A. Hirsch, Soluble graphene: generation of aqueous graphene solutions aided by a perylenebisimide-based bolaamphiphile, *Adv. Mater.*, 2009, **21**, 4265; (d) B. G. Choi, W. H. Hong, Y. M. Jung and H. S. Park, Charge transfer interactions between conjugated block copolymers and reduced graphene oxides, *Chem. Commun.*, 2011, **47**, 10293; (e) R. Hao, W. Qian, L. Zhang and Y. L. Hou, Aqueous dispersions of TCNQ-anion-stabilized graphene sheets, *Chem. Commun.*, 2008, 6576; (f) J. Malig, N. Jux, D. Kiessling, J.-J. Cid, P. Vázquez, T. Torres and D. M. Guldi, Towards tunable graphene/phthalocyanine-PPV hybrid systems, *Angew. Chem., Int. Ed.*, 2011, **50**, 3561; (g) Y. W. Hu, F. H. Li, X. X. Bai, D. Li, S. C. Hua, K. K. Wang and L. Niu, Label-free electrochemical impedance sensing of DNA hybridization based on functionalized graphene sheets, *Chem. Commun.*, 2011, **47**, 1743; (h) M. Castelain, H. J. Salavagione, R. Gomez and J. Luis Segura, Supramolecular assembly of graphene with functionalized poly(fluorene-*alt*-phenylene): the role of the anthraquinone pendant groups, *Chem. Commun.*, 2011, **47**, 7677; (i) J. Geng, B.-S. Kong, S. B. Yang and H.-T. Jung, Preparation of graphene relying on porphyrin exfoliation of graphite, *Chem. Commun.*, 2010, **46**, 5091.

10. (a) X. Y. Zhang, L. L. Hou, A. Cnossen, A. C. Coleman, O. Ivashenko, P. Rudolf, B. J. van Wees, W. R. Browne and B. L. Feringa, One-pot functionalization of graphene with porphyrin through cycloaddition reactions, *Chem. Eur. J.*, 2011, **17**, 8957; (b) M. Quintana, K. Spyrou, M. Grzelczak, W. R. Browne, P. Rudolf and M. Prato, Functionalization of graphene via 1,3-dipolar cycloaddition, *ACS Nano*, 2010, **4**, 3527; (c) V. Georgakilas, A. B.

Bourlinos, R. Zboril, T. A. Steriotis, P. Dallas, A. K. Stubos and C. Trapalis, Organic functionalisation of graphenes, *Chem. Commun.*, 2010, **46**, 1766.

11. (a) K. Loh, Q. Bao, P. Ang and J. Yang, The chemistry of graphene, *J. Mater. Chem.*, 2010, **20**, 2277; (b) L. Yan, Y. B. Zheng, F. Zhao, S. J. Li, X. F. Gao, B. Q. Xu, P. S. Weiss and Y. L. Zhao, Chemistry and physics of a single atomic layer: strategies and challenges for functionalization of graphene and graphene-based materials, *Chem. Soc. Rev.*, 2012, **41**, 97.

12. E. Bekyarova, M. E. Itkis, P. Ramesh, C. Berger, M. Sprinkle, W. A. de Heer and R. C. Haddon, Chemical modification of epitaxial graphene: spontaneous grafting of aryl groups, *J. Am. Chem. Soc.*, 2009, **131**, 1336.

13. (a) T. A. Strom, E. P. Dillon, C. E. Hamilton and A. R. Barron, Nitrene addition to exfoliated graphene: a one-step route to highly functionalized graphene, *Chem. Commun.*, 2010, **46**, 4097; (b) X. Xu, W. Lv, J. Huang, J. Li, R. Tang, J. Yan, Q. Yang, J. Qin and Z. Li, Functionalization of graphene by tetraphenylethylene using nitrene chemistry, *RSC Adv.*, 2012, **2**, 7042.

14. A. Mukherjee, J. Kang, O. Kuznetsov, Y. Sun, R. Thaner, A. Bratt, J. Lomeda, K. Kelly and W. E. Billups, Water-soluble graphite nanoplatelets formed by oleum exfoliation of graphite, *Chem. Mater.*, 2011, **23**, 9.

15. (a) H.-X. Wang, K.-G. Zhou, Y.-L. Xie, J. Zeng, N.-N. Chai, J. Li and H.-L. Zhang, Photoactive graphene sheets prepared by "click" chemistry, *Chem. Commun.*, 2011, **47**, 5747; (b) Z. Jin, T. P. McNicholas, C. Shih, Q. Wang, G. L. C. Paulus and M. S. Strano, Click chemistry on solution-dispersed graphene and monolayer CVD graphene, *Chem. Mater.*, 2011, **23**, 3362; (c) M. Castelaín, G. Martínez, P. Merino, J. Á. Martín-Gago, J. L. Segura, G. Ellis and H. J. Salavagione, Graphene functionalisation with a conjugated poly(fluorene) by click coupling: striking electronic properties in solution, *Chem. Eur. J.*, 2012, **18**, 4965.

16. (a) W. Zhang and T. M. Swager, Functionalization of single-walled carbon nanotubes and fullerenes via a dimethyl acetylenedicarboxylate-4-dimethylaminopyridine zwitterion approach, *J. Am. Chem. Soc.*, 2007, **129**, 7714; (b) W. Zhang, J. K. Sprafke, M. Ma, E. Y. Tsui, S. A. Sydlik, G. C. Rutledge and T. M. Swager, Modular functionalization of carbon nanotubes and fullerenes, *J. Am. Chem. Soc.*, 2009, **131**, 8446.

17. ^{13}C NMR spectroscopy of the two functionalized graphene samples were attempted without success, possibly due to slow relaxation due to limited

rotation rates of the large graphene flakes and the limited concentrations achieveable.

18. (a) A. C. Ferrari, J. C. Meyer, V. Scardaci, C. Casiraghi, M. Lazzeri, F. Mauri, S. Piscanec, D. Jiang, K. S. Novoselov, S. Roth and A. K. Geim, Raman spectrum of graphene and graphene layers, *Phys. Rev. Lett.*, 2006, **97**, 187401; (b) M. A. Pimenta, G. Dresselhaus, M. S. Dresselhaus, L. G. Cancado, A. Jorio and R. Saito, Studying disorder in graphite-based systems by Raman spectroscopy, *Phys. Chem. Chem. Phys.*, 2007, **9**, 1276.

19. (a) X. Zhong, J. Jin, S. W. Li, Z. Y. Niu, W. Q. Hu, R. Li and J. T. Ma, Aryne cycloaddition: highly efficient chemical modification of graphene, *Chem. Commun.*, 2010, **46**, 7340; (b) M. Quintana, A. Montellano, A. E. del Rio Castillo, G. V. Tendeloo, C. Bittencourt and M. Prato, Selective organic functionalization of graphene bulk or graphene edges, *Chem. Commun.*, 2011, **47**, 9330.

20. S. Mao, H. H. Pu and J. H. Chen, Graphene oxide and its reduction: modeling and experimental progress, *RSC Adv.*, 2012, **2**, 2643.

21. F. Reineri, A. Viale, G. Giovenzana, D. Santelia, W. Dastrù, R. Gobetto and S. Aime, New hyperpolarized contrast agents for ^{13}C-MRI from *para*-hydrogenation of oligooxyethylenic alkynes, *J. Am. Chem. Soc.*, 2008, **130**, 15047.

Chapter 5

One-pot functionalization of graphene with porphyrin through cycloaddition reactions

Abstract

Two graphene based hybrid materials, graphene-TPP (TPP: tetraphenylporphyrin) and graphene-PdTPP (PdTPP: palladium tetraphenylporphyrin) were prepared directly from pristine graphene using one pot cycloaddition reactions. The hybrid materials were characterized by UV/Vis, FTIR, TGA, TEM and Raman, luminescence spectroscopy and fluorescence/phosphorescence lifetime measurements. The covalent linkage between graphene and porphyrin was confirmed by FTIR, Raman spectroscopy and further supported by control experiments. The presence of TPP (or PdTPP) in the hybrid material was demonstrated by UV/Vis spectroscopy, and TGA data indicate that graphene-TPP and graphene-PdTPP hybrid materials contain approximately 18% TPP and 20% PdTPP by mass, respectively. The quenching and reduced lifetime of fluorescence (or phosphorescence) suggests that excited state energy/electron transfer between graphene and the covalently attached TPP (or PdTPP).

This chapter has been published:

Xiaoyan Zhang, Lili Hou, Arjen Cnossen, Anthony C. Coleman, Oleksii Ivashenko, Petra Rudolf, Bart J. van Wees, Wesley R. Browne and Ben L. Feringa, ***Chem. Eur. J.***, 2011, 17, 8957-8964.

5.1 Introduction

Graphene, a single-atom-thick layer of graphite, has attracted intense scientific interest because of its extraordinary properties,[1] such as the existence of massless Dirac fermions, a room temperature quantum Hall effect, high charge carrier mobility and gas sensing at the molecular level. It is widely anticipated that graphene will see applications in supercapacitors,[2] nanoelectronic devices,[3] chemical sensors,[4] and reinforced composite materials[5] in the near future. For such applications, large scale preparation of high purity graphene flakes is essential. Currently, graphene is typically prepared by one of the following methods: mechanical,[6] epitaxial,[7] reduction of graphene oxide[8] or solvent dispersion of graphite.[9] Further manipulation of graphene itself is rendered difficult due to its tendency to aggregate as a result of the strong π-π interactions between individual flakes. This aggregation makes fabrication of graphene-based materials difficult. For this reason, non-covalent[10] and covalent[11] methods for the functionalization of graphene have been developed. In this context, graphene-based hybrid nanomaterials (combining graphene with other functional components) have attracted widespread attention.[12-14] The hybrid nanomaterials not only combine the unique optical, electrical, magnetic, and chemical properties of each component, but also have the potential to introduce novel properties that can be applied to a diverse range of applications. The majority of reports of graphene-based hybrid nanomaterials use graphene oxide as the starting material.[15] However, the oxygen-containing functional groups of this material greatly change the intrinsic properties of graphene, therefore potentially affecting the final properties of graphene-based hybrid nanomaterials.[16] Consequently, the development of alternative routes is required. Recently, preparation of graphene using solvent dispersion methods developed by a number of groups,[9] including our group,[9f] have attracted particular interest because it holds the advantage of retaining the intrinsic properties of graphene and at the same time it maintains the dispersibility of

graphene in certain solvents. The functionalization of graphene using cycloaddition on pristine graphene is a promising approach.[17] Compared with non-covalent methods, covalent functionalization of pristine graphene with other molecules provides for stable and well defined systems. Furthermore, rational design of the process enable control over the degree of functionalization with retention of the properties of graphene. Porphyrin, a well-known and studied aromatic compound itself possesses exceptional optical and electronic properties, and has been used in fields as diverse as solar cells, sensors, catalysis and biology.[18] C_{60}-porphyrin and carbon nanotube-porphyrin hybrid materials have been prepared for a number of applications.[19] Due to the similarity of graphene with C_{60} and carbon nanotubes, hybrid materials combining graphene with porphyrin can be envisaged as being useful for applications such as in solar cells, sensors and catalysis. A distinct difference however between C_{60}/carbon nanotubes and graphene is the accessibility of the edge as well as both faces of the carbon sheet to chemical reaction.

Here we show that graphene-TPP (TPP: tetraphenylporphyrin) and graphene-PdTPP (PdTPP: palladium tetraphenylporphyrin) hybrid materials can be readily prepared using one pot cycloaddition reactions. The hybrid materials prepared are stable in solution and are characterized using a number of spectroscopic and microscopic methods.

5.2 Results

The method used for the preparation of graphene-TPP and graphene-PdTPP is shown in Scheme 1. Graphene in *ortho*-dichlorobenzene (ODCB) was prepared according to the procedure reported by Barron *et al.*[9a] Tetraphenylporphyrin monoaldehyde (TPP-CHO) and palladium tetraphenylporphyrin monoaldehyde (PdTPP-CHO) were synthesized according to literature procedures (see experimental section).[20,21] In brief, graphene in ODCB, sarcosine, and TPP-

CHO (or PdTPP-CHO) were reacted at 160 ^{o}C for one week, and the hybrid materials were purified by multiple filtration/redispersion cycles.

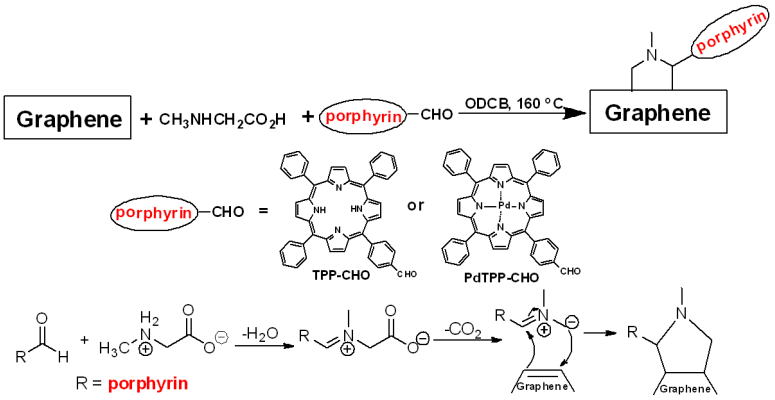

Scheme 1. Synthesis of graphene-TPP and graphene-PdTPP hybrid materials, and the accepted mechanism for the reaction.

The presence of TPP (or PdTPP) in the graphene-TPP (or graphene-PdTPP) hybrid material is confirmed by UV/Vis absorption spectroscopy. As shown in Figure 1a, TPP-CHO in DMF shows a Soret band at 419 nm together with, relatively less intense, Q bands.[22] The absorption spectrum of graphene-TPP in DMF shows a broader absorption peak at ca. 421 nm and weaker Q-bands, that are attributed to the absorption of the TPP unit in the graphene-TPP hybrid material. The absorption spectra for PdTPP and graphene-PdTPP are shown in Figure 1b. A strong Soret absorption band at 416 nm and also a weaker Q band at 523 nm were observed.[23] For the graphene-PdTPP hybrid material, two broadened bands are observed at 419 and 525 nm and assigned to the absorption of the covalently tethered PdTPP. In control reactions for both TPP and PdTPP, where the reaction was performed without sarcosine (see experimental section), the UV/Vis absorption spectra of the graphene materials recovered do not exhibit the typical porphyrin absorption bands. This supports the conclusion that the porphyrin molecules in the graphene-TPP and graphene-

PdTPP hybrid materials are not physisorbed but instead attached covalently. In addition, the Soret band of both porphyrins show a small red-shift when covalently attached to graphene, which suggests that there may be interactions between graphene and porphyrin molecules in the hybrid materials.

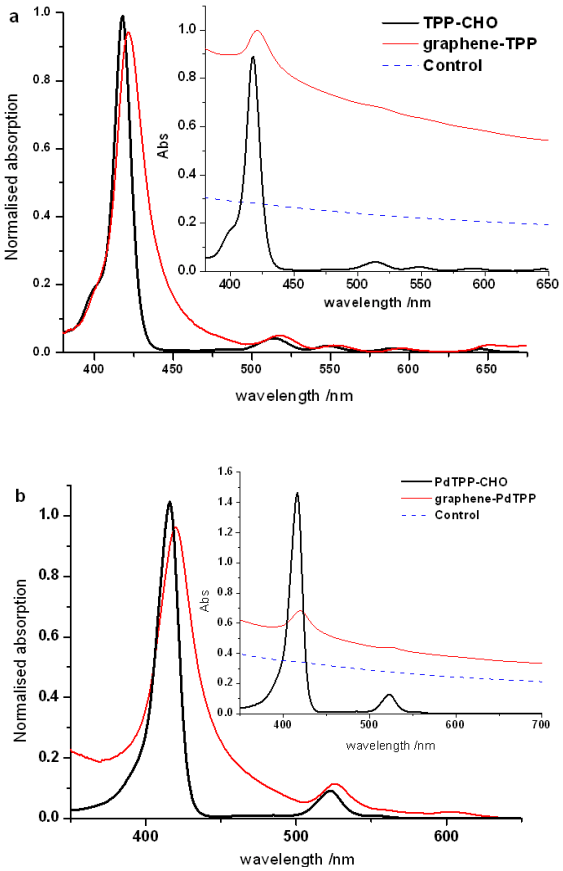

Figure 1. UV/Vis absorption spectra of (a) TPP-CHO (black solid line), graphene-TPP (red solid line, baseline corrected) {Inset: TPP-CHO (black solid line), graphene-TPP (red solid line) and the control sample (blue dashed line)} in DMF. (b) PdTPP-CHO (black solid line), graphene-PdTPP (red solid line, baseline corrected) {Inset: PdTPP-CHO (black solid line), graphene-PdTPP (red solid line) and the control sample (blue dashed line)} in DMF.

Additional confirmation of the successful hybridization of PdTPP with graphene comes from the X-ray photoelectron spectrum collected on a dropcast film of the hybrid material on a polycrystalline copper substrate. Figure 2 shows the Pd 3d core level region which indicates the presence of Pd. The Pd $3d_{5/2}$ binding energy of 338.5 eV is in agreement with Pd bond to N as observed for similar compounds.[24]

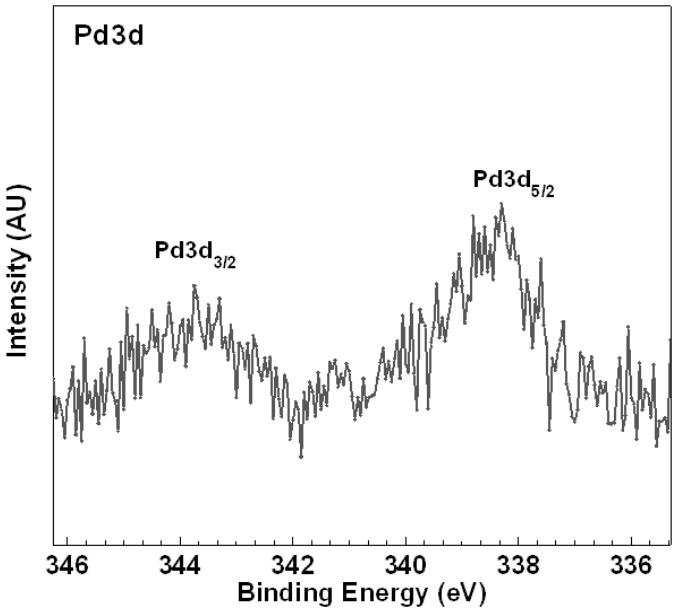

Figure 2. X-ray photoelectron spectrum of the Pd 3d core level region measured on a dropcast graphene-PdTPP film on Cu.

The loading of TPP or PdTPP in the graphene-TPP and graphene-PdTPP hybrid materials was determined by TGA. Figure 3 shows the TGA curves of graphene, graphene-TPP and graphene-PdTPP. The weight loss observed for graphene is assigned to the defects caused by sonication, which are apparent also from the D/G band ratio in the Raman spectra and release of trapped solvents. Compared to graphene, graphene-TPP and graphene-PdTPP show approximately 18% and 20% weight loss between 250 ^{o}C and 500 ^{o}C,

respectively. This weight loss corresponds to the loss of TPP or PdTPP molecules attached covalently to graphene. Accordingly, the degree of functionalization was estimated to be one TPP group per 235 carbon atoms in graphene-TPP (0.42%), and one PdTPP group per 240 carbon atoms in graphene-PdTPP (0.41%).[25]

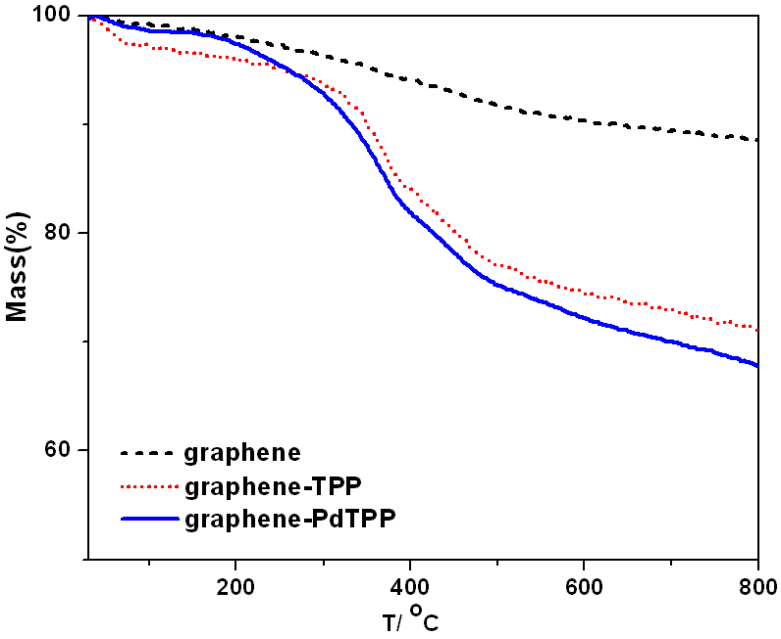

Figure 3. TGA curves of graphene (black solid line), graphene-TPP (red solid line) and graphene-PdTPP (blue solid line).

Figure 4a shows the FTIR spectra of graphene, graphene-TPP and graphene-PdTPP. The spectrum of graphene is almost featureless, indicative of a low content of defects. While for the graphene-TPP and graphene-PdTPP, some features of TPP and PdTPP were observed in the range between 1000–1500 cm^{-1}. The absence of a carbonyl stretch at about 1700 cm^{-1} for the graphene-TPP and graphene-PdTPP hybrid compared to the spectra of free TPP-CHO and PdTPP-CHO (Figure 4b) indicates reaction of the aldehyde moieties.

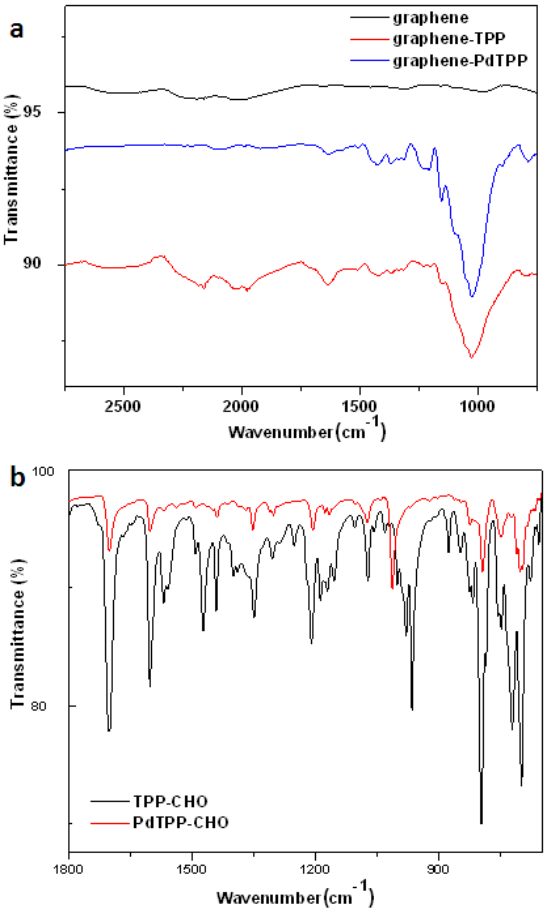

Figure 4. (a) FTIR spectra of graphene (top, black), graphene-PdTPP (middle, blue) and graphene-TPP (bottom, red). (b) FTIR spectra of TPP-CHO (black) and PdTPP-CHO (red).

Additional evidence of functionalization is provided by Raman spectroscopy. The Raman spectra of graphite, graphene, graphene-TPP and graphene-PdTPP are shown in Figure 5. For the graphitic materials, the typical Raman bands are: a defect-induced D band at 1350 cm^{-1}, an in-plane vibration mode of sp^2 hybridized carbon at 1580 cm^{-1} (G band), and a two phonon double resonance process at ca. 2700 cm^{-1} (2D band). The D band of graphite is almost completely absent, and the 2D band consists of two components with the main

peak at ca. 2718 cm^{-1}.[26] Graphene shows a weak D band and a strong G band at 1580 cm^{-1}, with a D/G ratio of 0.22. Both graphene-TPP and graphene-PdTPP show an increased D/G ratio (0.40 and 0.42, respectively) compared with graphene. The increased D/G ratio is consistent with the functionalization of graphene through covalent bonding.[17] It is worth mentioning that, the 2D band for graphene and functionalized graphene is shifted to 2700 cm^{-1} compared with graphite. Due to the small size of the graphene flakes and the aggregation of graphene when deposited on the substrate, it is difficult to distinguish single-layer graphene by Raman spectroscopy in the present case. However, by comparing the position and shape of the spectra of graphene and functionalized graphene with graphite, we identify the graphene flakes as a mixture of single and few-layer graphene.[26,17a]

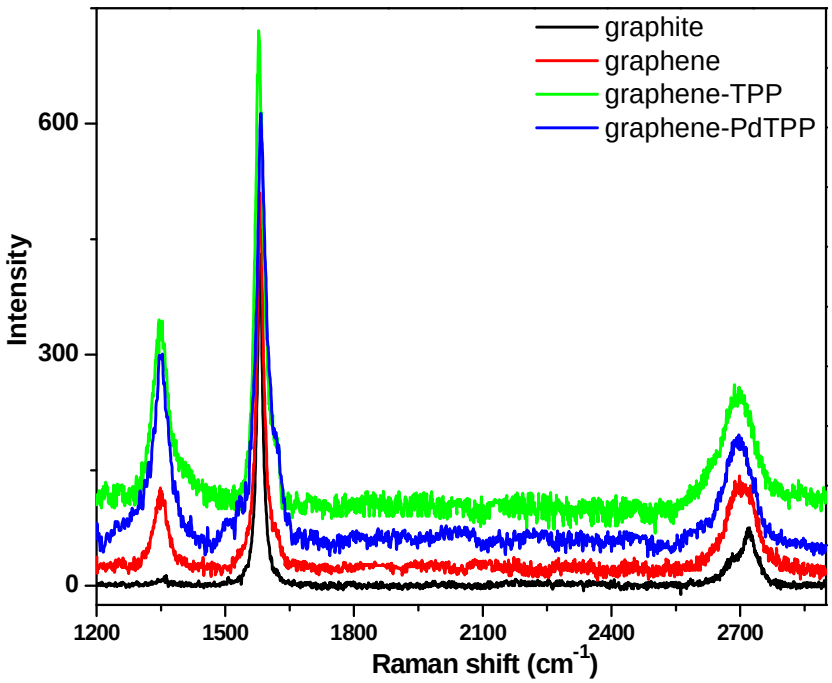

Figure 5. Raman spectra (bottom to top) of graphite, graphene, graphene-PdTPP and graphene-TPP (λ_{exc} = 532 nm).

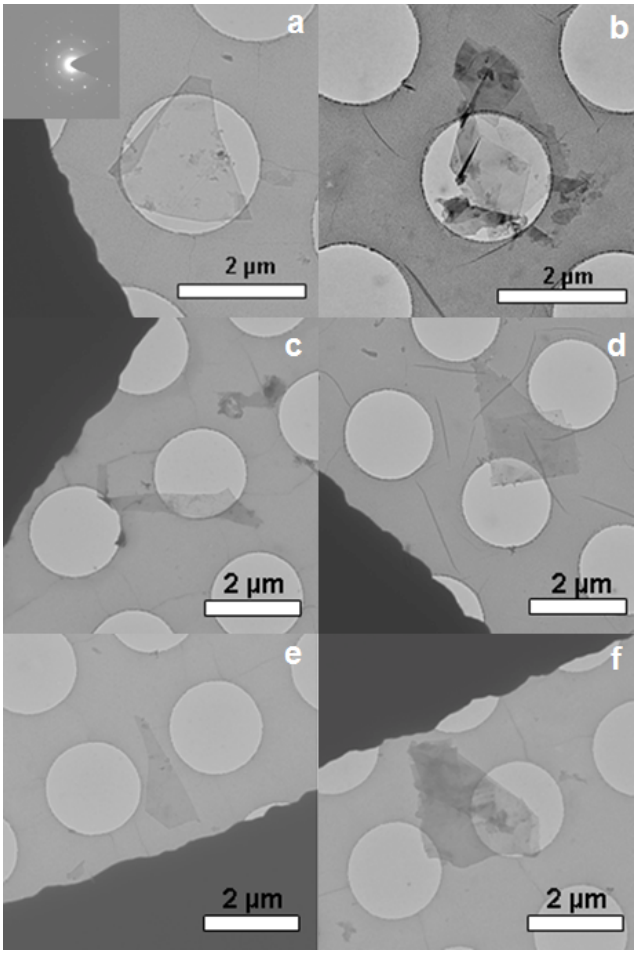

Figure 6. TEM images of graphene (a, b), graphene-TPP (c, d) and graphene-PdTPP (e, f). The samples were prepared by drop casting onto holey carbon grids.

The morphology of graphene, graphene-TPP and graphene-PdTPP were investigated by TEM analysis. Figure 6a shows a single-layer graphene flake, as indicated by the electron diffraction pattern (Figure 6a, inset, the intensity of the innermost spots is stronger than the outer spots).[9b,9f] There are also a large proportion of few-layer graphene flakes (Figure 6b). As expected,[9a] the graphene starting material consists of single- and few-layer graphene flakes.

After the cycloaddition reactions, little change in the morphology of graphene-TPP and graphene-PdTPP hybrid materials was observed (Figure 6c-6f, Figure 7 and 8).

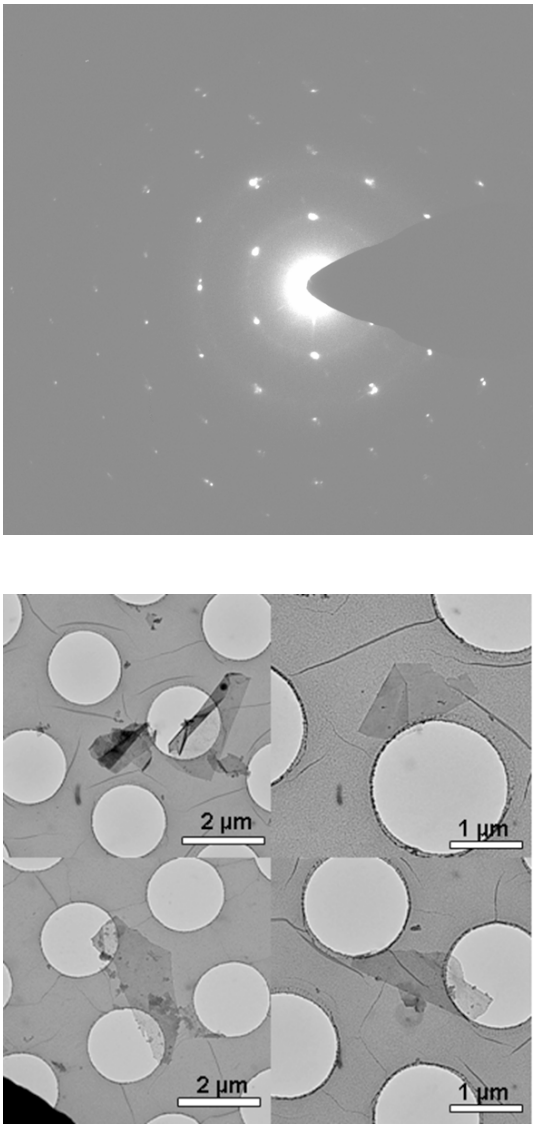

Figure 7. The diffraction pattern shown in Figure 6a (upper image) and additional TEM images of graphene-TPP hybrid material (bottom image).

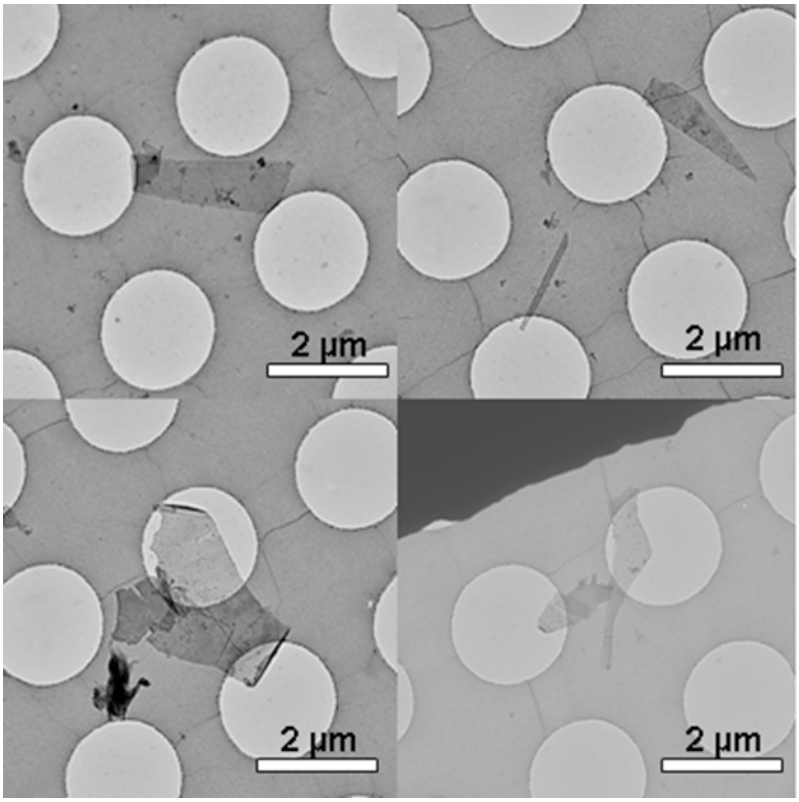

Figure 8. Additional TEM images of graphene-PdTPP hybrid material.

The interaction between graphene and porphyrin in the hybrid materials was studied by fluorescence (or phosphorescence, in the case of PdTPP) spectroscopy. The Soret band absorption intensities in the graphene-porphyrin hybrids were equivalent to the free porphyrin for luminescence measurements, taking into consideration the scattering by graphene (Figure 9a). When excited at 410 nm, free TPP-CHO shows strong fluorescence at 650 nm and 710 nm (Figure 9b, solid line). In contrast, for the graphene-TPP hybrid, the fluorescence is quenched significantly (Figure 9b, dotted line). The fluorescence quantum yield is reduced from 4% to 0.3% for TPP-CHO and graphene-TPP, respectively.

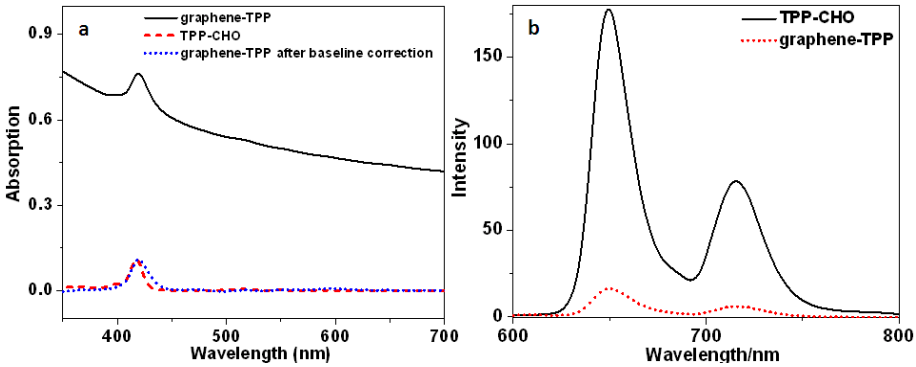

Figure 9. (a) UV/Vis absorption spectra of graphene-TPP (solid line) and TPP-CHO (dashed line) used to obtain the emission spectra shown in Figure 9b and of graphene-TPP after baseline correction (dotted line). The concentrations of porphyrin in both TPP-CHO and graphene-TPP were equivalent (0.7 µM) according to the intensity of the Soret band. (b) Fluorescence emission spectra of TPP-CHO (solid line) and graphene-TPP (dotted line) at λ_{exc} = 410 nm in DMF. The concentration of porphyrin in both samples (*i.e.* TPP-CHO and graphene-TPP) was equivalent (0.7 µM), as determined by the intensity of the Soret band taking into account the background due to scattering of graphene.

A similar quenching behavior is observed for the graphene-PdTPP hybrid material (Figure 10b). The strong phosphorescence at 710 nm for PdTPP is also quenched in the hybrid material. The phosphorescence quantum yield is reduced from 0.62% for PdTPP to below 0.01% for graphene-PdTPP.

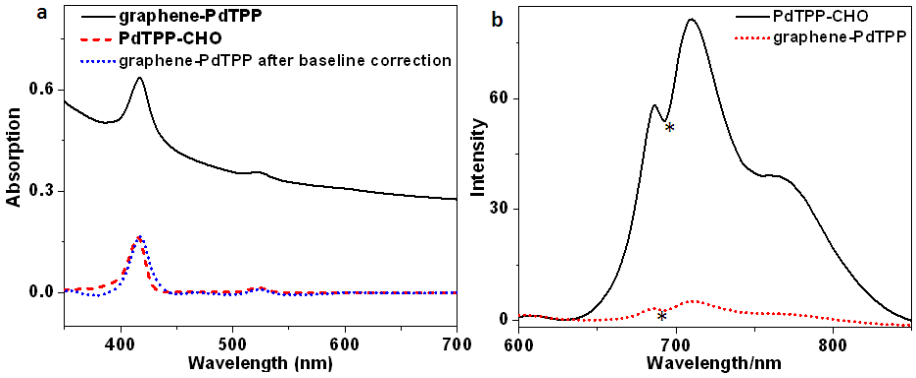

Figure 10. (a) UV/Vis absorption spectra of graphene-PdTPP (solid line) and PdTPP-CHO (dashed line) used to obtain the emission spectra shown in Figure 10b and of graphene-PdTPP after baseline correction (dotted line). The concentrations of porphyrin in both PdTPP-CHO and graphene-PdTPP were equivalent (0.6 μM) according to the intensity of the Soret band. (b) Phosphorescence emission spectra of PdTPP-CHO (solid line) and graphene-PdTPP (dotted line) at λ_{exc} = 410 nm. The concentration of porphyrin in both PdTPP-CHO and graphene-PdTPP were kept the same (0.6 μM) according to the Soret band absorption intensity (Figure 8a). *The dip in the spectrum is an instrumental artifact.

The luminescence lifetimes of both TPP-CHO (or PdTPP-CHO) and graphene-TPP (or PdTPP) show that there are strong interactions between the graphene and TPP (or PdTPP). For graphene-TPP the fluorescence decay is biexponential, with a short component of <500 ps and a longer component of 6.2 ns. The short component accounts for the major part of the decay and confirms that rapid quenching of the porphyrin singlet excited state occurs. The biexponential nature of the decay may reflect the location of the porphyrin on the graphene, i.e. on the basal plane or near the edge. The relatively minor contribution of the longer lifetime component is consistent with such an assignment. Comparison of the fluorescence spectra of the covalently modified

graphene-TPP with both free TPP-CHO and a matched mixture of TPP-CHO with graphene show that collisonal (dynamic) quenching is not significant (Figure 11).

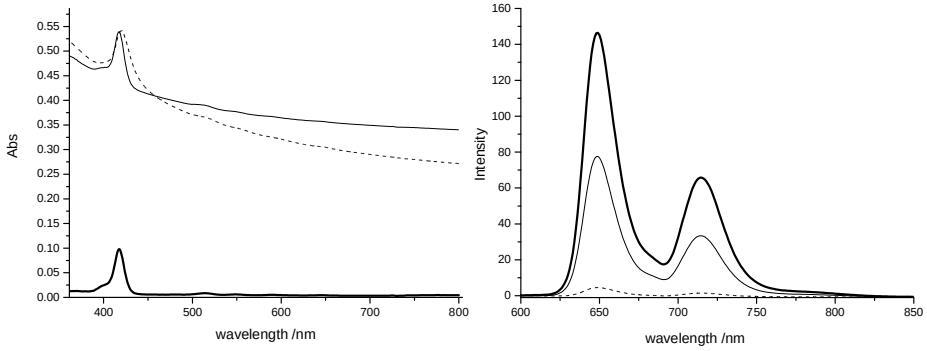

Figure 11. (left) UV/Vis absorption and (right) fluorescence (λ_{exc} = 410 nm) spectra of solutions of TPP-CHO (thick solid line), graphene-TPP (thin dotted line) and a mixture of TPP-CHO and graphene (thin solid line). The absorption at 410 nm (attributable to the porphyrin component in each case was matched for comparison of the intensity of the emission spectra. The attenuation due to scattering by the graphene in the wavelength range of the fluorescence spectrum and at 410 nm is estimated to result in a 50% loss in emission intensity. Hence the decrease in emission intensity of the TPP-CHO in the presence of graphene is attributable primarily to attenuation and not only dynamic quenching.

The phosphorescence decay lifetime of PdTPP-CHO is 44 μs whereas for the graphene-PdTPP hybrid material the phosphorescence quantum yield and lifetime are diminished considerably and are non-exponential. Fitting of the decay of graphene-PdTPP with a biexponential function gives the values 80 and 660 ns, with the latter component being the lesser of the two components. The phosphorescence decay lifetime of the palladium porphyrin is in the microsecond time range and hence in contrast to fluorescence,

phosphorescence can be quenched dynamically as well as statically. Dynamic quenching is, however, not as efficient as static quenching as shown by matched solutions, of PdTPP-CHO mixed with graphene, and of graphene-PdTPP, where the emission intensity of the covalently attached porphyrin is substantially less than that of the free PdTPP-CHO/graphene mixture (Figure 12).

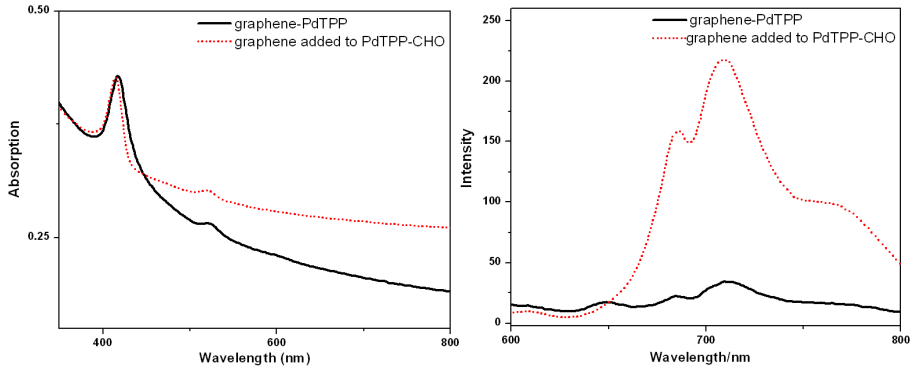

Figure 12. (left) UV/Vis absorption and (right) phosphorescence (λ_{exc} = 410 nm) spectra of solutions of graphene-PdTPP (solid line) and a mixture of PdTPP-CHO with graphene (dotted line). The absorption at 410 nm (attributable to the porphyrin component in each case) was matched for comparison of the intensity of the emission spectra. The attenuation due to scattering by the graphene in the wavelength range of the phosphorescence spectrum and at 410 nm is estimated to result in a ca. 40% loss in emission intensity. Hence the decrease in emission intensity of the PdTPP-CHO in the presence of graphene is attributable primarily to attenuation and not only dynamic quenching.

The absence of absorption bands of the porphyrin in UV/Vis absorption spectra for the control samples, prepared by the same procedures as for graphene-TPP and graphene-PdTPP, the disappearance of aldehyde absorption bands in the FTIR spectra of graphene-TPP and graphene-PdTPP, the presence of Pd

determined by XPS and the increased D/G ratio in the Raman spectra for both of the hybrid materials, all indicate the successful functionalization of graphene. Based on TGA data, the degree of functionalization of these two hybrid materials is relatively low, which allows for extended patches of undisturbed graphene. The reduced emission lifetimes for both of the hybrid materials is in agreement with the fluorescence (or phosphorescence) quenching and the reduction in emission quantum yield, indicates that either energy or electron transfer processes between graphene and the attached porphyrin molecules occurs.[27]

5.3 Conclusions

In summary, graphene-TPP and graphene-PdTPP hybrid materials have been successfully prepared using one pot cycloaddition reactions. The presence of TPP or PdTPP in the hybrid materials was confirmed by UV/Vis absorption spectroscopy and XPS. Fluorescence and phosphorescence quenching is observed with a concomitant decrease in excited state lifetimes. These observations confirm that energy and/or electron transfer quenching between graphene and the covalently bound porphyrin molecules occurs. The amount of TPP or PdTPP present in the hybrid materials was determined by TGA, and the covalent linkage was confirmed by Raman, FTIR, and further supported by control experiments. TEM images show that the morphology of the hybrid materials is not affected by the cycloaddition functionalization processes. The relatively low degree of functionalization of these two hybrid materials may allow for retention of graphene's intrinsic properties, especially in comparison with materials prepared via graphene oxides for example. Considering the remarkable properties of both graphene and porphyrin, these two hybrid materials may have potential applications in a number of areas, such as solar cells, sensors and catalysis.[19]

5.4 Perspective

Combining photoactive materials with graphene to form donor-acceptor hybrid systems are rapidly developing, mainly aiming at solar energy harvesting applications. In addition to porphyrin, other aromatic compounds such as phthalocyanines, have been covalently attached onto graphene using similar approaches as described in this chapter.[28] For future directions, fundamental studies on the electron and/or energy transfer processes and applications in photoelectrochemical cells should be performed.

5.5 Acknowledgement

We thank Dr I. Melián-Cabrera for TGA measurements, H.M.M. Hesp for assistance with TCSPC and Raman spectroscopy, Oleksii Ivashenko for recording the XPS spectrum, Arjen Cnossen for providing TPP-CHO, and Lili Hou for quantum yield measurements.

5.6 Experimental

Chemicals: Graphite flakes (Sigma-Aldrich), sarcosine (98%, Sigma-Aldrich) and *ortho*-dichlorobenzene (ODCB, 98%, AR, Merck) were used as received without further purification. 5-(4-Methylcarboxyphenyl)-10,15,20-triphenylporphyrin (TPP-COOMe) was obtained according to literature procedures.[20] 5-(4-Formylphenyl)-10,15,20-triphenylporphyrin (TPP-CHO) was synthesized from TPP-COOMe by a reduction/oxidation method (see below). Palladation of TPP-CHO was performed according to the general method published by Lindsey and co-workers.[21]

Instruments: Sonication was conducted using a low power sonication bath (Bransonic, PC 620). Centrifugation was performed on a Hermle Z323K Centrifuge. Filtration was carried out using a Sintered Micro Filter holder through a 0.45 μm nylon membrane. UV/Vis absorption spectra were obtained

on a JASCO V-630 UV/Vis Spectrometer. Fluorescence and phosphorescence spectra were measured on a JASCO FP-6200 Spectrofluorometer. Quantum yield measurements were determined using $[Ru(bpy)_3](PF_6)_2$ in water as a reference.[29] Fluorescence lifetime measurements were performed using a time-correlated single photon counting system, and detected using a microchannel plate PMT coupled with 630 nm long pass filter. The light source is a Ti:Sapphire laser (400 nm, 1.9 MHz). Phosphorescence lifetime measurements were obtained using a home built system comprising of a Zolix Omni-λ 300 monochromator coupled with a Zolix PMTH-S1-CR131 PMT detector. Transients were digitized using a Tektronix DPO 4032 Digital Phosphor Oscilloscope. The light source is an Innolas 400 Nd:YAG laser (excitation at 532 nm, 10 Hz, 40 mW) with a Si-diode trigger sensor. Solutions for phosphorescence measurements were degassed by at least three freeze-pump-thaw cycles. X-ray photoelectron spectroscopy (XPS) data were collected on a dropcast sample of graphene-PdTPP on polycrystalline Cu using a Surface Science SSX-100 ESCA instrument equipped with a monochromatic Al K_α X-ray source ($h\nu$ = 1486.6 eV). The takeoff angle between the spectrometer detector and the normal to the surface was 37°. Binding energies (± 0.1 eV) were referenced to the $Cu2p_{3/2}$ photoemission line at a binding energy of 932.7 eV.[30] Thermal gravimetric analysis (TGA) was performed under N_2 atmosphere on a Mettler Toledo TGA/SDTA851e system. Transmission electron microscopy (TEM) characterization was performed using a PHILIPS CM10 operating at 100 KV. Raman spectra were recorded on a JOBIN-YVON model T 64000 triple grating spectrometer (excitation at 532 nm). Raman samples were prepared by drop casting a few drops of the graphene and functionalized graphene on clean gold substrates and then dried under vacuum. Fourier Transform Infrared Spectroscopy (FTIR) were collected using a Perkin Elmer Spectrum 400 equipped with a UATR attachment.

Synthesis of TPP-CHO: TPP-COOMe (87 mg, 0.129 mmol) was dissolved in freshly distilled CH_2Cl_2 (5 mL) at 0 ºC. $LiAlH_4$ (0.3 mL of a 1.0 M solution in CH_2Cl_2, 0.3 mmol) was added dropwise. The mixture was allowed to warm to RT and stirred for 2 h, followed by the addition of MeOH (1 mL). The reaction mixture was partitioned between CH_2Cl_2 (30 mL) and sat. aqueous Rochelle salt solution (30 mL). The organic layer was separated, dried on Na_2SO_4 and concentrated. The residue was dissolved in THF (5 mL) and MnO_2 (56 mg, 0.64 mmol) was added. The mixture was vigorously stirred at 40 ºC for 4 h and then filtered through a silica plug (CH_2Cl_2). The filtrate was concentrated and recrystallized (CH_2Cl_2/MeOH, layer addition) to give TPP-CHO (63 mg, 76%) as a purple solid. Spectroscopic data is in accordance with the literature.[31]

Preparation of graphene: Graphite (100 mg) was sonicated for 2 h in ODCB (100 mL), and then centrifuged at 3000 rpm for 30 min. The supernatant was decanted to obtain graphene in ODCB. The concentration of graphene in ODCB was 0.01 mg/ml.

Preparation of graphene-TPP and graphene-PdTPP hybrid materials: The procedure for the preparation of graphene-TPP and graphene-PdTPP hybrid materials is shown in Scheme 1. Graphene in ODCB (50 mL), sarcosine (25 mg), and TPP-CHO (or PdTPP-CHO) (20 mg) were placed in a 100 mL round-bottom flask, and stirred at 160 ºC under a N_2 atmosphere for 1 week. The reaction mixture was filtered through a 0.45 μm nylon membrane. The obtained filter cake was washed subsequently with ODCB, DMF, and $CHCl_3$ several times using repeated redispersion, sonication and filtration steps. The final suspension in $CHCl_3$ was centrifuged at 5000 rpm for 30 min. The precipitate was dried under vacuum to obtain the desired graphene-TPP or graphene-PdTPP hybrid materials.

Control samples: In order to confirm the covalent linkage between TPP (or PdTPP) and graphene, control samples were prepared. Graphene in ODCB (50

mL), and TPP-CHO (or PdTPP-CHO) (20 mg) were placed in a 100 mL round-bottom flask, and stirred at 160 ^{o}C under a N_2 atmosphere for 1 week (in the absence of sarcosine). The handling procedures were as above for the hybrid materials.

5.7 Notes and references

1. (a) A. K. Geim and K. S. Novoselov, The rise of graphene, *Nat. Mater.*, 2007, **6**, 183; (b) A. K. Geim, Graphene: status and prospects, *Science*, 2009, **324**, 1530; (c) M. J. Allen, V. C. Tung and R. B. Kaner, Honeycomb carbon: a review of graphene, *Chem. Rev.*, 2010, **110**, 132; (d) C. N. R. Rao, A. K. Sood, K. S. Subrahmanyam and A. Govindaraj, Graphene: the new two-dimensional nanomaterial, *Angew. Chem. Int. Ed.*, 2009, **48**, 7752; (e) K. P. Loh, Q. L. Bao, P. K. Ang and J. X. Yang, The chemistry of graphene, *J. Mater. Chem.*, 2010, **20**, 2277; (f) Y. Zhu, S. Murali, W. Cai, X. Li, J. Suk, J. Potts and R. Ruoff, Graphene and graphene oxide: synthesis, properties, and applications, *Adv. Mater.*, 2010, **22**, 3906.

2. (a) M. D. Stoller, S. Park, Y. W. Zhu, J. An and R. S. Ruoff, Graphene-based ultracapacitors, *Nano Lett.*, 2008, **8**, 3498; (b) H. Wang, H. Casalongue, Y. Liang and H. J. Dai, $Ni(OH)_2$ nanoplates grown on graphene as advanced electrochemical pseudocapacitor materials, *J. Am. Chem. Soc.*, 2010, **132**, 7472; (c) Z. Wu, W. Ren, D. Wang, F. Li, B. Liu and H. M. Cheng, High-energy MnO_2 nanowire/graphene and graphene asymmetric electrochemical capacitors, *ACS Nano*, 2010, **4**, 5835;

3. (a) C. Jozsa, M. Popinciuc, N. Tombros, H. T. Jonkman and B. J. van Wees, Electronic spin drift in graphene field-effect transistors, *Phys. Rev. Lett.*, 2008, **100**, 236603; (b) K. S. Kim, Y. Zhao, H. Jang, S. Y. Lee, J. M. Kim, K. S. Kim, J.-H. Ahn, P. Kim, J.-Y. Choi and B. H. Hong, Large-scale pattern growth of graphene films for stretchable transparent electrodes, *Nature*, 2009, **457**, 706; (c) X. Wang, L. J. Zhi and K. Müllen, Transparent, conductive graphene electrodes for dye-sensitized solar cells, *Nano Lett.*, 2008, **8**, 323; (d) X. Wang, Y. Ouyang, X. Li, H. Wang, J. Guo and H. Dai, Room-temperature all-semiconducting sub-10-nm graphene nanoribbon field-effect transistors, *Phys. Rev. Lett.*, 2008, **100**, 206803; (e) C. Di, D. Wei, G. Yu, Y. Liu, Y. Guo and D. Zhu, Patterned graphene as source/drain electrodes for bottom-contact organic field-effect transistors, *Adv. Mater.*, 2008, **20**, 3289.

4. (a) F. Schedin, A. K. Geim, S. V. Morozov, E. W. Hill, P. Blake1, M. I. Katsnelson and K. S. Novoselov, Detection of individual gas molecules adsorbed on graphene, *Nat. Mater.*, 2007, **6**, 652; (b) J. D. Fowler, M. J. Allen,

V. C. Tung, Y. Yang, R. B. Kaner and B. H. Weiller, Practical chemical sensors from chemically derived graphene, *ACS Nano*, 2009, **3**, 301; (c) Y. Q. Wen, F. F. Xing, S. J. He, S. P. Song, L. H. Wang, Y. T. Long, D. Li and C. Fan, A graphene-based fluorescent nanoprobe for silver(I) ions detection by using graphene oxide and a silver-specific oligonucleotide, *Chem. Commun.*, 2010, **46**, 2596; (d) C. Lu, J. Li, J. Liu, H. Yang, X. Chen and G. Chen, Increasing the sensitivity and single-base mismatch selectivity of the molecular beacon using graphene oxide as the "nanoquencher", *Chem. Eur. J.*, 2010, **16**, 4889; (e) Q. Zhang, Y. Qiao, F. Hao, L. Zhang, S. Wu, Y. Li, J. Li and X. Song, Fabrication of a biocompatible and conductive platform based on a single-stranded DNA/graphene nanocomposite for direct electrochemistry and electrocatalysis, *Chem. Eur. J.*, 2010, **16**, 8133.

5. (a) S. Stankovich, D. A. Dikin, G. H. B. Dommett, K. M. Kohlhaas, E. J. Zimney, E. A. Stach, R. D. Piner, S. T. Nguyen and R. S. Ruoff, Graphene-based composite materials, *Nature*, 2006, **442**, 282; (b) J. F. Shen, Y. Z. Hu, C. Li, C. Qin and M. Ye, Synthesis of amphiphilic graphene nanoplatelets, *Small*, 2009, **5**, 82; (c) D. Cai and M. Song, Recent advance in functionalized graphene/polymer nanocomposites, *J. Mater. Chem.*, 2010, **20**, 7906; (d) T. Ramanathan, A. Abdala, S. Stankovich, D. Dikin, M. Herrera-Alonso, R. Piner, D. Adamson, H. Schniepp, X. Chen, R. Ruoff, S. Nguyen, I. Aksay, R. Prud'Homme and L. Brinson, Functionalized graphene sheets for polymer nanocomposites, *Nat. Nanotechnol.*, 2008, **3**, 327.

6. K. S. Novoselov, A. K. Geim, S. V. Morozov, D. Jiang, Y. Zhang, S. V. Dubonos, I. V. Grigorieva and A. A. Firsov, Electric field effect in atomically thin carbon films, *Science*, 2004, **306**, 666.

7. (a) P. W. Sutter, J. I. Flege and E. A. Sutter, Epitaxial graphene on ruthenium, *Nat. Mater.*, 2008, **7**, 406; (b) J. Coraux, A. T. N'Diaye, C. Busse and T. Michely, Structural coherency of graphene on Ir(111), *Nano Lett.*, 2008, **8**, 565.

8. (a) S. Stankovich, D. A. Dikin, R. D. Piner, K. A. Kohlhaas, A. Kleinhammes, Y. Jia, Y. Wu, S. T. Nguyen and R. S. Ruoff, Synthesis of graphene-based nanosheets via chemical reduction of exfoliated graphite oxide, *Carbon*, 2007, **45**, 1558; (b) D. Li, M. B. Muller, S. Gilje, R. B. Kaner and G. G. Wallace, Processable aqueous dispersions of graphene nanosheets, *Nat. Nanotechnol.*, 2008, **3**, 101; (c) H. L. Wang, J. T. Robinson, X. L. Li and H. J. Dai, Solvothermal reduction of chemically exfoliated graphene sheets, *J. Am. Chem. Soc.*, 2009, **131**, 9910; (d) J. L. Zhang, H. J. Yang, G. X. Shen, P. Cheng, J. Y. Zhang and S. W. Guo, Reduction of graphene oxide via L-ascorbic acid, *Chem. Commun.*, 2010, **46**, 1112; (e) M. Zhou, Y. L. Wang, Y. M. Zhai, J. F. Zhai, W. Ren, F. A. Wang and S. J. Dong, Controlled synthesis of large-area

and patterned electrochemically reduced graphene oxide films, *Chem. Eur. J.*, 2009, **15**, 6116; (f) G. Cravotto and P. Cintas, Sonication-assisted fabrication and post-synthetic modifications of graphene-like materials, *Chem. Eur. J.*, 2010, **16**, 5246.

9. (a) C. E. Hamilton, J. R. Lomeda, Z. Z. Sun, J. M. Tour and A. R. Barron, High-yield organic dispersions of unfunctionalized graphene, *Nano Lett.*, 2009, **9**, 3460; (b) Y. Hernandez, V. Nicolosi, M. Lotya, F. M. Blighe, Z. Y. Sun, S. De, I. T. McGovern, B. Holland, M. Byrne, Y. K. Gun'ko, J. J. Boland, P. Niraj, G. Duesberg, S. Krishnamurthy, R. Goodhue, J. Hutchison, V. Scardaci, A. C. Ferrari and J. N. Coleman, High-yield production of graphene by liquid-phase exfoliation of graphite, *Nat. Nanotechnol*., 2008, **3**, 563; (c) P. Blake, P. D. Brimicombe, R. R. Nair, T. J. Booth, D. Jiang, F. Schedin, L. A. Ponomarenko, S. V. Morozov, H. F. Gleeson, E. W. Hill, A. K. Geim and K. S. Novoselov, Graphene-based liquid crystal device, *Nano Lett.*, 2008, **8**, 1704; (d) A. B. Bourlinos, V. Georgakilas, R. Zboril, T. A. Steriotis and A. K. Stubos, Liquid-phase exfoliation of graphite towards solubilized graphenes, *Small*, 2009, **5**, 1841; (e) X. Q. Wang, P. F. Fulvio, G. A. Baker, G. M. Veith, R. R. Unocic, S. M. Mahurin, M. F. Chi and S. Dai, Direct exfoliation of natural graphite into micrometre size few layers graphene sheets using ionic liquids, *Chem. Commun*., 2010, **46**, 4487; (f) X. Y. Zhang, A. C. Coleman, N. Katsonis, W. R. Browne, B. J. van Wees and B. L. Feringa, Dispersion of graphene in ethanol using a simple solvent exchange method, *Chem. Commun.*, 2010, **46**, 7539; (g) D. Rangappa, K. Sone, M. Wang, U. K. Gautam, D. Golberg, H. Itoh, M. Ichihara and I. Honma, Rapid and direct conversion of graphite crystals into high-yielding, good-quality graphene by supercritical fluid exfoliation, *Chem. Eur. J.*, 2010, **16**, 6488.

10. (a) S. Stankovich, R. D. Piner, X. Q. Chen, N. Q. Wu, S. T. Nguyen and R. S. Ruoff, Stable aqueous dispersions of graphitic nanoplatelets via the reduction of exfoliated graphite oxide in the presence of poly(sodium 4-styrenesulfonate), *J. Mater. Chem.*, 2006, **16**, 155; (b) Y. X. Xu, H. Bai, G. W. Lu, C. Li and G. Q. Shi, Flexible graphene films via the filtration of water-soluble noncovalent functionalized graphene sheets, *J. Am. Chem. Soc.*, 2008, **130**, 5856; (c) Q. Su, S. Pang, V. Alijani, C. Li, X. Feng and K. Müllen, Composites of graphene with large aromatic molecules, *Adv. Mater.*, 2009, **21**, 3191; (d) A. Ghosh, K. V. Rao, S. J. George and C. N. R. Rao, Noncovalent functionalization, exfoliation, and solubilization of graphene in water by employing a fluorescent coronene carboxylate, *Chem. Eur. J.*, 2010, **16**, 2700; (e) X. Qi, K. Pu, H. Li, X. Zhou, S. Wu, Q. Fan, B. Liu, F. Boey, W. Huang and H. Zhang, Amphiphilic graphene composites, *Angew. Chem. Int. Ed.*, 2010, **49**, 9426.

11. (a) S. Niyogi, E. Bekyarova, M. E. Itkis, J. L. McWilliams, M. A. Hamon and R. C. Haddon, Solution properties of graphite and graphene, *J. Am. Chem. Soc.*, 2006, **128**, 7720; (b) S. Stankovich, R. D. Piner, S. T. Nguyen and R. S. Ruoff, Synthesis and exfoliation of isocyanate-treated graphene oxide nanoplatelets, *Carbon*, 2006, **44**, 3342; (c) R. Salvio, S. Krabbenborg, W. J. M. Naber, A. H. Velders, D. N. Reinhoudt and W. G. van der Wiel, The formation of large-area conducting graphene-like platelets, *Chem. Eur. J.*, 2009, **15**, 8235; (d) H. Yang, C. Shan, F. Li, D. Han, Q. Zhang and L. Niu, Covalent functionalization of polydisperse chemically-converted graphene sheets with amine-terminated ionic liquid, *Chem. Commun.*, 2009, 3880.

12. (a) I. V. Lightcap, T. H. Kosel and P. V. Kamat, Anchoring semiconductor and metal nanoparticles on a two-dimensional catalyst mat. Storing and shuttling electrons with reduced graphene oxide, *Nano Lett.*, 2010, **10**, 577; (b) F. Liu, J. Y. Choi and T. S. Seo, DNA mediated water-dispersible graphene fabrication and gold nanoparticle-graphene hybrid, *Chem. Commun.*, 2010, **46**, 2844; (c) A. N. Cao, Z. Liu, S. S. Chu, M. H. Wu, Z. M. Ye, Z. W. Cai, Y. L. Chang, S. F. Wang, Q. H. Gong and Y. F. Liu, A facile one-step method to produce graphene-CdS quantum dot nanocomposites as promising optoelectronic materials, *Adv. Mater.*, 2010, **22**, 103; (d) H. P. Cong, J. J. He, Y. Lu and S. H. Yu, Water-soluble magnetic-functionalized reduced graphene oxide sheets: in situ synthesis and magnetic resonance imaging applications, *Small*, 2010, **6**, 169; (e) Z. Tang, S. Shen, J. Zhang and X. Wang, Noble-metal-promoted three-dimensional macroassembly of single-layered graphene oxide, *Angew. Chem. Int. Ed.*, 2010, **49**, 4603.

13. (a) Y. X. Xu, L. Zhao, W. J. Hong, C. Li and G. Q. Shi, Chemically converted graphene induced molecular flattening of 5,10,15,20-tetrakis(1-methyl-4-pyridinio)porphyrin and its application for optical detection of cadmium(II) ions, *J. Am. Chem. Soc.*, 2009, **131**, 13490; (b) J. X. Geng, B. S. Kong, S. B. Yang and H. T. Jung, Preparation of graphene relying on porphyrin exfoliation of graphite, *Chem. Commun.*, 2010, **46**, 5091; (c) J. X. Geng and H. T. Jung, Porphyrin functionalized graphene sheets in aqueous suspensions: from the preparation of graphene sheets to highly conductive graphene films, *J. Phys. Chem. C*, 2010, **114**, 8227; (d) N. Karousis, S. P. Economopoulos, E. Sarantopoulou and N. Tagmatarchis, Porphyrin counter anion in imidazolium-modified graphene-oxide, *Carbon*, 2010, **48**, 854; (e) W. W. Tu, J. P. Lei, S. Y. Zhang and H. X. Ju, Characterization, direct electrochemistry, and amperometric biosensing of graphene by noncovalent functionalization with picket-fence porphyrin, *Chem. Eur. J.*, 2010, **16**, 10771.

14. (a) J. Balapanuru, J. Yang, S. Xiao, Q. Bao, M. Jahan, L. Polavarapu, J. Wei, Q.-H. Xu and K. P. Loh, A graphene oxide-organic dye ionic complex with DNA-sensing and optical-limiting properties, *Angew. Chem. Int. Ed.*,

2010, **49**, 6549; (b) Y. Wang, Z. Li, D. Hu, C. Lin, J. Li and Y. Lin, Aptamer/graphene oxide nanocomplex for in situ molecular probing in living cells, *J. Am. Chem. Soc.*, 2010, **132**, 9274; (c) C. Lu, J. Li, M. Lin, Y. Wang, H. Yang, X. Chen and G. Chen, Amplified aptamer-based assay through catalytic recycling of the analyte, *Angew. Chem. Int. Ed.*, 2010, **49**, 8454; (d) C. Shan, H. Yang, D. Han, Q. Zhang, A. Ivaska and L. Niu, Water-soluble graphene covalently functionalized by biocompatible poly-L-lysine, *Langmuir*, 2009, **25**, 12030.

15. (a) N. Karousis, A. S. D. Sandanayaka, T. Hasobe, S. P. Economopoulos, E. Sarantopoulou and N. Tagmatarchis, Graphene oxide with covalently linked porphyrin antennae: synthesis, characterization and photophysical properties, *J. Mater. Chem.*, 2011, **21**, 109; (b) X. D. Zhuang, Y. Chen, G. Liu, P. P. Li, C. X. Zhu, E. T. Kang, K. G. Neoh, B. Zhang, J. H. Zhu and Y. X. Li, Conjugated-polymer-functionalized graphene oxide: synthesis and nonvolatile rewritable memory effect, *Adv. Mater.*, 2010, **22**, 1731; (c) Y. Xu, Z. Liu, X. Zhang, Y. Wang, J. Tian, Y. Huang, Y. Ma, X. Zhang and Y. Chen, A graphene hybrid material covalently functionalized with porphyrin: synthesis and optical limiting property, *Adv. Mater.*, 2009, **21**, 1275; (d) M. Melucci, E. Treossi, L. Ortolani, G. Giambastiani, V. Morandi, P. Klar, C. Casiraghi, P. Samorì and V. Palermo, Facile covalent functionalization of graphene oxide using microwaves: bottom-up development of functional graphitic materials, *J. Mater. Chem.*, 2010, **20**, 9052; (e) D. Yu, Y. Yang, M. Durstock, J. Baek and L. Dai, Soluble P3HT-grafted graphene for efficient bilayer-heterojunction photovoltaic devices, *ACS Nano*, 2010, **4**, 5633; (f) P. Li, Y. Chen, J. Zhu, M. Feng, X. Zhuang, Y. Lin and H. Zhan, Charm-bracelet-type poly(N-vinylcarbazole) functionalized with reduced graphene oxide for broadband optical limiting, *Chem. Eur. J.*, 2011, **17**, 780.

16. (a) A. Lerf, H. Y. He, M. Forster and J. Klinowski, Structure of graphite oxide revisited, *J. Phys. Chem. B*, 1998, **102**, 4477; (b) W. S. Hummers Jr. and R. E. Offeman, Preparation of graphitic oxide, *J. Am. Chem. Soc.*, 1958, **80**, 1339; (c) R.Y.N. Gengler, K. Spyrou and P. Rudolf, A roadmap to high quality chemically prepared graphene, *J. Phys. D: Appl. Phys.*, 2010, **43**, 374015.

17. (a) M. Quintana, K. Spyrou, M. Grzelczak, W. R. Browne, P. Rudolf and M. Prato, Functionalization of graphene via 1,3-dipolar cycloaddition, *ACS Nano*, 2010, **4**, 3527; (b) V. Georgakilas, A. B. Bourlinos, R. Zboril, T. A. Steriotis, P. Dallas, A. K. Stubos and C. Trapalis, Organic functionalisation of graphenes, *Chem. Commun.*, 2010, **46**, 1766; (c) X. Zhong, J. Jin, S. W. Li, Z. Y. Niu, W. Q. Hu, R. Li and J. T. Ma, Aryne cycloaddition: highly efficient chemical modification of graphene, *Chem. Commun.*, 2010, **46**, 7340; (d) T. A. Strom, E. P. Dillon, C. E. Hamilton and A. R. Barron, Nitrene addition to exfoliated graphene: a one-step route to highly functionalized graphene, *Chem. Commun.*,

2010, **46**, 4097; (e) L.-H. Liu, M. M. Lerner and M. Yan, Derivitization of pristine graphene with well-defined chemical functionalities, *Nano Lett.*, 2010, **10**, 3754.

18. (a) P. Boyd and C. Reed, Fullerene-porphyrin constructs, *Acc. Chem. Res.*, 2005, **38**, 235; (b) M. Ethirajan, Y. Chen, P. Joshi and R. Pandey, The role of porphyrin chemistry in tumor imaging and photodynamic therapy, *Chem. Soc. Rev.*, 2011, **40**, 340; (c) M. Biesaga, K. Pyrzynska and M. Trojanowicz, Porphyrins in analytical chemistry. A review, *Talanta*, 2000, **51**, 209.

19. D. Guldi, A. Rahman, V. Sgobba and C. Ehli, Multifunctional molecular carbon materials–from fullerenes to carbon nanotubes, *Chem. Soc. Rev.*, 2006, **35**, 471.

20. J. Tomé, M. Neves, A. Tomé, J. Cavaleiro, A. Mendonça, I. Pegado, R. Duarte and M. Valdeira, Synthesis of glycoporphyrin derivatives and their antiviral activity against herpes simplex virus types 1 and 2, *Bioorg. Med. Chem.*, 2005, **13**, 3878.

21. D. Sharada, A. Muresan, K. Muthukumaran and J. Lindsey, Direct synthesis of palladium porphyrins from acyldipyrromethanes, *J. Org. Chem.*, 2005, **70**, 3500.

22. J. Geng, Y. Ko, S. Youn, Y. Kim, S. Kim, D. Jung and H. Jung, Synthesis of SWNT rings by non-covalent hybridization of porphyrins and single-walled carbon nanotubes, *J. Phys. Chem. C*, 2008, **112**, 12264.

23. M. Obata, N. Matsuura, K. Mitsuo, H. Nagai, K. Asai, M. Harada, S. Hirohara, M. Tanihara and S. Yano, Oxygen-sensing properties of 5,10,15,20-tetraphenylporphinato platinum(II) and palladium(II) covalently bound on poly(isobutyl-*co*-2,2,2-trifluoroethyl methacrylate), *J. Polym. Sci. Part A: Polym. Chem.*, 2010, **48**, 663.

24. (a) H. Chen, B. Liu, H. Wang, Z. Xiao, M. Chen and D. Qian, Metal-mediated layer-by-layer assembly of zinc 5,10,15,20-tetrapyridylporphine and pyridyl derivatives, *Mater. Sci. Eng.: C*, 2007, **27**, 639; (b) J. Fonseca, J. Tedim, K. Biernacki, A. Magalhães, S. Gurman, C. Freire and A. Hillman, Structural and electrochemical characterisation of [Pd(salen)]-type conducting polymer films, *Electrochim. Acta*, 2010, **55**, 7726.

25. The molar weight for TPP and PdTPP are 614 and 719 g/mol. Based on the weight loss of graphene-TPP and graphene-PdTPP, the functionalization degree is (0.82/12)/(0.18/614) = 233.1 for graphene-TPP, and (0.8/12)/(0.2/719) =239.6 for graphene-PdTPP. The Pd content in graphene-PdTPP was estimated to be 0.14 % by XPS.

26. (a) A. C. Ferrari, J. C. Meyer, V. Scardaci, C. Casiraghi, M. Lazzeri, F. Mauri, S. Piscanec, D. Jiang, K. S. Novoselov, S. Roth and A. K. Geim, Raman spectrum of graphene and graphene layers, *Phys. Rev. Lett*., 2006, **97**, 187401; (b) M. Lotya, Y. Hernandez, P. J. King, R. J. Smith, V. Nicolosi, L. S. Karlsson, F. M. Blighe, S. De, Z. M. Wang, I. T. McGovern, G. S. Duesberg and J. N. Coleman, Liquid phase production of graphene by exfoliation of graphite in surfactant/water solutions, *J. Am. Chem. Soc*., 2009, **131**, 3611; (c) S. De, P. J. King, M. Lotya, A. O'Neill, E. M. Doherty, Y. Hernandez, G. S. Duesberg and J. N. Coleman, Flexible, transparent, conducting films of randomly stacked graphene from surfactant-stabilized, oxide-free graphene dispersions, *Small*, 2010, **6**, 458.

27. (a) S. Campidelli, C. Sooambar, E. Lozano Diz, C. Ehli, D. Guldi and M. Prato, Dendrimer-functionalized single-wall carbon nanotubes: synthesis, characterization, and photoinduced electron transfer, *J. Am. Chem. Soc.*, 2006, **128**, 12544; (b) F. D'Souza, R. Chitta, A. Sandanayaka, N. Subbaiyan, L. D'Souza, Y. Araki and O. Ito, Self-assembled single-walled carbon nanotube:zinc-porphyrin hybrids through ammonium ion-crown ether interaction: construction and electron transfer, *Chem. Eur. J.*, 2007, **13**, 8277.

28. (a) M. E. Ragoussi, J. Malig, G. Katsukis, B. Butz, E. Spiecker, G. de la Torre, T. Torres and D. M. Guldi, Linking photo- and redoxactive phthalocyanines covalently to graphene, *Angew. Chem., Int. Ed.*, 2012, **51**, 6421; (b) N. Karousis, J. Ortiz, K. Ohkubo, T. Hasobe, S. Fukuzumi, A. Sastre-Santos and N. Tagmatarchis, Zinc phthalocyanine–graphene hybrid material for energy conversion: synthesis, characterization, photophysics, and photoelectrochemical cell preparation, *J. Phys. Chem. C*, 2012, **116**, 20564.

29. M. S. Lowry, W. R. Hudson, R. A. Pascal, Jr. and S. Bernhard, Accelerated luminophore discovery through combinatorial synthesis, *J. Am. Chem. Soc.*, 2004, **126**, 14129.

30. J. F. Moulder, W. F. Stickle and P. E. Sobol, *Handbook of X-Ray Photoelectron Spectroscopy*, Perkin-Elmer, Physical Electronics Division, 1993.

31. O. Wennerström, H. Ericsson, I. Raston, S. Svensson and W. Pimlott, *meso*-tetra(*meso*-tetraphenylporphyrinyl)porphyrin, a macrocycle with five covalently linked porphyrin units, *Tetrahedron Lett.*, 1989, **30**, 1129.

Chapter 6

Supramolecular chemistry on large area graphene field-effect transistors

Abstract

A combined study of the self-assembly of *bis*-urea-terthiophene (**T_3**) molecular wires on graphene and its effect on the electrical properties of graphene is presented using commercially available CVD graphene. It is shown that commercially available CVD graphene can be used as a substrate for the self-assembly of **T_3** molecular wires even when the graphene is highly undulating. Changes in doping levels and charge carrier mobility are observed in graphene transistors after **T_3** modification. Clean transistors reveal that the doping induced by the molecular wires in the graphene is at least an order of magnitude less than the doping induced by unwanted adsorbates.

This chapter is to be published:

Xiaoyan Zhang, Everardus H. Huisman, Mallikarjuna Gurram, Wesley R. Browne, Bart J. van Wees and Ben L. Feringa, *submitted*.

6.1 Introduction

Graphene, a one-atom thick two-dimensional honeycomb carbon lattice, has shown extraordinary properties and potential applications in numerous fields.[1] Since all atoms in graphene are surface atoms, a natural approach to tune graphene's electronic properties is to use surface chemistry.[2–4] Recently, a number of studies on self-assembly of organic molecules on graphene have been reported,[5–13] albeit with few reports combining both the surface organization *and* its effect on the electrical performance of graphene devices.[14,15] The dearth of combined studies is likely to be due to the specific limitations presented by each source of graphene used. For example, mechanically exfoliated flakes of graphene on an insulating dielectric allow fabrication of electronic devices, but are very challenging to approach with the tip of a scanning tunneling microscope (STM) due to their small dimensions.[16] On the other hand, large-area graphene grown epitaxially from silicon carbide or grown by chemical vapor deposition (CVD) on a metal is suitable for studying self-assembly, but is not readily used in field-effect transistors due to the lack of a back gate electrode in the substrate. In contrast, graphene grown by CVD and subsequently transferred to silicon/silicon dioxide wafers combines the accessibility of large-area graphene with the utility of a back gate present in the substrate.[17,18] Furthermore, wafer-scale CVD graphene transferred to silicon/silicon dioxide is now widely available through several commercial suppliers. In this communication, a combined study of the self-assembly and electronic properties of large-area graphene transistors (1 mm x 1 mm) modified by self-assembled *bis*-urea-terthiophene (**T_3**) and *bis*-urea-nonane (**C_9**) molecular wires is reported.[19] Self-assembled molecular wires up to several hundreds of nanometers in length were clearly observed both on CVD graphene on nickel and on transferred CVD graphene on silicon/silicon dioxide using STM at the liquid/solid interface. In the latter case, molecular wires were able to follow graphene's corrugation. Gate spectroscopy on

molecularly modified graphene transistors shows that the electronic interaction between the molecular wires and the graphene is weak compared to the effect of unwanted dopants.

6.2 Results

An important reason for the limited number of STM studies on CVD graphene transferred to insulating substrates is the high degree of undulation (corrugation) of the graphene on these substrates,[20] limiting the ability to obtain high resolution STM images. This problem can be circumvented by using self-assembly motifs that are readily discernable. In this study, a *bis*-urea-terthiophene derivative (**T_3**) with a well-defined and characteristic signature of self-assembly on graphite was chosen.

Figure 1a shows the molecular structure of **T_3**. The synthesis of **T_3** was reported previously.[21] **T_3** contains a urea group on each side of a central terthiophene moiety. Each of the urea groups is involved in up to four hydrogen bonds with neighboring molecules (Figure 1a). The hydrogen bonds drive the formation of one-dimensional molecular wires on highly oriented pyrolytic graphite (HOPG) in which the thiophene moieties arrange themselves as molecular wires with a well-defined spacing of ~ 6.2 nm detectable using STM at the liquid/solid interface at room temperature.[19,22]

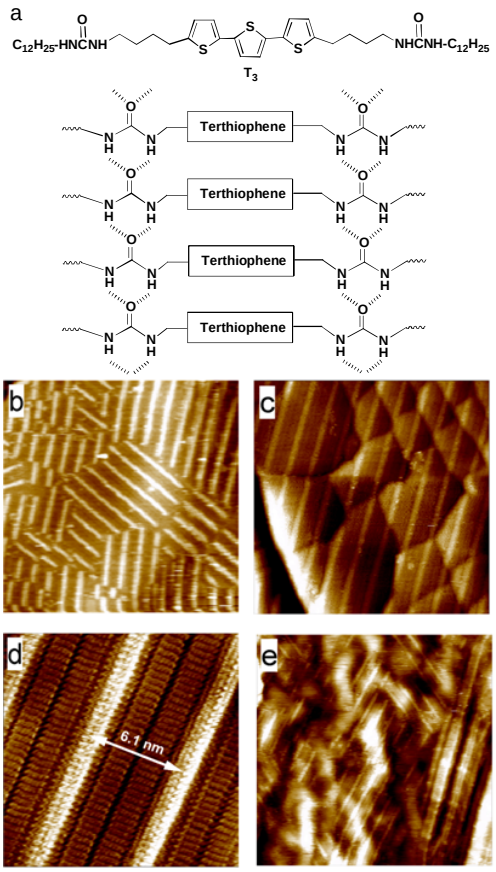

Figure 1. (a) Molecular structure of *bis*-urea-terthiophene $\mathbf{T_3}$ and a H-bonding scheme of self-assembled monolayers of $\mathbf{T_3}$. (b) An STM image displaying $\mathbf{T_3}$ molecular wires formation on CVD graphene on nickel. Imaging conditions: size (90 nm × 90 nm), I_{set} = 0.1 nA, V_{bias} = 0.65 V. (c) An STM image displaying $\mathbf{T_3}$ molecular wires formation on CVD graphene on nickel. Molecular wires are observed to cross several nickel grain boundaries. Imaging conditions: size (65 nm × 65 nm), I_{set} = 0.1 nA and V_{bias} = 0.65 V. (d) A submolecular resolution STM image showing a molecular wire separation of ~ 6.1 nm (part of the region imaged in Figure 1c). Imaging conditions: size (14.4 nm × 14.4 nm), I_{set} = 0.1 nA and V_{bias} = 0.6 V. (e) An STM image displaying $\mathbf{T_3}$ molecular wires formation on CVD graphene on silicon/silicon dioxide. Imaging conditions: size (90 nm × 90 nm), I_{set} = 0.06 nA and V_{bias} = 0.5 V.

Self-assembly of $\mathbf{T_3}$ on graphene grown on nickel was studied using STM at the liquid/solid interface at room temperature. Graphene containing mono- and few-layer graphene on nickel was obtained from Graphene Supermarket™. $\mathbf{T_3}$ was deposited on graphene/nickel by drop-casting a solution of $\mathbf{T_3}$ in octanoic acid (1 mM) and the STM tip was immersed into the liquid. Typical dimensions over which homogeneous self-assembly was observed (regions where the orientation of the molecular wires is well-defined) are of the order of 10-100 nm.[23] Interestingly, regions where molecular wires cross multiple nickel grain boundaries were also observed (Figure 1c). Furthermore, the angle between molecular wires in neighboring domains is found to be close to 60°. This suggests that the orientation of the molecular wires is directed by the underlying graphene lattice. Submolecular resolution of $\mathbf{T_3}$ could be obtained (Figure 1d), from which the separation between molecular wires was determined to be 6.1 ± 0.1 nm, as for $\mathbf{T_3}$ self-assembled on HOPG.[21]

Next, the self-assembly on graphene transferred to silicon/silicon dioxide was studied. Graphene on silicon/silicon dioxide was obtained from Graphene Supermarket™. The graphene films as received typically shows defects such as cracks and folds in addition to impurities/residues originating from CVD growth and/or transfer (Figure 2a and 2b). The single layer nature of the graphene was confirmed by Raman spectroscopy (Figure 2c). STM imaging confirmed an undulating graphene surface. Peak to peak height variations of 2.5 nm were observed in line cross sections in regions free of cracks, residues and ripples. This is in agreement with values reported for exfoliated graphene on silicon/silicon dioxide.[20,24] $\mathbf{T_3}$ was deposited on the graphene by drop-casting a solution of $\mathbf{T_3}$ in octanoic acid (1 mM) and a STM tip was immersed into the liquid. Although detection was found to be more challenging than on graphene on nickel, molecular wires were observed readily. Typical dimensions over which homogeneous self-assembly was observed are again in

the order of 10-100 nm. In the present case, the corrugation of the graphene prevents us from imaging **T_3** at the submolecular level.

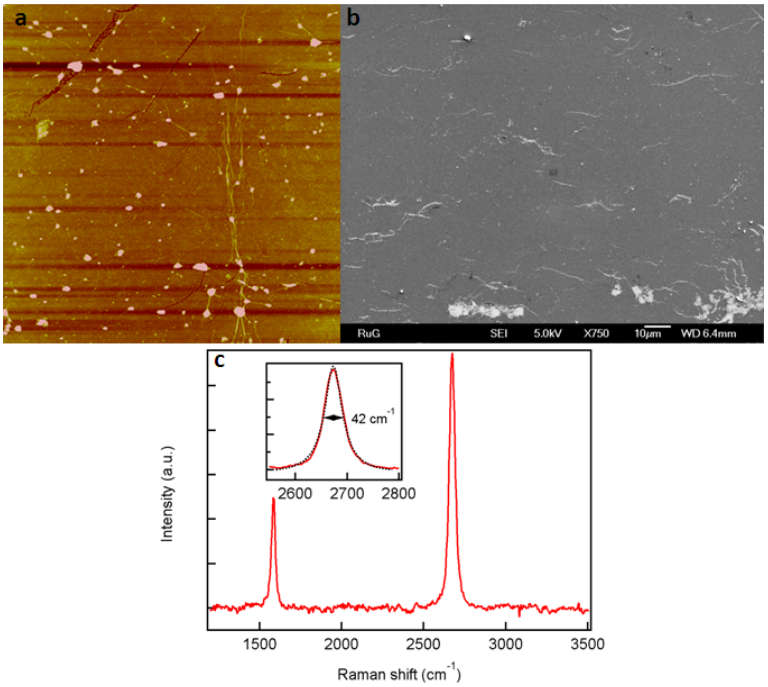

Figure 2. (a) An atomic force microscopy (AFM) image of a 10 µm × 10 µm region of graphene on SiO_2/Si as received from Graphene Supermarket. (b) An SEM image of region of graphene on SiO_2/Si as received from Graphene Supermarket. (c) Raman spectrum of graphene on SiO_2/Si substrate (λ_{exc} = 532 nm). The spectrum shows a symmetrical 2D band centered at 2673 cm^{-1} with a full-width at half maximum of ~ 42 cm^{-1}.

Interestingly, the STM image shows that **T_3** molecular wires follow the corrugation of the graphene. By taking the average of the interline spacings observed in Figure 1e, a line spacing of 6.0 nm ± 0.1 nm was determined. This value agrees with the line spacing obtained on graphene on nickel. Again, the angle between neighboring domains is typically found to be close to 60^o, which implies that graphene plays a role in the orientation of the molecular wires.

These observations constitute an important step: CVD grown graphene transferred to silicon/silicon dioxide, although strongly corrugated and displaying several defects and impurities, can still be used to self-assemble *bis*-urea molecules into molecular wires.

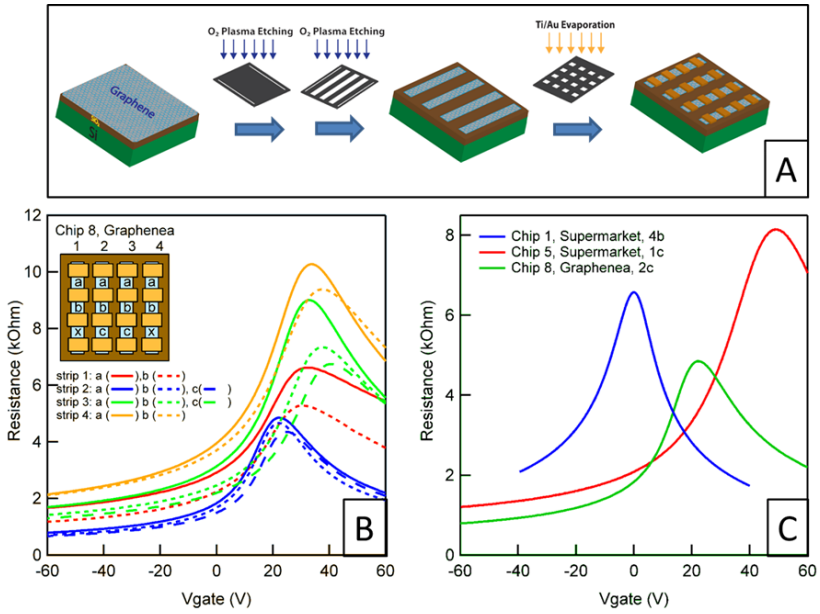

Figure 3. (a) Device preparation using a lithography-free process to pattern twelve large-area (1 mm × 1 mm) field-effect transistors (FET) on a 10 mm × 10 mm chip of graphene on silicon/silicon dioxide. (b) Transfer curves of 10 FETs on a chip. The inset displays a map of the chip. Within a chip the FETs display a spread in resistance. (c) Transfer curves for three FETs on different chips, showing that doping levels are uncontrolled, even after the annealing.

In order to study how the self-assembly of $\mathbf{T_3}$ modifies the electronic properties of graphene, a lithography-free procedure was developed to prepare large-area transistors that avoids introduction of polymer residues during the patterning of graphene.[25,26] Figure 3a schematically shows the procedure used. Graphene on silicon/silicon dioxide was obtained from both Graphene Supermarket™ and

Graphenea™. First, a 10 mm × 10 mm piece of fully covered monolayer graphene was covered with a shadow mask and etched in four strips of 1 mm × 9 mm using two reactive ion etching steps in an oxygen plasma.[27] Subsequently, four contacts were deposited on each strip to form twelve transistors in total (inset Figure 3b). After fabrication, the chip was glued to a chip carrier and wire bonded. When measuring the transfer characteristics of the transistors under ambient conditions, the charge neutrality point (CNP) was observed to be above the accessible gate voltage maximum (> 80 V). Therefore, the samples were loaded in a homebuilt vacuum chamber and annealed under high vacuum ($5 \cdot 10^{-6}$ mbar, 130 ºC) until the gate voltage position of the CNP saturated (typically after 10 h).

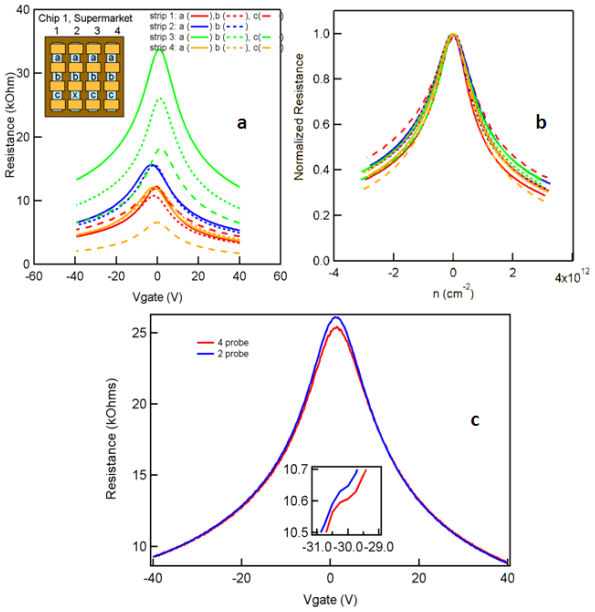

Figure 4. (a) 11 transfer curves of a chip obtained from Graphene Supermarket (chip 1). (b) Transfer curves normalized with respect to the resistance at the CNP. (c) 4 probe versus 2 probe transfer curve of a FET on a Graphene Supermarket chip. The inset shows a close-up graph, from which a contact resistance of each gold-graphene contact is estimated to be 25 Ohms.

Figure 3b shows the transfer curves of ten FETs and highlights the large variation (up to 240 %) in the resistance between FETs (see also Figure 4a). Interestingly, by normalization of each transfer curve with respect to the maximum resistance found at the CNP, all traces fall on a single curve (Figure 4b). Ill-defined contact resistances were excluded by comparing four-probe transfer curves with the two-probe transfer curves (Figure 4c). An etched area of 1.00 ± 0.05 mm × 1.00 ± 0.05 mm is confirmed by optical microscopy. We speculate that the spread in resistance comes from variations in defects in the graphene such as cracks. The effective graphene area of FETs with such defects might be reduced. Since the length of the transport channel is set by the electrode spacing this will result in an effective increase in the effective number of squares (> 1).[28] When assuming that the FET with the lowest resistance is free of such defects, a mobility of $3.3 \cdot 10^3$ $cm^2 V^{-1} s^{-1}$ is obtained (FET 3c, mobility at the inflection point on the electron side). This value is comparable to values previously reported for FETs prepared from CVD graphene.[17]

Although the gate voltage positions of the CNPs of all FETs within a chip were found to be reduced by annealing in vacuum and to saturate at a certain voltage, still a large variation in gate voltage positions of the CNPs between chips was observed. Figure 3c shows three FET transfer curves of identically processed FETs on various chips from different sources. Again, pristine graphene FETs were generally found to be p-doped, although one chip was found to be close to undoped (see Figure 4a). Several methods of annealing the pristine graphene devices such as thermal annealing in Ar/H_2[24,29] and current annealing[30,31] were explored as to yield reproducible clean graphene with a well-defined CNP, but were not successful.

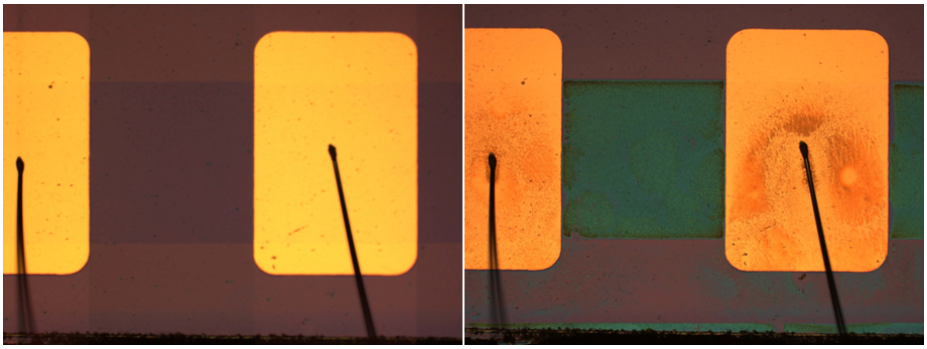

Figure 5. Optical images of graphene on SiO_2/Si FETs before (left) and after (right) self-assembly of $\mathbf{T_3}$.

After electrical characterization of the annealed devices, the chip was taken out of the vacuum chamber. Self-assembly of $\mathbf{T_3}$ on graphene on the same chip was performed by applying a drop of $\mathbf{T_3}$ in octanoic acid (1 mM) on top of the graphene FETs. Subsequently, the transistor was gently rinsed with isopropanol, blown dry using nitrogen, inspected for the presence of molecules using an optical microscope (Figure 5) and directly transferred to the vacuum chamber and annealed at 100 ^{o}C overnight under high vacuum. Gate spectroscopy analysis was performed at room temperature, after which the presence of molecules on the surface was again verified by optical microscopy (Figure 5).

In total, forty six devices on eight different chips from different sources were analyzed.[32] Figure 6a-c shows three examples of transfer curves before (blue curves) and after (red curves) $\mathbf{T_3}$ modification of the graphene. Figure 6d shows the difference in the gate voltage of the CNP before and after applying $\mathbf{T_3}$, $\Delta V_{CNP} = V_{CNP}^{pristine} - V_{CNP}^{T3}$ versus the initial gate voltage position of the CNP, $V_{CNP}^{pristine}$ for each transistor. Strikingly, the data is scattered around the line $\Delta V_{CNP} = V_{CNP}^{pristine}$ which shows that after applying molecules, the CNP shifts

close to zero gate voltage independent of the initial gate voltage position of the CNP.

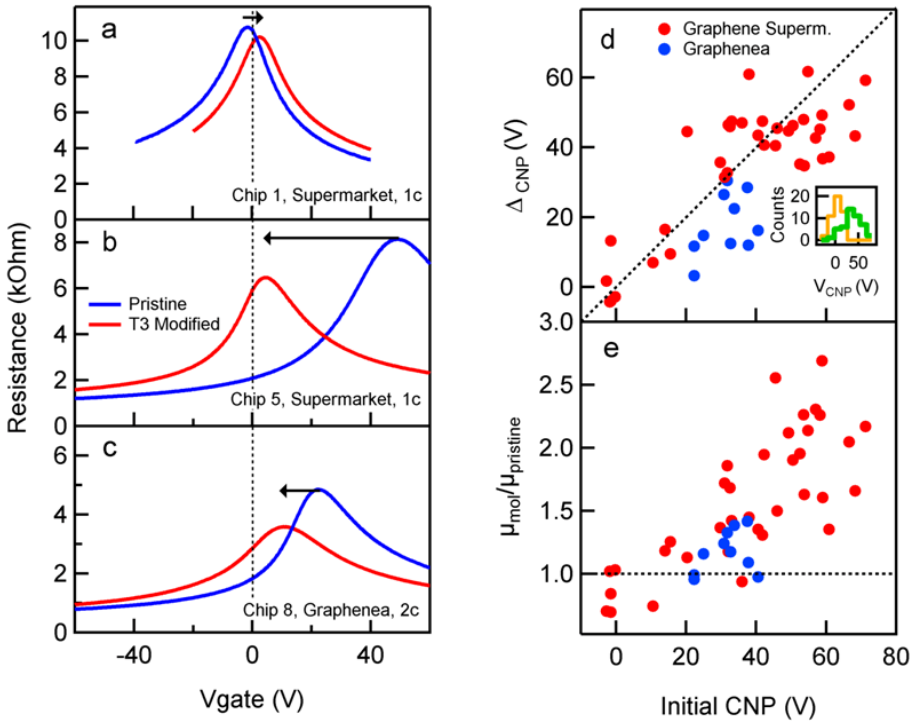

Figure 6. a), b), c) Examples of transfer curves before (blue curve) and after self-assembly of $\mathbf{T_3}$ (red curve) on graphene on silicon/silicon dioxide. Correlation plots of d) shift observed in the gate voltage position of the charge neutrality point (CNP) and e) mobility ratio as a function of the gate voltage position of the CNP before molecular modification. Inset Figure 6d: histogram displaying the distribution of the voltage position of the CNP before (green) and after (yellow) molecular modification.

Although an absolute value cannot be obtained exactly, the ratio of the mobilities before and after deposition of $\mathbf{T_3}$ ($\mu_{mol}/\mu_{pristine}$) can be used to deduce an increase or decrease in the mobility after molecular modifying the transistor (assuming the effective graphene area remains unaltered). Figure 6e shows

$\mu_{mol}/\mu_{pristine}$ as a function of $V_{CNP}^{pristine}$. We determined the mobility at the inflection point on the electron side (left of CNP) as described elsewhere.[33] FETs with a relatively large $V_{CNP}^{pristine}$ display a relatively high increase in mobility, whereas devices initially close to $V_{CNP}^{pristine}$ = 0 display almost no change, or even a small decrease in mobility.

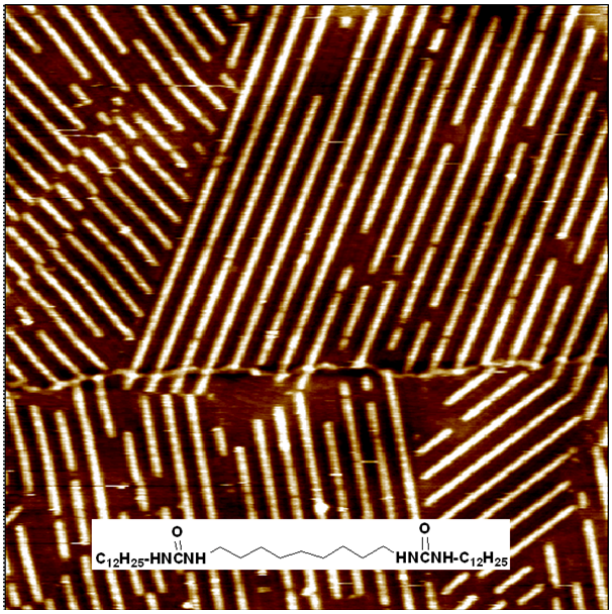

Figure 7. STM images of **C_9** self-assembly on graphene on nickel (obtained from Graphene Supermarket). Imaging conditions: size (154 × 154 nm^2), I_{set} = 0.06 nA and V_{bias} = 0.5 V. Inset: chemical structure of **C_9**.

To determine whether the observed changes in doping levels and increase in mobility are due to the terthiophene moieties in **T_3**, FETs modified with *bis*-urea compounds in which the central thiophene moiety was replaced by a saturated alkane (**C_9**) were also studied. A similar dedoping and mobility increase compared to **T_3** was observed (Figure 7 and Figure 8).

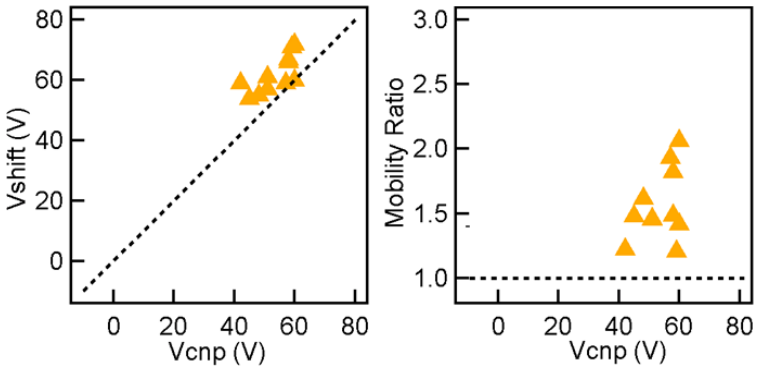

Figure 8. Reference measurements comparing the shift in the gate voltage position of the CNP (left image) and the mobility ratio (right image) before and after modifying graphene FETs with $\mathbf{C_9}$ as a function of the gate voltage position of the CNP before $\mathbf{C_9}$ modification.

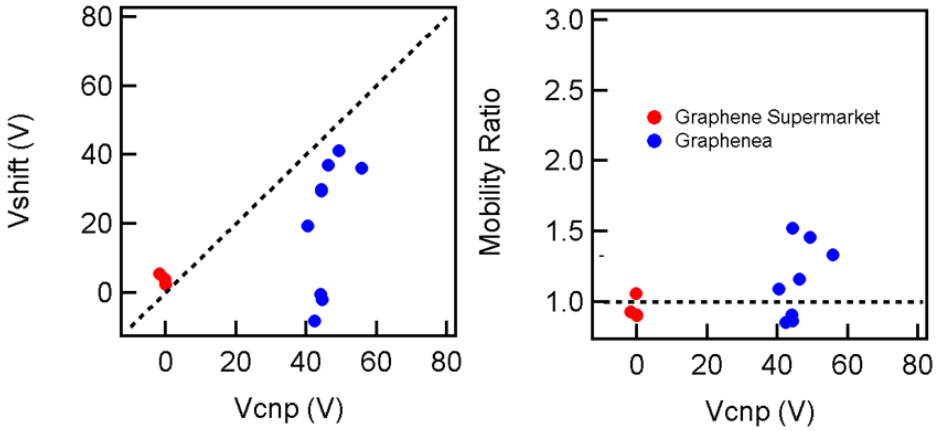

Figure 9. Reference measurements comparing the shift in the gate voltage position of the CNP (left image) and the mobility ratio (right image) before and after modifying graphene FETs with octanoic acid only (no molecules were dissolved) as a function of the gate voltage position of the CNP before applying octanoic acid.

Next, blank measurements on chips from each of the suppliers were performed as described above, using solvent only (i.e. no $\mathbf{T_3}$ dissolved, Figure 9).

Surprisingly, these FETs also show shifts in $\Delta V_{CNP} > 0$ for devices that were initially p-doped and almost no shift when $V_{CNP}^{pristine}$ was close to zero, indicating that the solvent itself plays an important role in the observed dedoping and mobility increase.

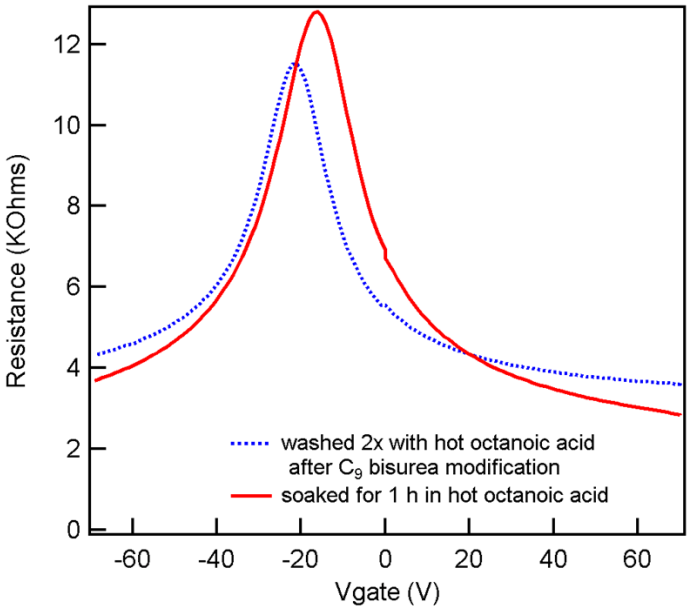

Figure 10. Transfer curves of a pristine FET soaked in hot octanoic acid (80 ^{o}C) for 1 hour (solid line). A **C$_9$** *bis*-urea modified FET was rinsed 2 × with hot octanoic acid as to remove **C$_9$** molecules (removal was verified using an optical microscope, dotted line).

Pristine FETs were soaked for an hour in hot octanoic acid (80 ºC) to study the effect of solvent. The gate voltage position of the CNP of these FETs was found to be between -15 and -20 V (Figure 10). Similar n-doping was observed by removing **C$_9$** from a FET by rinsing twice with hot octanoic acid (80 ºC). Previously, changes in charge carrier mobility for suspended graphene in

different liquid environments were reported, but solvent induced doping was not studied.[34]

To ascertain whether or not the presence of $\mathbf{T_3}$ monolayers influences the electronic properties of graphene, it is particularly interesting to examine the five pristine FETs that have their CNP initially close to 0 V. On average these 5 devices show a small n-doping shift (1 ± 7 V) and a mobility ratio of 0.86 ± 0.16. This indicates that $\mathbf{T_3}$ has only a weak interaction with the graphene and acts as a weak scatterer. This weak interaction can be understood when taking into account that due to stacking between adjacent terthiophene units, the thiophene rings will only partly interact with the graphene. Also note that the density of terthiophene units in a monolayer of $\mathbf{T_3}$ molecular wires on HOPG is about two orders of magnitude lower than the density of carbon atoms in graphene.

6.3 Conclusions

In conclusion, a combined study of the self-assembly of $\mathbf{T_3}$ molecular wires on graphene and its effect on the electrical properties of graphene is presented using commercially available CVD graphene. It is shown that commercially available CVD graphene can be used as a substrate for the self-assembly of $\mathbf{T_3}$ molecular wires even when the graphene is highly undulating. Changes in doping levels and charge carrier mobility are observed in graphene transistors after $\mathbf{T_3}$ modification. We attribute these changes mostly to solvent induced cleaning of initially p-doped graphene. Nevertheless, occasional clean transistors reveal that the doping induced by the molecular wires in the graphene is at least an order of magnitude smaller than the doping observed by unwanted adsorbates.

6.4 Methods

Measurements STM measurement was performed using a PicoSPM instrument (Molecular imaging, Scientec) at the liquid/solid interface. The STM tips were mechanically cut from Pt/Ir wire (80:20, diameter-0.25 mm, Goodfellow). Octanoic Acid (Sigma-Aldrich, ≥ 99%) and 2-propanol (Merck, UV grade) were used as received. Before STM imaging, *bis*-urea-terthiophene $\mathbf{T_3}$ was dissolved in octanoic acid (1 mM, 0.81 mg/ml) at ~ 90 ^{o}C. A drop of the solution was drop-casted onto graphene/SiO_2 or graphene/nickel surface. AFM measurement was performed on a Bruker NanoScope V instrument in tapping mode. SEM imaging was undertaken on a Jeol JSM 7000F Scanning Electron Microscope operated at 5 KV. Raman spectra at 532 nm were obtained using a home built system comprising of a iDus-DU420A CCD detector coupled to a Shamrock 163i spectrograph (Andor Technology) and a 25 mW 532 nm DPSS laser (Cobolt Lasers) fibre coupled to an Olympus BX51 microscope (equipped with laserline clean up and edge filters from Semrock) with long working distance objectives.

Transistor fabrication A shadow masks system was designed and realized in our workshop. Reactive Ion Etching was performed in a homebuilt system (Oxygen, 40W, 9 sccm, 20 seconds per step, 0.009 mbar). Titanium/gold contacts (5 nm/40 nm) were deposited using a Temescal e-gun evaporation system (TFC2000) with a base pressure of $5 \cdot 10^{-7}$ mbar. Devices were cut in two pieces prior to be glued to a chip carrier.

Electrical characterization 2-probe current biased measurements were performed using a 100 nA AC modulation (typically 300 Hz) from a homebuilt current source. The resistance was determined by measuring the voltage drop using a standard lock-in technique (Stanford SR830) and a homebuilt voltage amplifier. The gate voltage was applied by a Keithley 2400 Source Meter Unit.

In the 4-probe measurement the current was sent through the outer contacts, while the voltage drop across the inner contacts was measured.

6.5 Acknowledgement

E. H. H. and M. G. are acknowleged for their contributions and collaboration on the project, in particular regarding to device fabrication and characterization.

6.6 Notes and references

1. A. K. Geim and K. S. Novoselov, The rise of graphene, *Nat. Mater.*, 2007, **6**, 183.

2. V. Georgakilas, M. Otyepka, A. B. Bourlinos, V. Chandra, N. Kim, K. C. Kemp, P. Hobza, R. Zboril and K. S. Kim, Functionalization of graphene: covalent and non-covalent approaches, derivatives and applications, *Chem. Rev.*, 2012, **112**, 6156.

3. H. T. Liu, Y. Q. Liu and D. B. Zhu, Chemical doping of graphene, *J. Mater. Chem.*, 2011, **21**, 3335.

4. J. A. Mann and W. R. Dichtel, Noncovalent functionalization of graphene by molecular and polymeric adsorbates, *J. Phys. Chem. Lett.*, 2013, **4**, 2649.

5. Q. H. Wang and M. C. Hersam, Characterization and nanopatterning of organically functionalized graphene with ultrahigh vacuum scanning tunneling microscopy, *MRS Bull.*, 2011, **36**, 532.

6. M. Roos, B. Uhl, D. Künzel, H. E. Hoster, A. Groß and R. J. Behm, Intermolecular vs molecule–substrate interactions: a combined STM and theoretical study of supramolecular phases on graphene/Ru(0001), *Beilstein J. Nanotechnol.*, 2011, **2**, 365.

7. Q. H. Wang and M. C. Hersam, Room-temperature molecular-resolution characterization of self-assembled organic monolayers on epitaxial graphene, *Nat. Chem.*, 2009, **1**, 206.

8. A. J. Pollard, E. W. Perkins, N. A. Smith, A. Saywell, G. Goretzki, A. G. Phillips, S. P. Argent, H. Sachdev, F. Müller, S. Hüfner, S. Gsell, M. Fischer, M. Schreck, J. Osterwalder, T. Greber, S. Berner, N. R. Champness and P. H. Beton, Supramolecular assemblies formed on an epitaxial graphene superstructure, *Angew. Chem. Int. Ed.*, 2010, **49**, 1794.

9. J. Mao, H. Zhang, Y. Jiang, Y. Pan, M. Gao, W. Xiao and H.-J. Gao, Tunability of supramolecular Kagome lattices of magnetic phthalocyanines using graphene-based moire patterns as templates, *J. Am. Chem. Soc.*, 2009, **131**, 14136.

10. B. Long, M. Manning, M. Burke, B. N. Szafranek, G. Visimberga, D. Thompson, J. C. Greer, I. M. Povey, J. MacHale, G. Lejosne, D. Neumaier and A. J. Quinn, Non-covalent functionalization of graphene using self-assembly of alkane-amines, *Adv. Funct. Mater.*, 2012, **22**, 717.

11. P. Järvinen, S. K. Hämäläinen, K. Banerjee, P. Häkkinen, M. Ijäs, A. Harju and P. Liljeroth, Molecular self-assembly on graphene on SiO_2 and h-BN substrates, *Nano Lett.*, 2013, **13**, 3199.

12. S. Sarkar, H. Zhang, J.-W. Huang, F. Wang, E. Bekyarova, C. N. Lau and R. C. Haddon, Organometallic hexahapto functionalization of single layer graphene as a route to high mobility graphene devices, *Adv. Mater.*, 2013, **25**, 1131.

13. S. Lei, X. Sun, J. Zhang, X. Wang, C. Zhang, P. Hu, Y. Mu, X. Wan and Z. Guo, Oligothiophenes on CVD graphene grown on multi-crystalline copper foil: supramolecular assembly and impact of morphology, *Chem. Commun*., 2013, **49**, 10317.

14. T. Zhang, Z. Cheng, Y. Wang, Z. Li, C. Wang, Y. Li and Y. Fang, Self-assembled 1-octadecanethiol monolayers on graphene for mercury detection, *Nano Lett.*, 2010, **10**, 4738.

15. B. Li, A. V. Klekachev, M. Cantoro, C. Huyghebaert, A. Stesmans, I. Asselberghs, S. De Gendt and S. De Feyter, Toward tunable doping in graphene FETs by molecular self-assembled monolayers, *Nanoscale*, 2013, **5**, 9640.

16. E. Stolyarova, D. Stolyarov, L. Liu, K. T. Rim, Y. Zhang, M. Han, M. Hybersten, P. Kim and G. Flynn, STM studies of ultrathin graphitic (graphene) films on an insulating substrate under ambient conditions, *J. Phys. Chem. C*, 2008, **112**, 6681.

17. X. Li, W. Cai, J. An, S. Kim, J. Nah, D. Yang, R. Piner, A. Velamakanni, I. Jung, E. Tutuc, S. K. Banerjee, L. Colombo and R. S. Ruoff, Large-area synthesis of high-quality and uniform graphene films on copper foils, *Science*, 2009, **324**, 1312.

18. K. S. Kim, Y. Zhao, H. Jang, S. Y. Lee, J. M. Kim, K. S. Kim, J.-H. Ahn, P. Kim, J.-Y. Choi and B. H. Hong, Large-scale pattern growth of graphene films for stretchable transparent electrodes, *Nature*, 2009, **457**, 706.

19. J. van Esch, S. De Feyter, R. M. Kellogg, F. De Schryver and B. L. Feringa, Self-assembly of bisurea compounds in organic solvents and on solid substrates, *Chem. Eur. J.*, 1997, **3**, 1238.

20. V. Geringer, M. Liebmann, T. Echtermeyer, S. Runte, M. Schmidt, R. Rückamp, M. C. Lemme and M. Morgenstern, Intrinsic and extrinsic corrugation of monolayer graphene deposited on SiO_2, *Phys. Rev. Lett.*, 2009, **102**, 076102.

21. F. Schoonbeek, Making it all stick together, *PhD Thesis*, University of Groningen; F. S. Schoonbeek, J. H. van Esch, B. Wegewijs, D. B. A. Rep, M. P. de Haas, T. M. Klapwijk, R. M. Kellogg and B. L. Feringa, Efficient intermolecular charge transport in self-assembled fibers of mono- and bithiophene bisurea compounds, *Angew. Chem. Int. Ed.*, 1999, **38**, 1393; A. Gesquiére, M. M. S. Abdel-Mottaleb, S. De Feyter, F. C. De Schryver, F. Schoonbeek, J. van Esch, R. M. Kellogg, B. L. Feringa, A. Calderone, R. Lazzaroni and J. L. Bredas, Molecular organization of *bis*-urea substituted thiophene derivatives at the liquid/solid interface studied by scanning tunneling microscopy, *Langmuir*, 2000, **16**, 10385.

22. S. De Feyter and F. C. De Schryver, Two-dimensional supramolecular self-assembly probed by scanning tunneling microscopy, *Chem. Soc. Rev.*, 2003, **32**, 139.

23. This is subtantially smaller than the dimensions of 3-10 μm of typical graphene terraces.

24. M. Ishigami, J. H. Chen, W. G. Cullen, M. S. Fuhrer and E. D. Williams, Atomic structure of graphene on SiO_2, *Nano Lett.*, 2007, **7**, 1643.

25. N. Staley, H. Wang, C. Puls, J. Forster, T. N. Jackson, K. McCarthy, B. Clouser and Y. Liu, Lithography-free fabrication of graphene devices, *Appl. Phys. Lett.*, 2007, **90**, 143518.

26. W. Bao, G. Liu, Z. Zhao, H. Zhang, D. Yan, A. Deshpande, B. LeRoy and C. N. Lau, Lithography-free fabrication of high quality substrate-supported and freestanding graphene devices, *Nano Res.*, 2010, **3**, 98.

27. Similar results were obtained with an Ar plasma.

28. Alternatively, lack of intimate contact between the mask and sample during the etching might cause inhomogeneous damage to the graphene. This seems unlikely, since a clear slant direction is not directly deducable from the order of resistances in figure 3b. Also, the oxygen ion mean free path at the pressures used during etching is substantially longer than the estimated mask sample separation.

29. Y. Dan, Y. Lu, N. J. Kybert, Z. Luo and A. T. C. Johnson, Intrinsic response of graphene vapor sensors, *Nano Lett.*, 2009, **9**, 1472.

30. J. Moser, A. Barreiro and A. Bachtold, Current-induced cleaning of graphene, *Appl. Phys. Lett.*, 2007, **91**, 163513.

31. K. I. Bolotin, K. J. Sikes, Z. Jiang, M. Klima, G. Fudenberg, J. Hone, P. Kim and H. L. Stormer, Ultrahigh electron mobility in suspended graphene, *Solid State Commun.*, 2008, **146**, 351.

32. 7 Graphene Supermarket chips (78 FETs) and 1 Graphenea chip (12 FETs) were fabricated. 8 FETs were not measured due to a limit in the number of available bond pads on the chip carrier used, 23 FETs failed (mostly due to gate leakage). 13 transfer chracateristics were excluded due to ill-defined CNPs and/or ill-defined inflection points.

33. N. Tombros, A. Veligura, J. Junesch, J. Jasper van den Berg, P. J. Zomer, M. Wojtaszek, I. J. Vera Marun, H. T. Jonkman and B. J. van Wees, Large yield production of high mobility freely suspended graphene electronic devices on a polydimethylglutarimide based organic polymer, *J. Appl. Phys.*, 2011, **109**, 093702.

34. A. K. M. Newaz, Y. S. Puzyrev, B. Wang, S. T. Pantelides and K. I. Bolotin, Probing charge scattering mechanisms in suspended graphene by varying its dielectric environment, *Nat. Commun.*, 2012, **3**, 734.

Chapter 7

Self-assembly of alkyl-porphyrins on large area chemical vapor deposition (CVD) graphene on nickel and SiO_2 substrates and the interaction between graphene and alkyl-porphyrins

Abstract

The two-dimensional conjugated sp^2 structure of graphene makes it an ideal template for patterning oriented and ordered supermolecular self-assembled structures. Understanding the self-assembly of molecules on graphene is a key step for the further design of graphene-based electronic devices. In this chapter, the self-assembly of two alkyl-Ni(II)-porphyrins on large area chemical vapor deposition (CVD) graphene (both on nickel and SiO_2/Si substrates) was studied using scanning tunneling microscopy (STM). Graphene on a nickel substrate is flatter than on SiO_2/Si, enabling submolecular resolution of porphyrins on the former surface. On graphene/SiO_2, submolecular resolution of porphyrins could not be obtained mainly due to the corrugation of the graphene. The interaction between graphene and porphyrins was studied by Raman and UV/Vis spectroscopy, and the data indicate that graphene and porphyrins can interact electronically.

This chapter is to be published:

Xiaoyan Zhang, Wesley R. Browne, Bart J. van Wees and Ben L. Feringa, *to be submitted.*

7.1 Introduction

Over the last decade, graphene has attracted tremendous attention due to its excellent electrical, optical, thermal and mechanical properties.[1] It is expected that graphene can be potentially used in sensors, nanoelectronic devices, energy materials, composites, etc.[2] To realize these applications, preparation of large area high quality graphene in a controllable and reproducible manner is a prerequisite. Several methods have been reported to obtain graphene, including mechanical cleavage,[3] reduction of graphene oxide,[4] solvent dispersion of graphite,[5,6] organic synthesis,[7] growing on silicon carbide[8] and chemical vapor deposition (CVD),[9,10] as discussed in the introduction chapter. Among them, CVD growth of graphene on metal substrates is well developed and has attracted a lot of attention because it yields high quality graphene films on a large scale that are readily transferred to other substrates, including the commonly used SiO_2/Si. Several reports have described the fabrication of graphene/SiO_2 field effect transistors (FETs) and the recovery of the intrinsic properties of graphene from CVD graphene.[11,12] Although progress has been made in this area, major challenges remain. For example, precise control and tuning of the electronic properties of graphene is still limited by the lack of highly specific homogenous and reproducible methods, which are both important issues in graphene based electronic devices.[13] An interesting route to modify graphene's electronic properties is to use surface chemistry. Chemical functionalization of graphene is expected to be effective in modulating the electronic structure of graphene. Covalent functionalization normally induces damage to the carbon lattice and changes the electronic properties of graphene.[14] In contrast, surface functionalization of graphene through noncovalent approaches holds the potential to tune the electronic properties of graphene without disrupting the carbon sp^2 lattice.[15-20] Furthermore, the reactivity of graphene could be altered by the absorption of organic molecules.[21] The two-dimensional conjugated sp^2 structure of graphene makes

it an ideal template for patterning oriented and ordered supermolecular structures. Indeed it has been reported that periodic potential modulation on graphene induced by periodic strain or doping could be used to tune the band structure of graphene.[22,23]

Porphyrins are highly versatile in organic electronic devices due to their remarkable electronic properties.[24] However, from the point of view of device application, the performance of these materials not only depends on the molecular electronic structure, but also is affected by molecular packing, i.e., the morphology of the films. Highly ordered porphyrin structures usually yield enhanced charge carrier mobility and injection across an interface, and eventually better performance of the electronic devices.[25-27] Our group has previously demonstrated the self-assembly of alkyl-porphyrins on highly oriented pyrolytic graphite (HOPG).[28] Although molecular packing and morphology control on HOPG have been studied extensively over the last decades,[29,30] studying the self-assembly of molecules on graphene/SiO_2 devices is still challenging mainly due to: (i) the difficulty in approaching the STM tip exactly to the conducting graphene area on the insultating SiO_2 substrate,[31] (ii) the corrugation of the graphene itself on the SiO_2 substrate makes it difficult to obtain STM images with high resolution.[32] In this chapter, the self-assembly of alkyl-Ni(II)-porphyrins on large area CVD graphene deposited both on conducting nickel and insulating SiO_2/Si substrates is shown by STM measurements. The interaction between alkyl-Ni(II)-porphyrins and graphene is also discussed.

7.2 Results

The synthesis of alkyl-Ni(II)-porphyrins is shown in Scheme 1. Briefly, pyrrole was reacted with alkyl-aldehydes in nitrobenzene and acetic acid at reflux for 1 h. After purification, alkyl-porphyrins were obtained. The alkyl-porphyrins were further reacted with $Ni(OAc)_2 \cdot 4H_2O$ in ethanol/$CHCl_3$ mixture to yield

the alkyl-Ni(II)-porphyrins. The synthesis and characterization are provided in the experimental part.

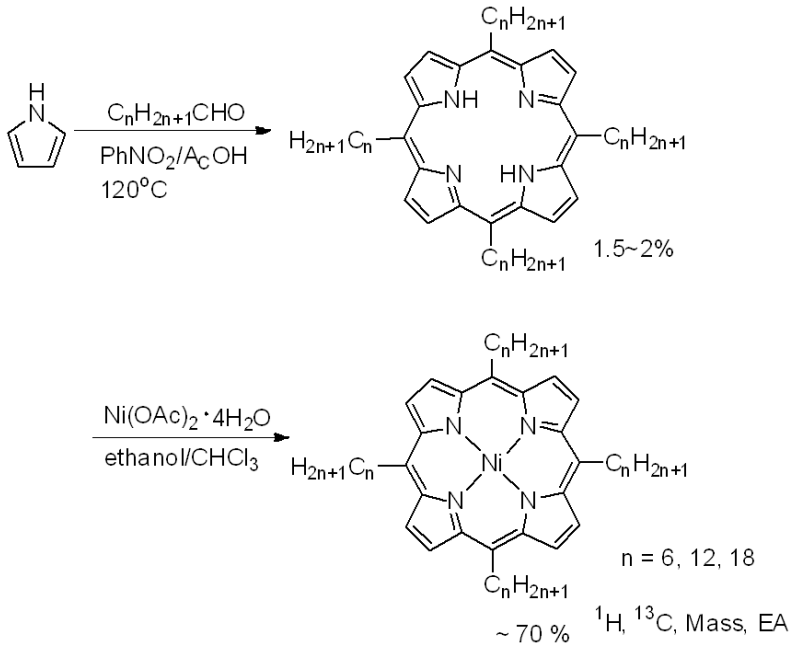

Scheme 1. Synthesis of C_n-Ni(II)-porphyrins.

The self-assembly of C_{12}- and C_{18}-Ni (II)-porphyrin was studied first on graphene on nickel, because the nickel substrate is conducting and therefore it is much easier to perform STM measurements. Graphene on nickel was purchased from Graphene Supermarket. C_n-Ni(II)-porphyrin was deposited on graphene/nickel substrate by drop-casting a solution of C_n-Ni(II)-porphyrin (tetradecane, 1 mM) and the STM tip was immersed into the liquid for the STM measurement (see methods).

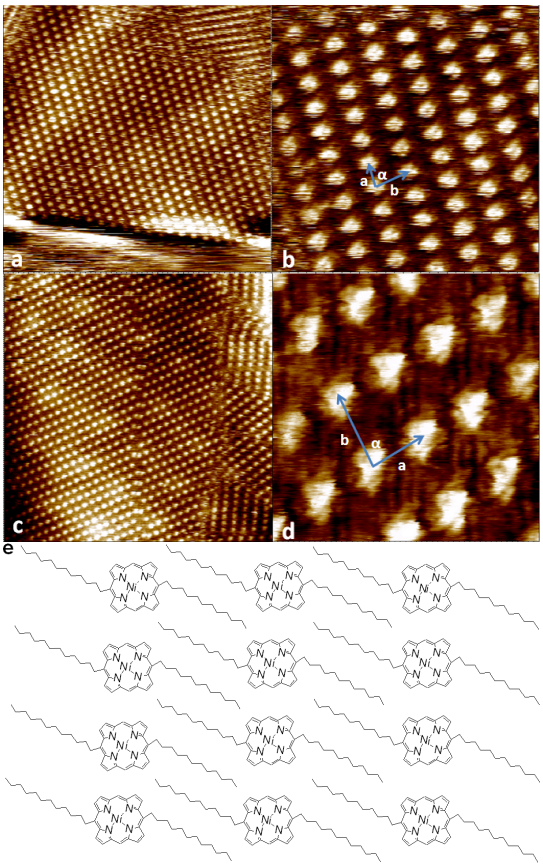

Figure 1. STM images of C_{12}-Ni (II)-porphyrin (a, b) and C_{18}-Ni (II)-porphyrin (c, d) self-assembled on graphene on nickel substrate. Imaging conditions: (a) size (52 × 52 nm^2), I_{set} = 0.1 nA and V_{bias} = 0.6 V. (b) size (15.2 × 15.2 nm^2), I_{set} = 0.1 nA and V_{bias} = 0.6 V. The unit cell is drawn: a = 1.7 ± 0.2 nm, b = 2.0 ± 0.2 nm, α = 80 ± 7º. (c) size (67.9 × 67.9 nm^2), I_{set} = 0.015 nA and V_{bias} = 0.5 V. (d) size (10 × 10 nm^2), I_{set} = 0.01 nA and V_{bias} = 0.5 V. The unit cell is drawn: a = 2.1 ± 0.1 nm, b = 2.4 ± 0.3 nm, α = 78 ± 6º. (e) Scheme of the packing model of C_{12}-Ni (II)-porphyrin on graphene/nickel. Two alkyl chains are physisorbed on the graphene surface.[28]

Figure 1 summarizes the STM images of the two porphyrins self-assembled on the graphene/nickel substrate. C_{12}-Ni(II)-porphyrin forms ordered patterns on

graphene on nickel (Figure 1a). When zoomed in, submolecular resolution of C_{12}-Ni (II)-porphyrin can be achieved (Figure 1b). The bright spots are ascribed to the core of the C_{12}-Ni(II)-porphyrin. The parameters of the unit cell consisting of four molecules are determined to be: a = 1.7 ± 0.2 nm, b = 2.0 ± 0.2 nm, α = 80 ± 7º. As for C_{18}-Ni(II)-porphyrin, it also forms an ordered monolayer on the graphene on nickel (Figure 1c). The core of C_{18}-Ni(II)-porphyrin appears as bright spots. The dark areas between the bright spots are occupied by the alkyl chains, which are less resolved (Figure 1d). The unit cells parameters are larger than those of C_{12}-Ni(II)-porphyrin, which is due to the longer alkyl length of C_{18}-Ni (II)-porphyrin (a = 2.1 ± 0.1 nm, b = 2.4 ± 0.3 nm, α = 78 ± 6º, Figure 1d).

Figure 2 shows STM images of C_{12}- and C_{18}-Ni(II)-porphyrin self-assembed on graphene on SiO_2. Graphene on SiO_2 was purchased from Graphene Supermarket. C_n-Ni(II)-porphyrin was deposited on graphene/SiO_2 substrate by drop-casting a solution of C_n-Ni(II)-porphyrin (tetradecane, 1 mM) and the STM tip was immersed into the liquid for the STM measurement (see methods). It is known that graphene interacts weakly with the underlying SiO_2 substrate, is not flat and tends to form corrugations.[32] The STM measurements are sensitive to corrugations, thus making high resolution of the two porphyrins challenging. Figure 2a and 2c shows the large area STM image of C_{12}- and C_{18}-Ni(II)-porphyrin on graphene/SiO_2. The two compounds both form ordered structures. The regular pattern formed by the two porphyrins even follows the corrugated zones. The bright areas are attributed to the corrugation of graphene (the relative higher areas are labeled with ovals in Figure 2). The height of the corrugation is mainly between 1.5 and 2.5 nm. Higher resolution of molecular structures could be obtained at a smaller scan range. However, submolecular images of the two compounds were not obtained mainly due to the corrugation of graphene.

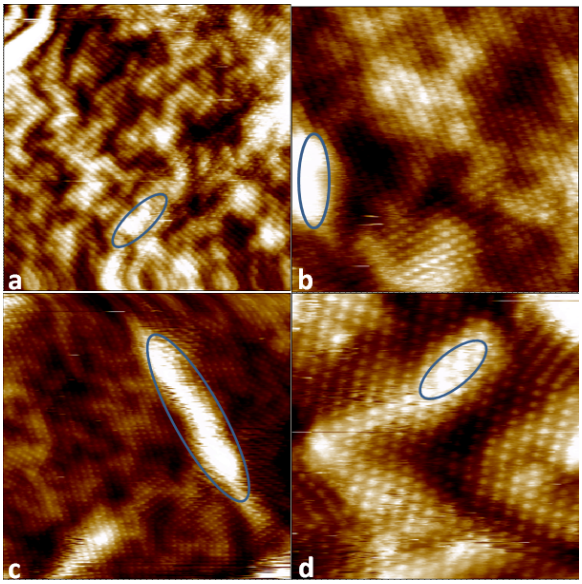

Figure 2. STM images of C_{12}-Ni(II)-porphyrin (a, b) and C_{18}-Ni(II)-porphyrin (c, d) self-assembled on graphene on SiO_2 substrate. Imaging conditions: (a) size (100 × 100 nm^2), I_{set} = 0.006 nA and V_{bias} = 0.5 V. (b) size (53.2 × 53.2 nm^2), I_{set} = 0.006 nA and V_{bias} = 0.5 V. (c) size (100 × 100 nm^2), I_{set} = 0.01 nA and V_{bias} = 0.5 V. (d) size (47.5 × 47.5 nm^2), I_{set} = 0.006 nA and V_{bias} = 0.5 V.

It was found that, the C_6-Ni(II)-porphyrin did not form ordered patterns on graphene on either of the substrates presumably due to the alkyl chain length (C_6) being too short, thus the hydrophobic interaction with graphene is too weak. Implying that the hydrophobic interaction of C_{12}- or C_{18}-Ni(II)-porphyrin with graphene plays an important role in the formation of ordered stuctures. This is also in agreement with the observations by Neves and co-workers, who demonstrated that short octylphosphonic acids did not fulfill the requirements for the formation of ordered structures on HOPG.[33] The authors attribute this to the decreased van der Waals interaction between the alkyl backbone and carbon atoms on HOPG, which are too small due to the short alkyl chain.

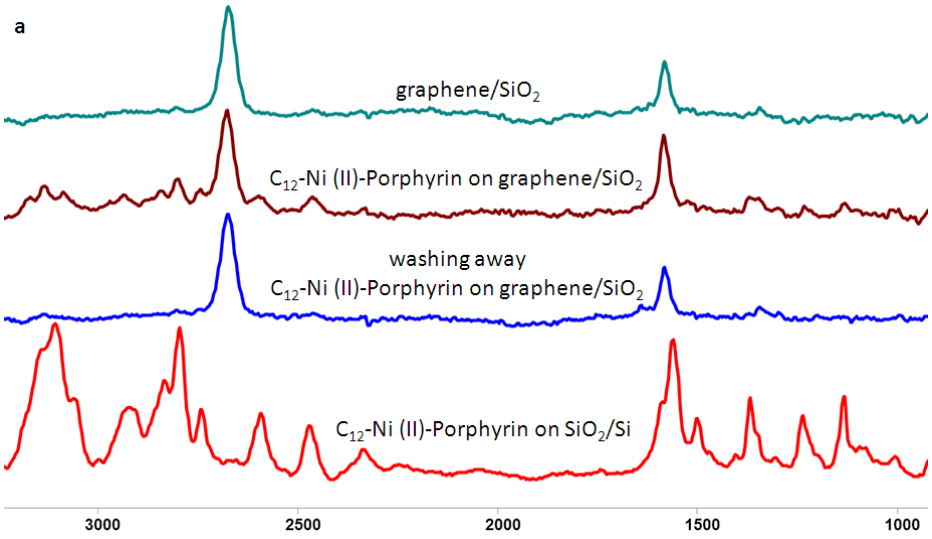
a
graphene/SiO2
C12-Ni (II)-Porphyrin on graphene/SiO2
washing away
C12-Ni (II)-Porphyrin on graphene/SiO2
C12-Ni (II)-Porphyrin on SiO2/Si
3000
2500
2000
1500
1000

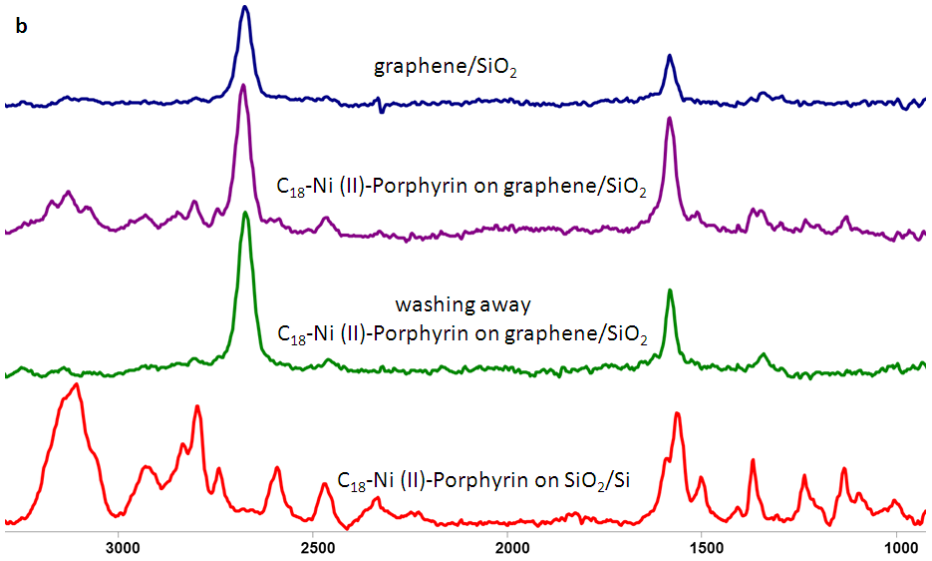
b
graphene/SiO2
C18-Ni (II)-Porphyrin on graphene/SiO2
washing away
C18-Ni (II)-Porphyrin on graphene/SiO2
C18-Ni (II)-Porphyrin on SiO2/Si
3000
2500
2000
1500
1000

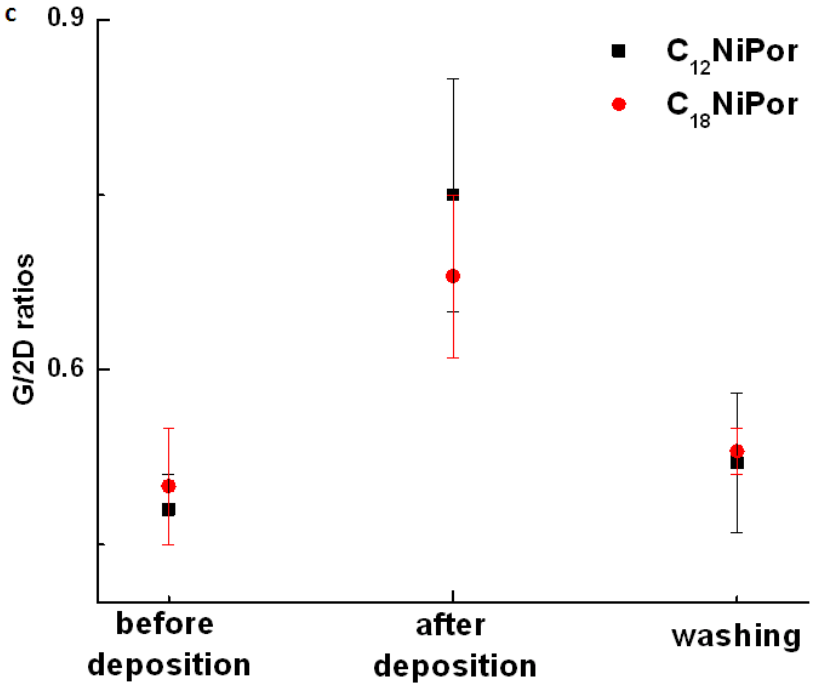

Figure 3. (a) Raman spectra (λ_{exc} = 532 nm) of graphene on SiO_2/Si, C_{12}-Ni(II)-porphyrin on SiO_2/Si, C_{12}-Ni(II)-porphyrin on graphene/SiO_2/Si and C_{12}-Ni(II)-porphyrin was removed by rinsing the graphene/SiO_2/Si substrate with $CHCl_3$. Spectra were background subtracted and baseline corrected. (b) Raman spectra (λ_{exc} = 532 nm) of graphene on SiO_2/Si, C_{18}-Ni(II)-porphyrin on SiO_2/Si, C_{18}-Ni(II)-porphyrin on graphene/SiO_2/Si and C_{18}-Ni(II)-porphyrin was removed by rinsing the graphene/SiO_2/Si substrate with $CHCl_3$. Spectra were background subtracted and baseline corrected. (c) Change in the G/2D band ratios before and after deposition of C_{12}-Ni(II)-porphyrin and C_{18}-Ni(II)-porphyrin, and after the removal of the porphyrins using $CHCl_3$ rinsing.

Raman spectroscopy was used to study the interaction between graphene and the porphyrins. The Raman spectrum of graphene on SiO_2/Si shows a typical G band at 1582 cm^{-1}, and also a 2D band at 2673 cm^{-1}.[34] The shape and full width at half maximum (FWHM) of the 2D band (~ 42 cm^{-1}) is a signature of single-

layer graphene.[34] After deposition of C_{12}-Ni(II)-porphyrin and C_{18}-Ni(II)-porphyrin, the position of the 2D band of graphene shifted towards 2679 cm^{-1}. After washed with $CHCl_3$, the position of the 2D band of graphene shifted back to the original position. Moreover, the ratios of the intensity between the G and 2D band (I_G/I_{2D}) of graphene after deposition of C_{12}-Ni(II)-porphyrin and C_{18}-Ni(II)-porphyrin increased, and they returned again to the original values after removing the porphyrins by washing with $CHCl_3$. The change of I_G/I_{2D} ratios can be attributed to a combination of electron-phonon and electron-electron scattering.[35] For C_{12}-Ni (II)-porphyrin and C_{18}-Ni (II)-porphyrin, their spectra were also shifted upon deposition onto graphene. The shifts of the 2D band of graphene, the increase of the G/2D ratios and also the shift of the porphyrin bands indicate that the interaction between graphene and porphyrins, and also graphene and porphyrins are sufficiently showing to alter their electronic and vibrational properties. However, there is no obvious difference of Raman spectra between C_{12}-Ni (II)-porphyrin and C_{18}-Ni (II)-porphyrin on graphene.

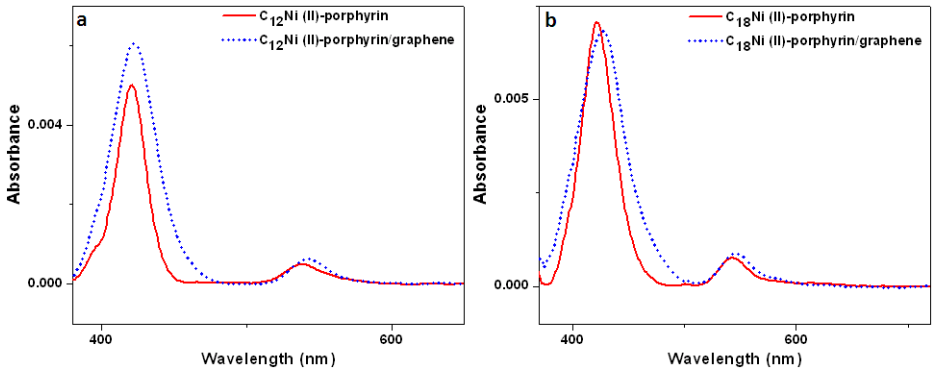

Figure 4. (a) UV/Vis absorption spectra of C_{12}-Ni(II)-porphyrin on quartz (solid line) and C_{12}-Ni(II)-porpyrin on graphene/quartz (dotted line). (b) UV/Vis absorption spectra of C_{18}-Ni(II)-porphyrin on quartz (solid line) and C_{18}-Ni(II)-porpyrin on graphene/quartz (dotted line).

The interaction between graphene and porphyrins was further studied by UV/Vis absorption spectroscopy. As shown in Figure 4a, C_{12}-Ni(II)-porphyrin on quartz shows a Soret band at 420 nm, together with a Q band at 538 nm. The absorption spectrum of C_{12}-Ni(II)-porphyrin on graphene/quartz shows a broadened band at 422 nm and also a band at 543 nm. The absorption spectra of C_{18}-Ni(II)-porphyrin on quartz and also on graphene/quartz are shown in Figure 4b. C_{18}-Ni(II)-porpyrin on quartz shows a Soret band at 422 nm and also a Q band at 542 nm. For C_{18}-Ni(II)-porphyrin on graphene/quartz, two broadened bands are observed at 427 nm and 546 nm, respectively. In both cases, the Soret and Q bands of porphyrins on graphene/quartz show red shifts compared with those of porphyrins on bare quartz, suggesting that the interactions between graphene and porphyrins (which are likely to be π-π interactions).

7.3 Conclusions

In summary, the self-assembly of two alkyl-Ni(II)-porphyrins on large area CVD graphene (both on nickel and SiO_2/Si substrates) was studied by STM. Graphene on nickel is flatter than on SiO_2/Si, submolecular resolution of porphyrins on graphene on nickel can be obtained. On the graphene/SiO_2 substrate, submolecular resolution of porphyrins could not be obtained due to the corrugation of graphene. An improvement could be achieved by deposition of graphene on boron nitride to obtain flatter graphene.[20] The interaction between graphene and porphyrins was studied by Raman and UV/Vis absorption spectroscopy, indicating that graphene and the porphyrins can interact electronically. The coordination metal of the porphyrins can also be replaced with other metal ions. It is reasonable to anticipate that the present strategy for templating porphyrins on graphene substrates could also be extended to other molecular systems.

7.4 Methods

Instruments NMR spectra were recorded using a Varian VXR-400 spectrometer (400 MHz). Raman spectra at 532 nm were obtained using a home built system comprising of a iDus-DU420A CCD detector coupled to a Shamrock163i spectrograph (Andor Technology) and a 25 mW 532 nm DPSS laser (Cobolt Lasers) fibre coupled to an Olympus BX51 microscope (equipped with laserline clean up and edge filters from Semrock) with long working distance objectives. Samples for Raman analysis were prepared by spin coating a few drops of the porphyrin solutions (0.05 mM in $CHCl_3$) on the graphene/SiO_2 substrate or SiO_2 substrate followed by drying under vacuum. STM measurements were performed using a PicoSPM instrument (Molecular imaging, Scientec). The STM tips were mechanically cut from Pt/Ir wire (80:20, diameter-0.25 mm, Goodfellow). Before STM imaging, porphyrins were dissolved in tetradecane (1 mM) at ~ 50 ^{o}C. A drop of the solution was drop-casted onto graphene on nickel or graphene on SiO_2. The STM tip was immersed into the liquid for the STM measurement and the scanning started ~ 5 min after drop-casting. UV/Vis spectra were obtained on a JASCO V-630 UV/Vis Spectrometer. Samples for UV/Vis analysis were prepared by spin coating a few drops of the porphyrin solutions (0.05 mM in $CHCl_3$) on graphene on quartz substrate or bare quartz substrate.

Chemicals and materials $C_6H_{13}CHO$ (Aldrich, 95%), $C_{12}H_{25}CHO$ (Alfa Aesar, 96%), pyrrole (Aldrich, 98%), nitrobenzene (Acros Organics, 99%), acetic acid (Merck, 100%), $Ni(OAc)_2{\cdot}4H_2O$ (Aldrich, 98%) and tetradecane (Sigma-Aldrich, $\geq$ 99%) were used as received. $C_{18}H_{37}CHO$ was synthesized according to a literature procedures.[36] Graphene on nickel, SiO_2 and quartz substrates were purchased from Graphene supermarket and used as received.[37]

C_n-porphyrin synthesis (n = 6, 12, 18)

C_n-CHO (25 mmol) was dissolved in nitrobenzene (200 ml) and acetic acid (125 ml). Pyrrole (25 mmol) was added and the mixture was heated at reflux for 1 h. The solvent was removed under reduced pressure and the crude product was purified by column chromatography to afford the C_n-porphyrin product (neutral Al_2O_3, DCM, 1.5-2%).

C_n-Ni (II)-porphyrin synthesis

C_n-porphyrin (0.05 mmol) and $Ni(OAc)_2 \cdot 4H_2O$ (0.2 mmol) were heated at reflux overnight in ethanol/$CHCl_3$ (9:1, 5 ml). The solvents were removed *in vacuo* and the crude product was purified by column chromatography to afford the desired product (neutral Al_2O_3, DCM, 60-75%).

C_6-Ni (II)-porphyrin

^{1}H NMR (400 MHz, $CDCl_3$) δ 0.88 (t, $^3J_{HH}$ = 6.0 Hz, 12H, $4CH_3$), 1.26–1.36 (m, 8H, $4CH_2$), 1.35–1.43 (m, 8H, $4CH_2$), 1.50–1.59 (m, 12H, $3CH_2$), 4.47 (t, $^3J_{HH}$ = 8 Hz, 8H, $4CH_2$), 9.23 (s, 8H, 8CH). ^{13}C NMR (100 MHz, $CDCl_3$) δ 14.2, 22.7, 30.0, 31.8, 33.9, 37.2, 116.8, 129.6, 141.1. HRMS (ESI) cal. for $C_{44}H_{60}N_4Ni$ [M+H] 703.42, found 703.42. Elemental analysis: cal.: C 75.1%, H 8.59%, N: 7.96%; found: C 74.8%, H 8.66%, N: 7.90%.

C_{12}-Ni (II)-porphyrin

^{1}H NMR (400 MHz, $CDCl_3$) δ 0.87 (t, $^3J_{HH}$ = 6.4 Hz, 12H, $4CH_3$), 1.20–1.34 (m, 56H, $28CH_2$), 1.36–1.45 (m, 8H, $4CH_2$), 1.48–1.59 (m, 8H, $4CH_2$), 2.17–2.27 (m, 8H, $4CH_2$), 4.47 (t, $^3J_{HH}$ = 6 Hz, 8H, $4CH_2$), 9.23 (s, 8H, 8CH). ^{13}C NMR (100 MHz, $CDCl_3$) δ 14.1, 22.7, 29.4, 29.6, 29.7, 30.4, 31.9, 33.9, 37.2, 116.8, 129.6, 141.1. HRMS (ESI) cal. for $C_{68}H_{108}N_4Ni$ [M+H] 1039.80, found

1039.80. Elemental analysis: cal.: C 78.5%, H 10.5%, N: 5.39%; found: C 78.6%, H 10.7%, N: 5.36%.

C_{18}-Ni (II)-porphyrin

^{1}H NMR (400 MHz, $CDCl_3$) δ 0.89 (t, $^{3}J_{HH}$ = 8.0 Hz, 12H, $4CH_3$), 1.20–1.34 (m, 104H, $52CH_2$), 1.35–1.44 (m, 8H, $4CH_2$), 1.50–1.56 (m, 8H, $4CH_2$), 2.19–2.26 (m, 8H, $4CH_2$), 4.46 (t, $^{3}J_{HH}$ = 8.0 Hz, 8H, $4CH_2$), 9.23 (s, 8H, 8CH). ^{13}C NMR (100 MHz, $CDCl_3$) δ 14.1, 22.7, 29.3, 29.5, 29.7, 30.3, 31.9, 33.9, 37.2, 116.8, 129.6, 141.1. HRMS (APCI) cal. for $C_{92}H_{156}N_4Ni$ [M+H] 1076.18, found 1076.18. Elemental analysis: cal.: C 80.3%, H 11.4%, N: 4.07%; found: C 80.4%, H 11.7%, N: 4.03%.

7.5 Notes and references

1. A. K. Geim and K. S. Novoselov, The rise of graphene, *Nat. Mater.*, 2007, **6**, 183.

2. A. K. Geim, Graphene: status and prospects, *Science*, 2009, **324**, 1530; M. J. Allen, V. C. Tung and R. B. Kaner, Honeycomb carbon: a review of graphene, *Chem. Rev.*, 2010, **110**, 132.

3. K. S. Novoselov, A. K. Geim, S. V. Morozov, D. Jiang, Y. Zhang, S. V. Dubonos, I. V. Grigorieva and A. A. Firsov, Electric field effect in atomically thin carbon films, *Science*, 2004, **306**, 666.

4. D. Li, M. B. Muller, S. Gilje, R. B. Kaner and G. G. Wallace, Processable aqueous dispersions of graphene nanosheets, *Nat. Nanotechnol.*, 2008, **3**, 101.

5. Y. Hernandez, V. Nicolosi, M. Lotya, F. M. Blighe, Z. Y. Sun, S. De, I. T. McGovern, B. Holland, M. Byrne, Y. K. Gun'ko, J. J. Boland, P. Niraj, G. Duesberg, S. Krishnamurthy, R. Goodhue, J. Hutchison, V. Scardaci, A. C. Ferrari and J. N. Coleman, High-yield production of graphene by liquid-phase exfoliation of graphite, *Nat. Nanotechnol.*, 2008, **3**, 563.

6. X. Y. Zhang, A. C. Coleman, N. Katsonis, W. R. Browne, B. J. van Wees and B. L. Feringa, Dispersion of graphene in ethanol using a simple solvent exchange method, *Chem. Commun.*, 2010, **46**, 7539.

7. J. S. Wu, W. Pisula and K. Müllen, Graphenes as potential material for electronics, *Chem. Rev.*, 2007, **107,** 718.

8. C. Berger, Z. M. Song, T. B. Li, X. B. Li, A. Y. Ogbazghi, R. Feng, Z. T. Dai, A. N. Marchenkov, E. H. Conrad, P. N. First and W. A. de Heer, Ultrathin epitaxial graphite: 2D electron gas properties and a route toward graphene-based nanoelectronics, *J. Phys. Chem. B*, 2004, **108**, 19912.

9. X. Li, W. Cai, J. An, S. Kim, J. Nah, D. Yang, R. Piner, A. Velamakanni, I. Jung, E. Tutuc, S. K. Banerjee, L. Colombo and R. S. Ruoff, Large-area synthesis of high-quality and uniform graphene films on copper foils, *Science*, 2009, **324**, 1312.

10. K. S. Kim, Y. Zhao, H. Jang, S. Y. Lee, J. M. Kim, K. S. Kim, J.-H. Ahn, P. Kim, J.-Y. Choi and B. H. Hong, Large-scale pattern growth of graphene films for stretchable transparent electrodes, *Nature*, 2009, **457**, 706.

11. D.-W. Shin, H. M. Lee, S. M. Yu, K.-S. Lim, J. H. Jung, M.-K. Kim, S.-W. Kim, J.-H. Han, R. S. Ruoff and J.-B. Yoo, A facile route to recover intrinsic graphene over large scale, *ACS Nano*, 2012, **6**, 7781.

12. N. Petrone, C. R. Dean, I. Meric, A. M. van der Zande, P. Y. Huang, L. Wang, D. Muller, K. L. Shepard and J. Hone, Chemical vapor deposition-derived graphene with electrical performance of exfoliated graphene, *Nano Lett.*, 2012, **12**, 2751.

13. H. T. Liu, Y. Q. Liu and D. B. Zhu, Chemical doping of graphene, *J. Mater. Chem.*, 2011, **21**, 3335.

14. V. Georgakilas, M. Otyepka, A. B. Bourlinos, V. Chandra, N. Kim, K. C. Kemp, P. Hobza, R. Zboril and K. S. Kim, Functionalization of graphene: covalent and non-covalent approaches, derivatives and applications, *Chem. Rev.*, 2012, **112**, 6156.

15. Q. H. Wang and M. C. Hersam, Room-temperature molecular-resolution characterization of self-assembled organic monolayers on epitaxial graphene, *Nat. Chem.*, 2009, **1**, 206.

16. A. J. Pollard, E. W. Perkins, N. A. Smith, A. Saywell, G. Goretzki, A. G. Phillips, S. P. Argent, H. Sachdev, F. Müller, S. Hüfner, S. Gsell, M. Fischer, M. Schreck, J. Osterwalder, T. Greber, S. Berner, N. R. Champness and P. H.

Beton, Supramolecular assemblies formed on an epitaxial graphene superstructure, *Angew. Chem. Int. Ed.*, 2010, **49**, 1794.

17. J. Mao, H. Zhang, Y. Jiang, Y. Pan, M. Gao, W. Xiao and H.-J. Gao, Tunability of supramolecular Kagome lattices of magnetic phthalocyanines using graphene-based moire patterns as templates, *J. Am. Chem. Soc.*, 2009, **131**, 14136.

18. T. Zhang, Z. Cheng, Y. Wang, Z. Li, C. Wang, Y. Li and Y. Fang, Self-assembled 1-octadecanethiol monolayers on graphene for mercury detection, *Nano Lett.*, 2010, **10**, 4738.

19. M. C. Prado, R. Nascimento, L. G. Moura, M. J. S. Matos, M. S. C. Mazzoni, L. G. Cancado, H. Chacham and B. R. A. Neves, Two-dimensional molecular crystals of phosphonic acids on graphene, *ACS Nano*, 2010, **5**, 394.

20. P. Järvinen, S. K. Hämäläinen, K. Banerjee, P. Häkkinen, M. Ijäs, A. Harju and P. Liljeroth, Molecular self-assembly on graphene on SiO_2 and h-BN substrates, *Nano Lett.*, 2013, **13**, 3199.

21. Q. H. Wang and M. C. Hersam, Characterization and nanopatterning of organically functionalized graphene with ultrahigh vacuum scanning tunneling microscopy, *MRS Bull.*, 2011, **36**, 532.

22. C.-H. Park, L. Yang, Y.-W. Son, M. L. Cohen and S. G. Louie, Anisotropic behaviours of massless Dirac fermions in graphene under periodic potentials, *Nat. Phys.*, 2008, **4,** 213.

23. J. A. Fürst, J. G. Pedersen, C. Flindt, N. A. Mortensen, M. Brandbyge, T. G. Pedersen and A.-P. Jauho, Electronic properties of graphene antidot lattices, *New J. Phys.*, 2009, **11**, 095020.

24. H. Imahori, T. Umeyama, K. Kurotobi and Y. Takano, Self-assembling porphyrins and phthalocyanines for photoinduced charge separation and charge transport, *Chem. Commun.*, 2012, **48**, 4032.

25. K. Xiao, W. Deng, J. K. Keum, M. Yoon, I. V. Vlassiouk, K. W. Clark, A.-P. Li, I. I. Kravchenko, G. Gu, E. A. Payzant, B. G. Sumpter, S. C. Smith, J. F. Browning, and D. B. Geohegan, Surface-induced orientation control of CuPc molecules for the epitaxial growth of highly ordered organic crystals on graphene, *J. Am. Chem. Soc.*, 2013, **135**, 3680.

26. S. S. Roy, D. J. Bindl and M. S. Arnold, Templating highly crystalline organic semiconductors using atomic membranes of graphene at the anode/organic interface, *J. Phys. Chem. Lett.*, 2012, **3**, 873.

27. S. Mohnani and D. Bonifazi, Supramolecular architectures of porphyrins on surfaces: the structural evolution from 1D to 2D to 3D to devices, *Coord. Chem. Rev.*, 2010, **254**, 2342.

28. J. Visser, N. Katsonis, J. Vicario and B. L. Feringa, Two-dimensional molecular patterning by surface-enhanced Zn-porphyrin coordination, *Langmuir*, 2009, **25**, 5980; N. Katsonis, J. Vicario, T. Kudernac, J. Visser, M. M. Pollard and B. L. Feringa, Self-organized monolayer of *meso*-tetradodecylporphyrin coordinated to Au(111), *J. Am. Chem. Soc.*, 2006, **128**, 15537.

29. S. De Feyter and F. C. De Schryver, Two-dimensional supramolecular self-assembly probed by scanning tunneling microscopy, *Chem. Soc. Re*v., 2003, **32,** 139.

30. L. C. Giancarlo and G. W. Flynn, Raising flags: applications of chemical marker groups to study self-assembly, chirality, and orientation of interfacial films by scanning tunneling microscopy, *Acc. Chem. Res.*, 2000, **33**, 491.

31. E. Stolyarova, D. Stolyarov, L. Liu, K. T. Rim, Y. Zhang, M. Han, M. Hybersten, P. Kim and G. W. Flynn, Scanning tunneling microscope studies of ultrathin graphitic (graphene) films on an insulating substrate under ambient conditions, *J. Phys. Chem. C*, 2008, **112**, 6681.

32. V. Geringer, M. Liebmann, T. Echtermeyer, S. Runte, M. Schmidt, R. Rückamp, M. C. Lemme and M. Morgenstern, Intrinsic and extrinsic corrugation of monolayer graphene deposited on SiO_2, *Phys. Rev. Lett.*, 2009, **102**, 076102.

33. G. N. Fontes and B. R. A. Neves, Effects of substrate polarity and chain length on conformational and thermal properties of phosphonic acid self-assembled bilayers, *Langmuir*, 2005, **21**, 11113.

34. A. C. Ferrari, J. C. Meyer, V. Scardaci, C. Casiraghi, M. Lazzeri, F. Mauri, S. Piscanec, D. Jiang, K. S. Novoselov, S. Roth and A. K. Geim, Raman spectrum of graphene and graphene layers, *Phys. Rev. Lett*., 2006, **97**, 187401.

35. D. M. Basko, S. Piscanec and A. C. Ferrari, Electron-electron interactions and doping dependence of the two-phonon Raman intensity in graphene, *Phys. Rev. B,* 2009, **80**, 165413.

36. A. A. Khan, S. H. Chee, B. L. Stocker and M. S. M. Timmer, The synthesis of long-chain α-alkyl-β-hydroxy esters using allylic halides in a Fráter–Seebach alkylation, *Eur. J. Org. Chem.*, 2012, **2012**, 995.

37. https://graphene-supermarket.com/

Summary and outlook

Since 2004, considerable progress has been made on graphene, mainly due to contributions by physicists, chemists and material scientists from all over the world. Preparation of high quality graphene flakes and precisely modulating the properties of graphene through functionalization are amongst the most pressing topics in graphene research.

This thesis focused on the preparation of graphene dispersions, and also functionalization of graphene (graphene dispersions and CVD grown graphene) using covalent and noncovalent supermolecular approaches.

The preparation of graphene using the solvent dispersion method has already seen impressive progress over the last five years. Single- and few-layer graphene flakes with relatively small sizes can be prepared in various solvents, as described in Chapter 2 and 3. In Chapter 3, a simple solvent exchange method to prepare graphene in a low boiling point solvent, ethanol, was developed. Relatively stable graphene dispersions were studied by several spectroscopic and microscopy techniques, and the films formed showed good conductivity. Toward future improvements of the solvent dispersion method of graphene, the preparation of graphene with large flake size and a low content of defects is highly desirable. Also, developing new mild and effective methods to exfoliate graphite to prepare graphene is appealing. Controlling the nature of the graphene flakes and selecting graphene flakes with uniform thickness and size, and avoiding contamination are important aspects for device applications.

The functionalization of graphene using covalent approaches has seen major developments over the past few years, in order to increase the dispersibility and processibility of graphene. In Chapter 4, highly functionalized stable graphene dispersions notably in water were obtained through a zwitterion intermediate cycloaddition reaction onto exfoliated graphene flakes. The functionalized

graphene was characterized by several spectroscopic and microscopic techniques. The functionalized graphene films show conductivity several orders of magnitude higher than graphene oxide.

Combining graphene with functional molecules bearing photoactive or redox active units through covalent approaches has also drawn a lot of attention. In Chapter 5, two types of graphene-porphyrin hybrid materials were prepared using one pot cycloaddition reactions. The graphene-porphyrin hybrid materials were characterized using a number of spectroscopic and microscopy techniques. The relatively low degree of functionalization of these two hybrid materials may allow for the retention of graphene's intrinsic properties, especially in comparison with materials prepared via graphene oxide for example.

Covalent functionalization on graphene may change the electronic properties of graphene. Therefore, controlling the degree of functionalization of graphene is important for graphene-based device applications (as described in Chapter 4 and 5). Site selective functionalized graphene, for example, edge selective functionalized graphene, is expected to preserve the intrinsic properties of graphene and at the same time may introduce novel properties to these hybrid materials. On the other hand, incorporating covalently functionalized graphene into polymers or other matrices is expected to allow nanocomposites with enhanced mechanical, electrical and thermal properties to be fabricated. In particular, milder approaches to covalent functionalization of graphene still need to be developed to broaden the chemistry of graphene and their applications.

In Chapter 6, commercially available large area CVD graphene was used as a substrate for the self-assembly of *bis*-urea-terthiophene $\mathbf{T_3}$ molecular wires even when the graphene is highly corrugated, as revealed by scanning tunneling microscopy (STM) measurement. Clean transistors reveal that the

doping induced by the molecular wires and the graphene is at least an order of magnitude less than the doping produced by unwanted adsorbates.

In Chapter 7, the self-assembly of two alkyl-Ni (II)-porphyrins on large area CVD graphene was studied using scanning tunneling microscopy (STM). The interaction between graphene and porphyrins was studied by Raman and UV/Vis absorption spectroscopy. The data indicate that graphene and porphyrins can affect each other electronically.

The unique two-dimensional structure of graphene makes it an ideal template for self-assembly of molecules. Chapter 6 and 7 focus on the self-assembly of *bis*-urea-terthiophene and alkyl-Ni(II)-porphyrins both on graphene on nickel and SiO_2 substrates. Submolecular resolution of the molecules on graphene/SiO_2 could not be obtained due to the corrugation of graphene. Graphene on a boron nitride substrate might be a better option to obtain higher resolution of the molecules. Self-assembly molecular layer can be used to tune the electronic properties of graphene. Furthermore, self-assembly of both donor and acceptor molecules on graphene could be an optional approach to achieve P-N junctions, without the need to cut or etch graphene. For the noncovalent functionalization of graphene, methodology for understanding the charge transfer process and the spatial distribution of charge carriers will be fundamentally important to further design novel graphene-based hybrid materials.

总结与展望

从 2004 年以来，有关石墨烯的研究已经取得了很大的进展，这得益于全世界的物理学家、化学家以及材料学家的贡献。制备高质量的石墨烯以及通过功能化修饰手段精确调控石墨烯的性质是石墨烯研究领域的热点之一。

本论文的研究重点在于：制备溶液中分散的石墨烯，以及通过共价和非共价（超分子）手段修饰石墨烯（所使用的石墨烯的制备方法包括溶液分散法和化学气相沉积法）。

在过去五年中，溶剂分散法制备石墨烯取得了显著的进展。正如第二、三章中所讨论的，尺寸较小的单层、寡层石墨烯可以被分散在多种溶剂之中。在第三章中，采用溶剂置换的方法制备了可在低沸点溶剂乙醇中均匀分散的石墨烯，并通过各种光谱和显微技术表征了石墨烯在乙醇中的分散态，并且所制备出来的石墨烯膜具有良好的导电性。溶剂分散法制备石墨烯可以进一步提高的方面包括：制备缺陷较少的大尺寸的石墨烯；发展更加有效和温和的方法分散石墨烯；制备尺寸和层数均一的石墨烯以提高其在器件应用方面的性能。

在过去的几年中，通过共价手段修饰石墨烯以提高其分散性和可加工性的研究也取得了较大的进展。在第四章中，通过在溶剂分散的石墨烯上进行两性离子环加成反应，成功制备出功能化程度较高的石墨烯。这种功能化修饰的石墨烯可以分散在水中，进而通过各种光谱和显微手段表征了功能化修饰的石墨烯，其导电性比氧化石墨烯高几个数量级。

通过共价手段将具有光学活性或氧化还原活性的分子接枝到石墨烯上也引起了广泛的兴趣。在第五章中，通过一步环加成反应制备出两种石墨烯-卟啉杂化材料，并通过各种光谱和显微手段表征了这两种杂化材料。

相对通过氧化石墨烯功能化修饰的途径而言，本章中制备的杂化材料具有较低的功能化程度，这有助于保持石墨烯的本征特性。

正如第四、五章中所讨论的，通过共价手段修饰石墨烯可能会改变石墨的性质，因此调控石墨烯的功能化程度就十分必要。例如，边缘选择性功能化的石墨烯有望既保留石墨烯的本征特性，还有可能引入新的性质。另一方面，将共价功能化修饰的石墨烯添加到聚合物或其它基质材料中可以用来提高复合材料的力学、电学和热力学性能。同时，发展更加温和的共价修饰石墨烯的方法有利于扩展石墨烯化学及其应用。

在第六章中，利用扫描隧道显微镜研究了含双脲基寡聚噻吩 $\mathbf{T_3}$ 在化学气相沉积法制备的大面积石墨烯上的自组装行为。即使石墨烯存在很多褶皱，$\mathbf{T_3}$ 分子仍然能够在石墨烯表面自组装成有序结构。晶体管器件研究表明，$\mathbf{T_3}$ 分子对石墨烯的掺杂要比其它吸附物至少低一个数量级。

在第七章中，利用扫描隧道显微镜研究了烷基长链卟啉在化学气相沉积法制备的大面积石墨烯表面的自组装行为。并通过拉曼和紫外光谱研究了石墨烯和烷基长链卟啉之间的相互作用，证明了两者之间存在的电子相互作用。

石墨烯独特的二维结构使其可以作为分子自组装的基底材料。第六、七章研究了含双脲基寡聚噻吩和烷基长链卟啉在大面积石墨烯上（包括在金属镍和二氧化硅基底上制备的石墨烯）的自组装行为。由于石墨烯在二氧化硅表面上存在褶皱，没有能够获得亚分子尺度的扫描隧道显微镜图。使用硼氮作为基底材料可以得到相对较为平整的石墨烯，因此有望得到更为清晰的分子图像。石墨烯上的自组装分子层可以用来调控石墨烯的电子性质。同时组装给体和受体分子可以在石墨烯表面形成 P-N 结，避免裁剪或刻蚀石墨烯的过程。更进一步研究石墨烯与分子界面上

的电荷转移和载流子分布对设计新的基于石墨烯的杂化材料具有十分重要的指导意义。

Samenvatting en vooruitzichten

Sinds 2004 heeft het onderzoek aan grafeen een aanzienlijke ontwikkeling doorgemaakt door bijdrages van natuurkundigen, scheikundigen en materiaalonderzoekers van over de hele wereld. Het produceren van grafeen met een hoge kwaliteit en het afstemmen van de eigenschappen van grafeen door middel van chemische functionalisatie behoren tot de meest urgente onderwerpen in het grafeen onderzoek.

Dit proefschrift richt zich op de bereiden van dispersies van grafeen en op het chemisch functionaliseren van grafeen (dispersies van grafeen en grafeen gemaakt met CVD-neerslagtechnieken) door gebruik te maken van zowel covalente als niet-covalente supermoleculaire methodes.

In de afgelopen vijf jaar heeft het bereiden van grafeen vanuit een dispersie een indrukwekkende ontwikkeling doorgemaakt. In hoofdstuk 2 en 3 staat beschreven hoe schilfertjes grafeen van één of twee laagjes dik met relatief kleine afmetingen in verschillende oplosmiddelen kunnen worden gedispergeerd. In hoofdstuk 3 staat beschreven hoe grafeen in ethanol, een oplosmiddel met een laag kookpunt, bereid kan worden met een eenvoudige oplosmiddel uitwisselingsmethode. Deze relatief stabiele grafeen dispersies werden onderzocht met behulp van spectroscopische en microscopische technieken en de dunne lagen die uit deze dispersies werden gemaakt hadden een goede elektrische geleidbaarheid. Wenselijke verbeteringen van de dispersies van grafeen zijn het vergroten van de grafeen schilfers en het verminderen van het aantal defecten. Ook het ontwikkelen van nieuwe milde en meer effectieve methodes om grafeen te isoleren door grafiet laag na laag af te schilferen is aantrekkelijk. Het controleren van de aard van grafeen schilfers, het selecteren van grafeen met een uniforme dikte en grootte en het reduceren van vervuiling zijn belangrijke aspecten voor het ontwikkelen van toepassingen.

Het chemisch functionaliseren van grafeen met covalente methoden om grafeen makkelijker in een dispersie te krijgen, en daarmee beter te verwerken, heeft de afgelopen jaren sterke ontwikkelingen doorgemaakt. In hoofdstuk 4 werd een stabiele dispersie van grafeen in water gerealiseerd door een zogenaamde zwitterion gemedieerde cycloadditie reactie op mechanisch afgeschilferd grafeen toe te passen. Het gefunctionaliseerde grafeen werd gekarakteriseerd door middel van spectroscopische en microscopische technieken. De dunne lagen die uit deze dispersies werden gemaakt hebben een elektrische geleidbaarheid die enkele ordes van groottes hoger is dan die van grafeenoxide.

Ook is er veel belangstelling voor het aanbrengen van moleculen met fotoactieve groepen of redox groepen door middel van covalente methoden. In hoofdstuk 5 werden twee typen grafeen-porfyrine hybride materiaal gemaakt door middel van een zogenaamde ‘one pot’ cycloadditie reactie. De grafeen-porfyrine hybride materialen werden gekarakteriseerd door verschillende spectroscopische en microscopische technieken. In vergelijking tot grafeenoxide werd het grafeen slechts in geringe mate gefunctionaliseerd, waardoor het de oorspronkelijke eigenschappen grotendeels heeft behouden.

Het aanbrengen van functionele groepen op grafeen door middel van covalente bindingen kan de elektrische eigenschappen van het grafeen beïnvloeden. Daarom is het beheersen van de mate waarin het grafeen chemische gefunctionaliseerd wordt van groot belang (beschreven in hoofdstuk 4 en 5). Het controleren van de precieze locatie op het grafeen waar functionele groepen aangebracht kunnen worden, bijvoorbeeld alleen aan de randen, biedt wellicht de mogelijkheid om de elektrische eigenschappen te behouden, terwijl er andere nieuwe eigenschappen worden toegevoegd. Ook het vermengen van dit gemodificeerde grafeen met polymeren of andere matrices kan nieuwe composietmaterialen opleveren met verbeterde mechanische, elektrische en

thermische eigenschappen. In het bijzonder is het relevant om mildere condities te vinden voor covalente chemische functionalisatie van grafeen.

Hoofdstuk 6 laat zien dat commercieel verkrijgbaar CVD grafeen met relatief grote oppervlaktes gebruikt kan worden om de zelf-assemblage van *bis*-urea-terthiophene (**T_3**) moleculen tot nanodraadjes te realiseren, zelfs als het grafeen verre van vlak is. De draadjes werden gevisualiseerd met een scanning tunneling microscoop. De studie laat zien dat de mogelijk geïnduceerde dotering van het grafeen door de aanwezigheid van de **T_3** nanodraadjes ten minste een orde van grootte lager is dan de achtergronddotering die vaak nog ongewenst in dit grafeen aanwezig is.

In hoofdstuk 7 wordt de spontane ordening van twee verschillende alkyl-Ni(II) porfyrines op CVD grafeen met behulp van een rasterelektronenmicroscoop bestudeerd. De invloed van de porfyrines op het grafeen werd onderzocht met Raman en UV/Vis spectroscopie. De resultaten laten zien dat grafeen en porfyrines elkaar elektronisch kunnen beïnvloeden.

De unieke twee-dimensionale structuur van grafeen maakt het een ideaal substraat voor de spontane ordening van moleculen. Hoofdstuk 6 en hoofdstuk 7 richten zich op de zelf-assemblage van alkyl-Ni(II) porfyrines op grafeen op nikkel en op grafeen op SiO_2. Submoleculaire resolutie van de moleculen op grafeen op SiO_2 kon niet verkregen worden vanwege de golving in grafeen wanneer het op SiO_2 is aangebracht. Het bestuderen van zelf-assemblage op grafeen op een vlak substraat zoals boor nitride is wellicht geschikter om moleculen met een hogere resolutie zichtbaar te maken. Zelf-geassembleerde monolagen kunnen gebruikt worden om de elektronische eigenschappen van grafeen precies af te stemmen. Bovendien kan het doteren van grafeen met zowel acceptoren als donoren een aanpak opleveren om zogenaamde P-N overgangen te realiseren zonder dat het grafeen daarbij gesneden of geëtst hoeft te worden. Voor het verder ontwerpen van nieuwe materialen met behulp van

niet-covalente chemische functionalisatie van grafeen is het van belang om methodes te ontwikkelen die het ladingsoverdracht proces tussen grafeen en de moleculen en de ruimtelijk invloed hiervan op het grafeen in kaart brengen.

Acknowledgements

How time flies! Back in September 2009, when I decided to come to Groningen for my PhD study, it has already been four years. But I still remember clearly the first day I arrived in Groningen. I like the city of Groningen very much (it is really quiet and quite different from the cities I have lived in in China) and I really enjoyed such an environment to have enough time to think about everything.

Now, it is time to acknowledge the people who gave me help during my PhD period. I would not be able to finish my PhD without their contributions.

First of all, I would like to start with the acknowledgement of Ben. Dear Ben, as one of your PhD students in the group, I am quite impressed and inspired by your enthusiasm, attitude and energy towards science. Thank you very much for giving me the opportunity to work in your excellent group. I have learned a lot during the past years, from the group meetings, subgroups, lectures, etc. Also, I am quite grateful for your continuous support of the projects, especially of the joint project (with many discussions and suggestions). Please accept my most sincere thanks.

Next, I would like to express my deep gratitude to Bart. Dear Bart, thanks for giving me the opportunity to work in the Physics of Nanodevices (FND) group on the joint projects, and also for your suggestions, discussions on the joint project during the meetings. Also, thanks for your critical reading of the chapters (with a lot of useful comments).

Wesley, to be honest, it is still not so easy for me to get used to your style even after four years. I am quite impressed that you can keep everything under control every day. Thanks for your kind help, suggestions, corrections of papers and thesis, etc., during my PhD period. Good luck to you for your future career.

Prof. Tamalika Banerjee, Prof. Jonathan N. Coleman and Prof. Marcel Mayor, thank you for being my reading committee, and for the critical reading and feedback on the thesis.

Then I express my deep thanks to the collaborators during the past years.

Eek, thanks a lot for the close collaboration on the project and also for translating the summary into Dutch. I really enjoyed the time we worked together (especially the scientific discussions every time), although it was always mixed with excitement and frustrations. I have learned a lot from you and would like to wish you all the best for your future career. Mallik, thanks for the time we spent together on the self-assembly project and also for the time during the Graphene 2013 conference in Bilbao. Best wishes for your PhD in the group of FND.

Willem, it is my great pleasure to have worked together with you on the project of using graphene as a substrate to deposit (single) metal complexes. The collaborations are fruitful with two nice papers published (hopefully we can still have the chance to collaborate in the future). Good luck to you for your future career.

I would like to thank the people who gave me support during my PhD studies. Tibor for introducing me to the world of STM, Nathalie and Greg for the help with AFM measurements, Marc for the assistance with the TEM measurements, Tony for the help with checking two of the papers, and the subgroup members for the discussions and suggestions during the meetings.

I also want to thank the people in my lab 16.238Z and other two labs in the C wing for the nice working atmosphere: Derk-Jan, Francesca, Paula, Robby, Matea, Jos, Bin, Jiaobing, Thomas, Ana, Nathalie, Diederik, Martin, Kuang-Yen, Jiawen, Anouk, Arjen, Thom, Tom, Jort, Jurica, Jochem, Petra, Wen-Hao, Sander, Sander, Peter, Stefeno, Sonia, Romina, etc. I also thank others for

creating a great international atmosphere: Adi, Anne, Alaric, Almudena, Antonio, Arjan, Appu, Celine, Claudia, Carlos, Davide, Duenpen, Emma, Erik, Francesco, Jack, Jiajia, Jianwei, Jeffrey, Jens, Johnny, Krzys, Lorina, Massimo, Mathieu, Milon, Nikki, Oleksii, Pat, Pitor, Sandeep, Shaghayegh, Shuo, Suresh, Tao, Tati, Valentin, Wiktor, Wim and some others I forgot to mention here.

Next, my thanks go to the members in the group of Physics of Nanodevices (FND): Paul, Ivan, Niko, Arramel, Magda, Jasper, Marcos, Siddhartha, Juliana and also Johan, Martijn, Anna, for the help and suggestions whenever I had questions in the group during the past years. Thanks to all the group members of the FND for the great atmosphere.

I thank Hans for the help with the elemental analysis measurements (also for weighing accurate amounts of samples for the STM measurements). Theodora is thanked for mass measurements. Also, Tineke and Hilda are thanked for their kind help whenever I had questions.

Many thanks to the Chinese community here, Depeng Zhao, Zhongtao Wu, Yun Liu, Lei Zhang, Jiajia Dong, Bin Mao, Jiawen Chen, Yange Huang, Zhiyuan Zhao, Zheng Zhang, Kai Liu, Jiaobing Wang, Qian Li, Jiawei Rong, Lifei Zheng, Jingyi Huang, Shuo Yang, etc. It is my great pleasure to meet you all in Groningen and I wish you all a bright future.

Special thanks to Derk-Jan and Depeng for being my paranymphs during the promotion. Thank you very much for your help.

Last but not least, I would like to thank my family. First, my lovely wife, Lili, for spending the time together with me in Groningen, always supporting me on everything and also collaborating on the projects. We had a lot of happy time here and also travelled to several countries in Europe. I enjoyed your nice meals especially the dinners a lot. My deepest thanks to our parents for

continuous support for us studying abroad and also sharing everything with Lili and me. 我爱你们!

最后，再次深深感谢一路走来所有给我帮助的人!

Groningen,

Xiaoyan